

Tracer Gas Investigation of Reingestion of Building Exhaust in an Urban Environment

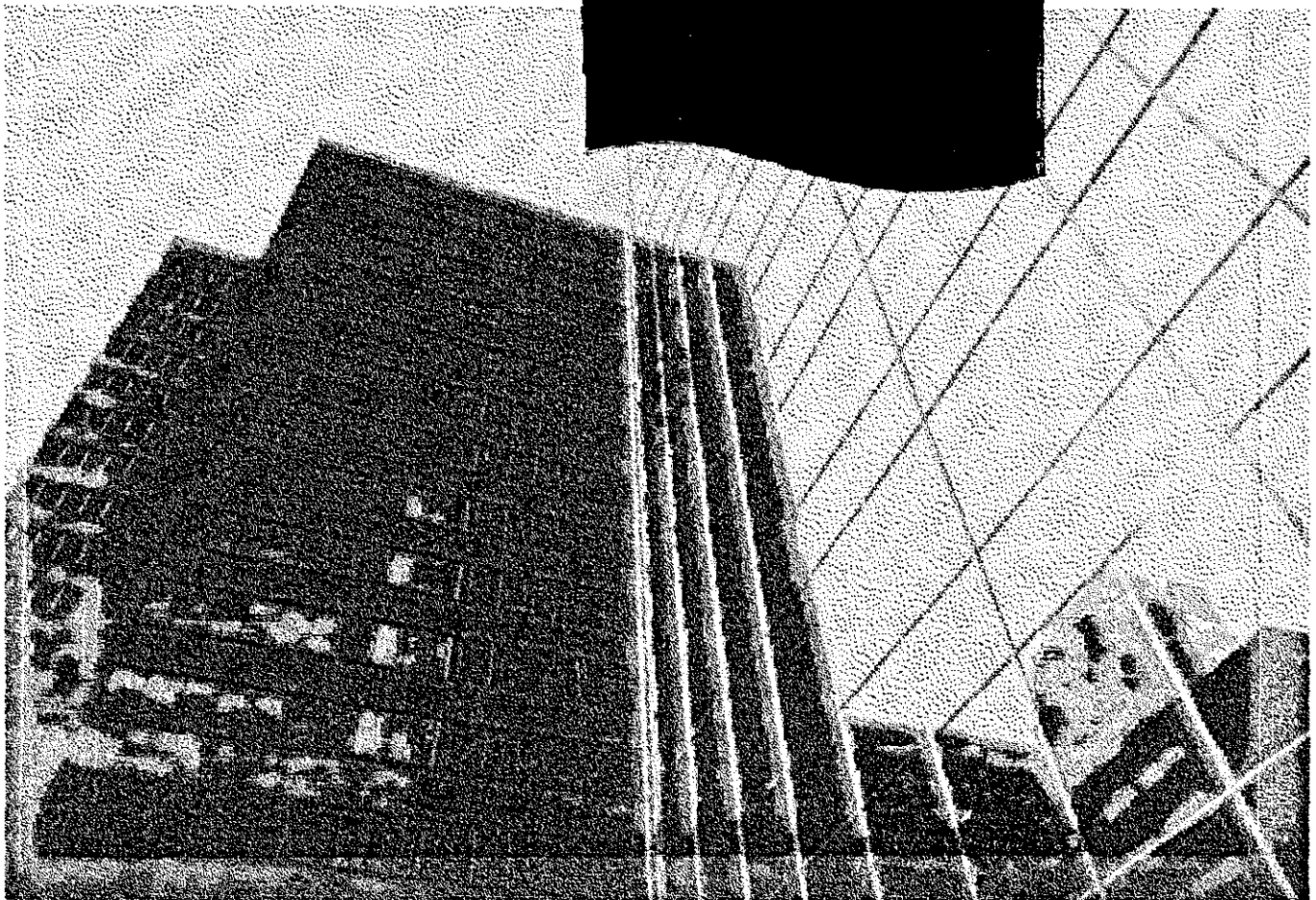
ÉTUDES ET RECHERCHES

Ted Stathopoulos
Louis Lazure
Patrick Saathoff

Février 1999

R-213

RAPPORT



IRSST
Institut de recherche
en santé et en sécurité
du travail du Québec

La recherche, pour mieux comprendre

L'Institut de recherche en santé et en sécurité du travail du Québec (IRSST) est un organisme de recherche scientifique voué à l'identification et à l'élimination à la source des dangers professionnels, et à la réadaptation des travailleurs qui en sont victimes. Financé par la CSST, l'Institut réalise et finance, par subvention ou contrats, des recherches qui visent à réduire les coûts humains et financiers occasionnés par les accidents de travail et les maladies professionnelles.

Pour tout connaître de l'actualité de la recherche menée ou financée par l'IRSST, abonnez-vous gratuitement au magazine *Prévention au travail*, publié conjointement par la CSST et l'Institut.

Les résultats des travaux de l'Institut sont présentés dans une série de publications, disponibles sur demande à la Direction des communications.

Il est possible de se procurer le catalogue des publications de l'Institut et de s'abonner à *Prévention au travail* en écrivant à l'adresse au bas de cette page.

ATTENTION

Cette version numérique vous est offerte à titre d'information seulement. Bien que tout ait été mis en œuvre pour préserver la qualité des documents lors du transfert numérique, il se peut que certains caractères aient été omis, altérés ou effacés. Les données contenues dans les tableaux et graphiques doivent être vérifiées à l'aide de la version papier avant utilisation.

Dépôt légal
Bibliothèque nationale du Québec

IRSST - Direction des communications
505, boul. de Maisonneuve Ouest
Montréal (Québec)
H3A 3C2
Téléphone : (514) 288-1 551
Télécopieur: (514) 288-7636
Site internet : www.irsst.qc.ca
© Institut de recherche en santé
et en sécurité du travail du Québec,

**Tracer Gas Investigation
of Reingestion of Building Exhaust
in an Urban Environment**

Ted Stathopoulos¹, Louis Lazure² et Patrick Saathoff¹

¹Centre d'études sur le bâtiment, Université Concordia

²Programme soutien analytique, IRSST

**ÉTUDES ET
RECHERCHES**

RAPPORT

Abstract

The dispersion of building exhaust was investigated using field and wind tunnel experiments. The major purposes of the study were: 1) to evaluate minimum dilution models that are currently used by building designers, 2) to assess the accuracy of wind tunnel modelling, and 3) to provide guidelines for reducing the risk of reingestion of stack emissions.

A total of seven field tests were carried out using two buildings on the campus of Concordia University in Montreal, Quebec. During the tests, a tracer gas was emitted from a short stack and air samples were obtained at up to fifteen locations on the roof using radio-controlled samplers that were designed and built by IRSST. A sampling period of 15-min was used for the field tests; usually ten samples were obtained at each location.

The field dilution data were compared with minimum dilution estimates obtained with three widely used design formulas, the Halitsky model, the Wilson-Chui model and the Wilson-Lamb model. The Halitsky model generally gave very conservative predictions of minimum dilution. The minimum dilution models of Wilson-Lamb and Wilson-Chui provide reasonable lower bounds for D_{\min} , although both models produced unconservative predictions of some of the field data. The Wilson-Chui model with a revised formula for initial dilution is recommended because it is simpler than the Wilson-Lamb model and also more conservative for urban environments.

Dilution data obtained in the wind tunnel study showed reasonably good comparison with the field data. In general, dilution values obtained in the wind tunnel were higher than the field values with

the discrepancy usually less than a factor of two. Thus, the wind tunnel appears to be slightly unconservative, at least for the particular case studies. Results of both the field study and the wind tunnel study indicate that the behavior of the plume may be dramatically affected when the momentum ratio, M , of the exhaust flow reaches a critical value. For Building 1, a large cubical building, dilution decreased significantly at all rooftop locations when M was between 3 and 4. Tests carried out with Building 2, a short rectangular building, showed that dilution decreased considerably when $M > 2$. These findings regarding the importance of M are noteworthy since, for typical building stacks, M values in the range of 2 to 4 are likely to occur frequently.

TABLE OF CONTENTS

<u>SECTION</u>		<u>PAGE</u>
	ABSTRACT	
1.0	INTRODUCTION	1
2.0	LITERATURE REVIEW	3
2.1	Dilution Models	3
2.1.1	The Halitsky Model	3
2.1.2	The Wilson-Chui Model	4
2.1.3	The Wilson-Lamb Model	5
2.2	Previous Field Dilution Studies	6
2.3	Comparison of Wind Tunnel and Field Data	7
3.0	METHODOLOGY	9
3.1	Experimental Procedures	9
3.2	Field Tests	10
3.2.1	Hall Building	10
3.2.2	The BE Building	22
3.3	Wind Tunnel Tests	30
3.3.1	Wind Tunnel Modelling Criteria	30
3.3.2	Experimental Methodology	32
4.0	RESULTS	38
4.1	Hall Building	38
4.1.1	Field Study	38
4.1.2	Wind Tunnel Study	57
4.1.3	Summary of Findings from the Hall Building Study	63
4.2	BE Building	65
4.2.1	Field Study	67
4.2.2	Wind Tunnel Study	83
4.2.3	Summary of Findings from the BE Building Study	93
5.0	GUIDELINES FOR DESIGN	94
6.0	ACKNOWLEDGMENTS	96
7.0	REFERENCES	96
	APPENDIX A	A1
	APPENDIX B	B1

LIST OF FIGURES

		<u>PAGE</u>
Figure 1	Location of Montreal city centre relative to Mount Royal and Dorval Airport.	11
Figure 2	Location of the Hall Building and the BE Building and surrounding buildings.	12
Figure 3	The Hall Building viewed from the south.	13
Figure 4	Wind rose for Dorval Airport.	15
Figure 5	Wind rose for McGill Observatory.	16
Figure 6	Plan view of Hall Building roof showing locations of the stack, samplers and the anemometer.	20
Figure 7	The BE Building viewed from the west.	24
Figure 8a	Photo of the Strobic stack on the BE Building.	25
Figure 8b	Dimensions of the Strobic stack	25
Figure 9	Exhaust velocity distribution in Strobic stack (BE Building)	27
Figure 10a	Plan view of the BE Building showing locations of the stack, anemometer and sampling locations (numbers indicate wind tunnel model tappings).	29
Figure 10b	Perspective view of the BE Building showing relative heights of the stack and rooftop structures.	30
Figure 11a	Wind tunnel model of the Hall Building.	34
Figure 11b	Wind tunnel model of the BE Building.	34
Figure 12	Vertical profiles of mean velocity and turbulence intensity obtained with a suburban exposure in the CBS boundary layer wind tunnel.	36
Figure 13a	Wind speed during Hall Building Test No. 1 (June 26, 1997).	39
Figure 13b	Wind direction during Hall Building Test No. 1 (June 26, 1997).	39
Figure 14a	Wind speed during Hall Building Test No. 2 (July 2, 1997).	40

		<u>PAGE</u>
Figure 14b	Wind direction during Hall Building Test No. 2 (July 2, 1997).	40
Figure 15a	Wind speed during Hall Building Test No. 3 (July 30, 1997).	41
Figure 15b	Wind direction during Hall Building Test No. 3 (July 30, 1997).	41
Figure 16a	Wind speed during Hall Building Test No. 4(August 7, 1997).	42
Figure 16b	Wind direction during Hall Building Test No. 4 (August 7, 1997)	42
Figure 17a	Concentration distribution for sample period No.1 on June 26.	44
Figure 17b	Concentration distribution for sample period No.2 on June 26.	44
Figure 18	Dilution data obtained at all samplers during Hall Test No. 1 compared with ASHRAE minimum dilution curves.	46
Figure 19	Dilution data obtained at all samplers during Hall Test No. 4 compared with ASHRAE minimum dilution curves.	48
Figure 20	Dilution data obtained at all samplers during Hall Test No. 2 compared with ASHRAE minimum dilution curves.	50
Figure 21	Dilution data obtained at all samplers during Hall Test No. 3 compared with ASHRAE minimum dilution curves.	51
Figure 22	Variation of dilution with time during Hall Test No. 1.	53
Figure 23	Variation of dilution with time during Hall Test No. 2.	54
Figure 24	Variation of dilution with time during Hall Test No. 3.	55
Figure 25	Variation of dilution with time during Hall Test No. 4.	56
Figure 26	Distributions of wind tunnel and field dilution obtained with $M=3$ for $\theta \sim 205$ deg.	58
Figure 27	Distributions of wind tunnel and field dilution obtained with $M=3$ for $\theta \sim 215$ deg.	59
Figure 28a	Variation of D_{wt} with M at tappings 2, 5, 8 and 12 for $\theta=210$ deg	61
Figure 28b	Variation of D_{wt} with M at tappings 2, 5, 8 and 12 for $\theta=215$ deg	61
Figure 29	Effect of wind direction on wind tunnel and field dilution measured at locations 2, 5, 8, 12 and 15.	63

		<u>PAGE</u>
Figure 30	Wind speed and wind direction during BE Building Test No. 1 (Oct. 1, 1997).	68
Figure 31	Wind speed and wind direction during BE Building Test No. 2 (Oct. 10, 1997).	69
Figure 32	Wind speed and wind direction during BE Building Test No. 3 (Dec. 2, 1997).	70
Figure 33	Wind data obtained during two 15-min intervals at the end of BE Test No. 1	72
Figure 34	Variation of dilution with time during BE Test No. 1.	73
Figure 35	Variation of dilution with time during BE Test No. 2.	74
Figure 36	Variation of dilution with time during BE Test No. 3.	75
Figure 37	Dilution data obtained at all samplers during BE Test No. 1 compared with ASHRAE minimum dilution curves.	77
Figure 38	Dilution data obtained at all samplers during BE Test No. 2 compared with ASHRAE minimum dilution curves.	78
Figure 39	Dilution data obtained at all samplers during BE Test No. 3 compared with ASHRAE minimum dilution curves.	79
Figure 40	Contour plots of wind tunnel and field dilution for the BE Building ($M \sim 3, \theta \sim 300$ deg.)	86
Figure 41	Contour plots of wind tunnel and field dilution for the BE Building ($M \sim 2, \theta \sim 270$ deg.)	87
Figure 42	Effect of wind direction on wind tunnel and field dilution measured on the penthouse of the BE Building.	88
Figure 43	Variation of D_{wt} with M at location 10 for $\theta = 280$ deg.	89
Figure 44	Effect of wind direction on wind tunnel and field dilution measured on the main roof of the BE Building.	92

1. Introduction

The reingestion of toxic or odorous gases emitted from rooftop stacks can significantly affect the indoor air quality of a building. Precautions taken during the design and construction phases to ensure proper air quality may be completely overwhelmed under certain atmospheric conditions. Industrial and institutional laboratories are especially susceptible to reingestion problems due to the large number of potential emission sources. This phenomenon has been suspected as a cause of indoor air quality problems at university laboratory buildings as well as various industrial facilities and manufacturing plants.

Determining a safe distance between the pollution sources and air intakes is a complex exercise that involves several parameters such as wind speed, wind direction, the degree of atmospheric stratification, the ratio of exhaust velocity to wind speed, the height and geometry of the building, the development of zones under positive and negative pressure, emission characteristics and the topography of the sites. Ideally, the exhaust system of a building must be designed so that exhaust gases are not reingested at fresh air intakes. For instance, in the province of Quebec, the regulation respecting the quality of the work environment [S-2.1, r.15 (1994)] stipulates that fresh air intakes must be located so that no air already evacuated from an establishment is reintroduced.

Estimates of maximum concentration as a function of downwind distance from a stack or vent can be obtained using dispersion models provided by the American Society of Heating, Refrigerating and Air Conditioning Engineers [ASHRAE (1997)]. Alternatively, a wind tunnel study can be carried out to predict peak concentrations at critical locations. The latter method is generally

preferred when surrounding structures or topography will significantly affect the flow patterns around the building. It is important to note, however, that neither modelling technique has been thoroughly validated with full-scale data. The ASHRAE formulas have primarily been evaluated by comparing dilution estimates with **wind tunnel** results for a number of case studies. Results of these comparisons have been contradictory. For example, Petersen and Wilson (1989) concluded that the ASHRAE formulas give very conservative estimates of plume dilution for high velocity or large diameter stacks. On the other hand, results of other studies indicate that the ASHRAE formulas do not provide conservative dilution estimates in all cases. [Perera et al. (1991), Schuyler and Turner (1989)].

The accuracy of empirical formulas and wind tunnel modelling can only be verified by comparing predicted concentrations with field data. However, few field studies have investigated the particular case of near-source diffusion of emissions from rooftop stacks. In the present comparative study, tracer gas experiments were performed using two institutional laboratories in Montreal. Air samples were collected at a number of locations on the roof of the buildings and the concentration profiles were correlated with meteorological data obtained on the roof. The field tests were then modeled in a boundary layer wind tunnel.

The main purpose of the wind tunnel study was to evaluate the accuracy of this modelling technique. It would be expected, that the accuracy will depend on various factors such as the distance from the emission source to the receptor and the degree to which the modelling criteria have been satisfied.

2. Literature Review

2.1 Dilution Models

A number of semi-empirical models exist for the evaluation of minimum dilution ($D_{min}=C_e/C_{max}$) of exhaust from rooftop stacks, where C_e is the exhaust concentration and C_{max} is the maximum concentration at a receptor for a particular wind speed. Three of the most widely-used models are those developed by Wilson and Chui (1985, 1987), Wilson and Lamb (1994) and Halitsky (1963). The latter two models are included in the ASHRAE Fundamentals Handbook (1997).

2.1.1 The Halitsky Model

Based on wind tunnel experiments, Halitsky (1963) developed the following minimum dilution model, hereafter designated as the H model, for block-shaped buildings with short stacks which have an emission velocity or exhaust area which is large enough to give significant plume rise.:

$$D_{min} = [\alpha + 0.11(1 + 0.2\alpha)S/A_e^{0.5}]^2 \quad (1)$$

where S is the distance from the source, A_e is the exhaust area and α is a parameter that depends on building shape, momentum ratio and orientation of the building. Chapter 15 of ASHRAE (1997) states that:

“the smallest D_{min} occurs along the elevated centerline of the jet plume, where $\alpha = 1.0$ is the appropriate value. Larger values of D_{min} occur on the building surfaces, where α ranges from 2 to 20.”

In the present study, α is conservatively assumed to be 2.0, as recommended by Petersen and Wilson (1989) and Halitsky (1990).

2.1.2 The Wilson-Chui Model

The Wilson-Chui model, hereafter designated as WC, was developed using results of numerous wind tunnel experiments which were carried out with isolated building models [Wilson and Chui (1985,1987), Chui and Wilson (1988)]. In this model, minimum dilution along the plume centerline is given by:

$$D_{\min} = (D_o^{0.5} + D_d^{0.5})^2 \quad (2)$$

where D_o is the initial dilution at the exhaust location and D_d is the distance dilution which is produced by atmospheric and building-generated turbulence. The ASHRAE(1993) formulas for D_o and D_d are:

$$D_o = 1 + 7\beta M^2 \quad (3)$$

$$D_d = B_1 S^2 / M A_e \quad (4)$$

where B_1 is the distance dilution parameter and M is the ratio of exhaust gas velocity, w_e , to the mean wind speed at the building height, U_h . The parameter, β , is the stack capping factor and is set equal to 1.0 for uncapped stacks. The parameter, B_1 , is set at a constant value with the magnitude dependent on the location of the receptors. The previous model specified constant values of $B_1 = 0.0625$ for rooftop receptors and $B_1 = 0.2$ for wall receptors. Note that Eq. (2) is applicable for a flush vent (i.e. $h_s=0$). For stacks with $h_s>0$, the critical dilution, D_{crit} , for the worst case wind speed, U_{crit} , can be estimated by:

$$D_{\text{crit}} = D_{\text{crit},0} (U_{\text{crit}} / U_{\text{crit},0} \exp[Y + Y^{0.5}(Y+1)^{0.5}]) \quad (5)$$

where $D_{\text{crit},0}$ is the dilution at the critical wind speed $U_{\text{crit},0}$ for a flush vent. The variable Y relates the plume height with the vertical spread of the plume and is a function of h_s and S . Expressions for $D_{\text{crit},0}$, $U_{\text{crit},0}$, U_{crit} are provided in ASHRAE (1993,1997).

2.1.3 The Wilson-Lamb Model

Dilution data obtained in a field study [Wilson and Lamb (1994)] and a wind tunnel study [Wilson and Chui (1987)] indicate that B_1 is strongly affected by the level of atmospheric turbulence in the approaching flow. Wilson and Lamb (1994) proposed a revised version of the WC D_{min} model that has since been included in ASHRAE (1997). In the new model, designated as WL in this report, Eq. 2 remains the same. However, the effect of upstream turbulence on the distance dilution parameter is approximated by the following formula:

$$B_1 = 0.027 + 0.0021\sigma_\theta \quad (6)$$

where σ_θ is the standard deviation of wind direction fluctuations in degrees and varies between 0° and 30° . The model suggests that distance dilution has two components -- the dilution due to building-generated turbulence and that due to atmospheric turbulence. It assumes that D_d is significantly enhanced by atmospheric turbulence. For an urban environment, ASHRAE (1997) recommends a typical value of $\sigma_\theta=15^\circ$, which gives a value of 0.032 for the atmospheric component of the distance dilution parameter, $B_1=0.059$. Thus, more than 50% of D_d is assumed to be due to upstream turbulence.

The WL model also includes a revised formula for the initial dilution:

$$D_o = 1 + 13\beta M \quad (7)$$

Eq. 6 is believed to be a reasonable approximation of the dilution that occurs near the stack due only to turbulence associated with the exhaust jet. Note that the previous formula for D_o (Equ. 3) also includes the apparent dilution due to plume rise. Equation 7 is expected to provide a better approximation of the actual initial dilution of the plume than Eq. 3; it is believed to be more

applicable to situations where receptors may be located above the stack. [Wilson and Lamb (1994)]

2.2 Previous Field Dilution Studies

A number of field studies have investigated the dispersion of exhaust from rooftop stacks. Several of these have used relatively small building models in a field setting to evaluate the influence of various atmospheric parameters [e.g. Ogawa et al. (1983a,b), Higson et al. (1994,1995), Oikawa and Meng (1997)]. However, the following section focuses on studies involving real buildings in an urban or suburban environment, which is the topic of the present study.

Lam et al. (1985) carried out a tracer gas study to evaluate plume dilution at a fresh air intake on a large building at the University of Hong Kong. Dilution data were obtained for a sampling period of only 10-seconds and therefore are not appropriate for the evaluation of minimum dilution models, which are generally applicable to an averaging time of 10-minutes. In a similar study, Lam and Kot (1993) carried out tracer gas experiments using a single source/receptor pair and evaluated the influence of wind speed on D . As with the previous study, tracer gas concentrations were obtained for samples of short duration. Furthermore, the influence of wind direction fluctuations may have been significant since only one receptor was used. Consequently, comparison with minimum dilution model estimates is probably not warranted.

Georgakis et al. (1995) carried out a series of tracer gas experiments using two buildings at the

University of Toronto. A number of different stacks of varying height and diameter were used in the study. The sampling period was 15-minutes and thus, the data can be used to evaluate minimum dilution models. However, the wind direction was often not in direct line with the stack/receptor pairs. As a result, some of the dilution measurements are not appropriate for evaluation of the models.

The most extensive set of tracer gas data involving emissions from rooftop stacks was obtained by Lamb and Cronn (1986) using a building on the campus of Washington State University (WSU). A number of experiments were carried out using a variety of stacks with different heights and flow rates. An array of rooftop and ground-level receptors provided a good description of plume dispersion under different atmospheric conditions. Consequently, the data are more appropriate for evaluation of minimum dilution models than data of the previously mentioned studies that used relatively few receptors. However, since the sampling period used in the WSU study was 1-hr, an averaging time correction is required to allow comparison with model estimates of D_{min} .

Wilson and Lamb (1994) analyzed the WSU data set and concluded that an increase in atmospheric turbulence tends to increase plume dilution. The Wilson/Chui minimum dilution model was revised to take into account the influence of turbulence on the distance dilution parameter, B_1 .

2.3 Comparison of Wind Tunnel and Field Data

The validity of wind tunnel results has been based largely on comparisons with data from field

studies that have not involved emissions from rooftop stacks. For example, Petersen and Ratcliff (1991) note that wind tunnel simulations of dense gas dispersion have generally compared well with field results. Petersen (1986) has also obtained excellent agreement between wind tunnel and field concentrations measured far downwind (6 km) of a stack on an offshore oil rig. Bachlin et al. (1991) found that wind tunnel concentrations were within a factor of two of field values for a ground-level source located in a chemical plant.

Martin (1965) measured plume dilution at ground-level locations downwind of a nuclear reactor at the university of Michigan and compared the results with wind tunnel dilution values. He concluded that when the plume is affected by building downwash, mean field concentrations compared well with mean concentrations measured in the wind tunnel. However, when the plume was not influenced by the building, peak concentrations obtained in the field correlate well with wind tunnel average concentrations.

Allwine et al. (1980) carried out wind tunnel simulations of field tests performed at the Rancho Seco Nuclear Power Station by Start et al. (1977). Wind tunnel concentrations were obtained at ground-level receptors located from 100m to 800m from the source. It was concluded that the wind tunnel over-predicted the field concentrations by a factor of 1.7.

It is important to note that the latter two studies compared wind tunnel and field data obtained at ground-level receptors. The accuracy of wind tunnel modelling of concentrations at receptors on the roof and walls of buildings has not been studied extensively. Ogawa et al. (1983b) compared

wind tunnel concentrations measured on the surface of a cubical building model with concentrations obtained in a field study carried out with a small test building. Ground-level concentrations measured in the wake of the model generally compared well with the field results. However, concentrations obtained on the model surfaces did not compare well. Consequently, it was recommended that concentrations measured on the roof and walls of a model building be used only as qualitative indicators of the dispersion of emissions from a rooftop source.

Results obtained by Ogawa et al. (1983b) may have been influenced by turbulence scale effects because of the small size of the structure used in the field tests. The size of turbulent eddies relative to the building dimension was much larger in the field tests than in the wind tunnel experiments.

Saathoff et al. (1996) compared wind tunnel results with those obtained in the WSU field study [Lamb and Cronn (1986)]. The evaluation was limited to field tests conducted with moderate to strong winds, since light winds cannot be modelled well with the wind tunnel. In general, wind tunnel dilution values compared well with the field data; dilution measurements at most receptors were within a factor of two of the field data.

3.0 Methodology

3.1 Experimental Procedures

Two buildings in the centre of Montreal, the Hall Building and the BE Building, were chosen for the study. Both of the test buildings are on the campus of Concordia University. In selecting the

buildings, several factors were considered. These factors included: stack height, stack location, exhaust flow rate, convenience of access and roof area covered by the plume. The Hall field tests were performed during the summer of 1997; the BE tests were performed in the autumn of 1997. After completion of the field experiments, a series of tracer gas tests were performed in the boundary layer wind tunnel at the Centre for Building Studies of Concordia University. The modelling parameters used in these tests were determined from data obtained in the field study.

3.2 Field Tests

3.2.1 Hall Building

The Hall Building, located in downtown Montreal, is one of the main buildings of Concordia University. It is a 62 m tall structure that contains many of the research and teaching laboratories of the university. It is surrounded by buildings of similar height and is approximately 500 m southeast of Mount Royal, a small hill with a peak elevation of 233 m . The relative location of the Hall Building with respect to Mount Royal is shown in Figure 1. Locations and heights of tall buildings surrounding the Hall and BE buildings are shown in Figure 2. A photograph of the Hall Building and surrounding buildings is shown in Figure 3.

This building was chosen for the study, in part, because previous wind tunnel studies have provided a significant amount of data for cubical buildings. Most of these studies have been carried out for isolated buildings; one purpose of the present study was to evaluate the influence of upstream buildings on the dilution process.

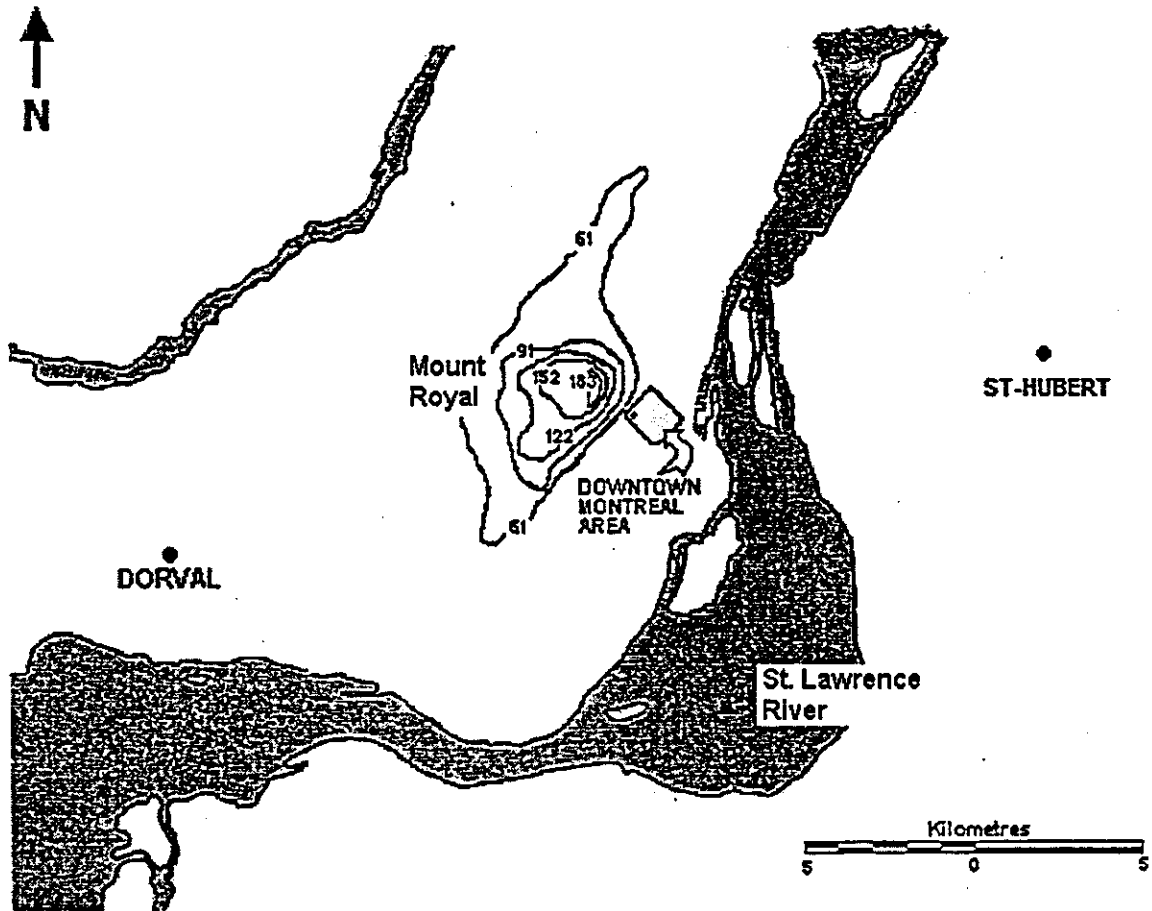


Figure 1 Location of Montreal city centre relative to Mount Royal and Dorval Airport. (Elevations are in meters).

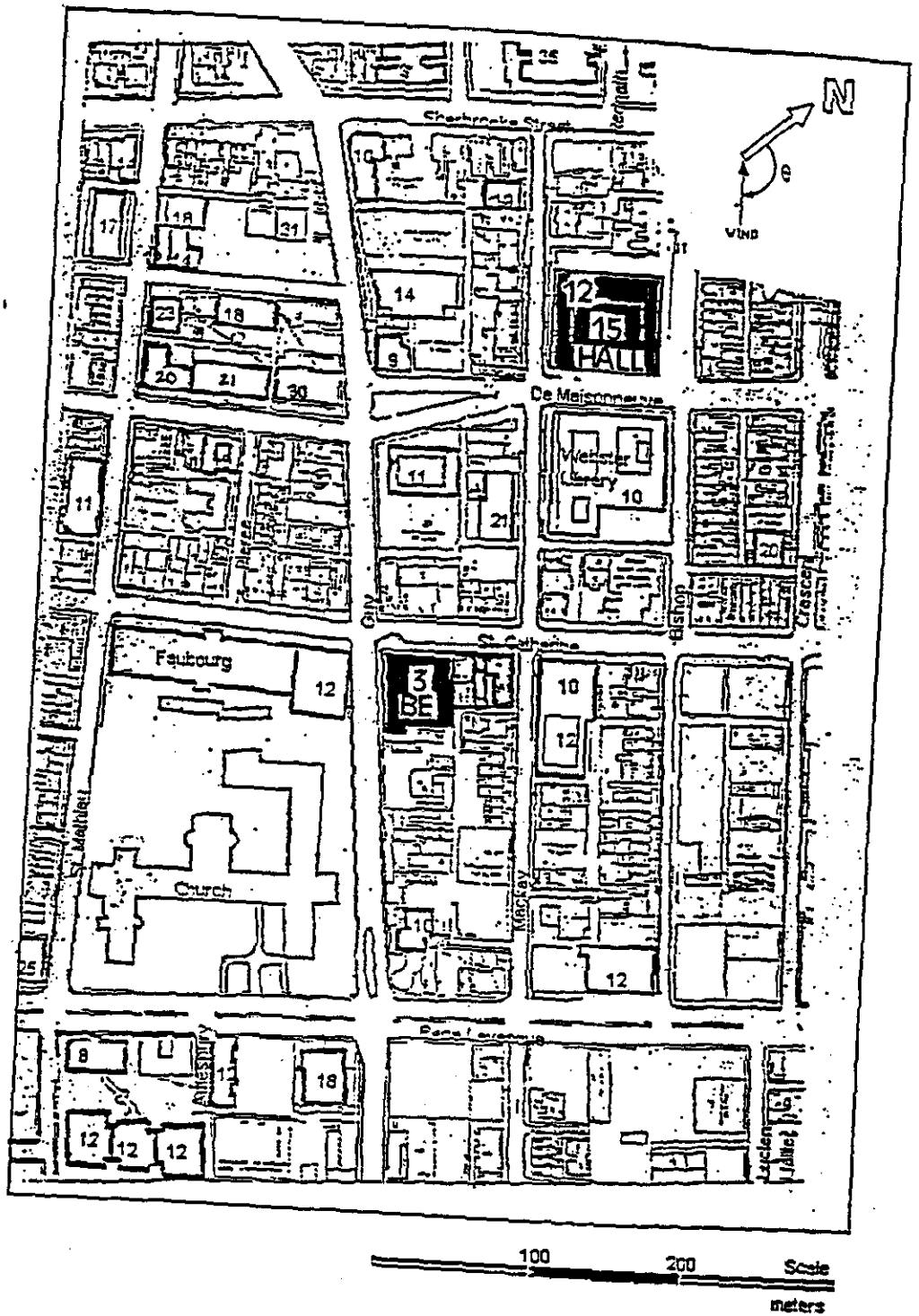


Figure 2 Location of the Hall Building and the BE Building and surrounding buildings. (Number of storeys are indicated for tall buildings).

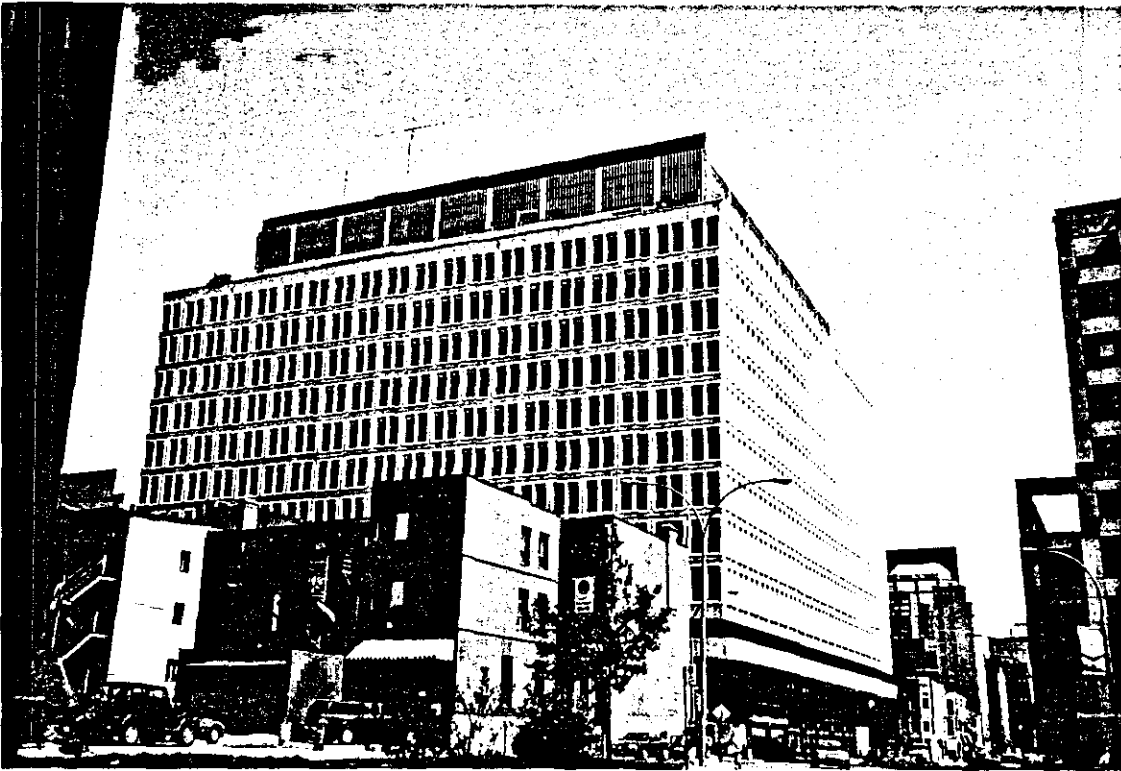


Figure 3 The Hall Building viewed from the south.

Previous field experiments involving the dispersion of a tracer gas have found that concentration data show a significant amount of scatter, even for nominally similar atmospheric conditions [e.g. Start et al. (1977), Georgakis et al. (1995)]. Therefore, rather than perform the field tests for a wide range of meteorological conditions, it was decided that it would be preferable to carry out the experiments on days with similar conditions so that firm conclusions could be made regarding the data.

The wind climate in the vicinity of the Hall Building is expected to be similar to that of Dorval Airport, located 20 km west of Montreal. The wind rose for Dorval Airport in Figure 4 shows that the predominant wind directions are west-southwest and northeast. However, the proximity of Mount Royal tends to reduce the frequency and magnitude of westerly winds in the city centre.

Wind data obtained on a 14 storey building on the campus of McGill University, located 1 km northeast of the Hall Building, shows the influence of Mount Royal. The McGill wind rose shown in Figure 5 indicates that in the city centre, the frequency of westerly winds is lower than at Dorval Airport.

The wind conditions chosen for the Hall Building tests were southwesterly winds with mean wind speed $> 5 \text{ m s}^{-1}$. This wind speed category generally corresponds to a neutral or slightly unstable atmosphere [Turner (1994)] and is therefore suitable for wind tunnel modelling. The decision to carry out a test on a given day was based on wind forecasts by Environment Canada (Dorval) and by the availability of personnel from IRSST and Concordia University. Tests were carried out on

WIND SPEEDS AT DORVAL

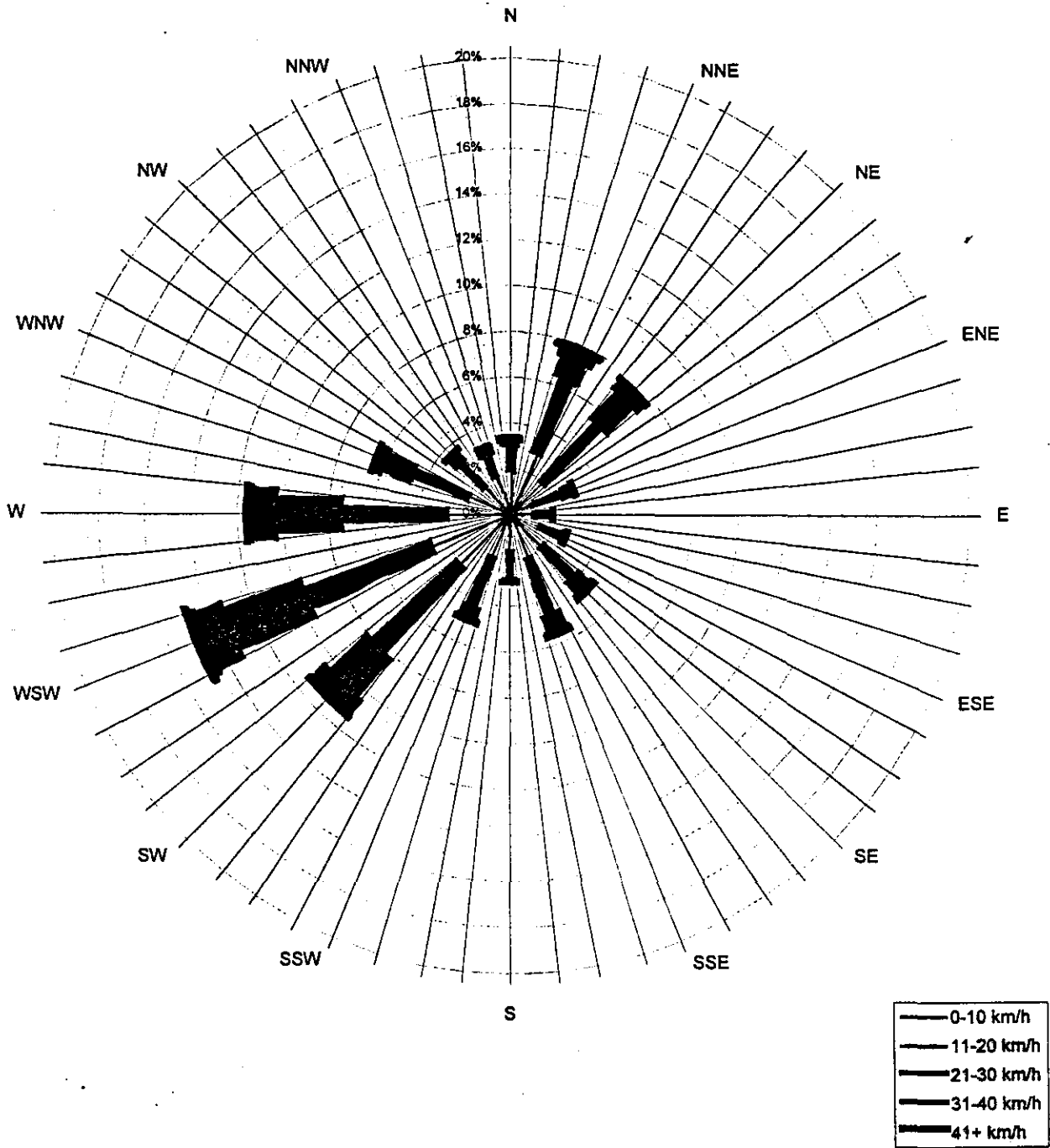


Figure 4 Wind frequency chart for Montreal (@ z=300 m) based on Dorval Airport data.

**WIND SPEEDS AT MCGILL 1980-1988
300 METERS ABOVE GROUND**

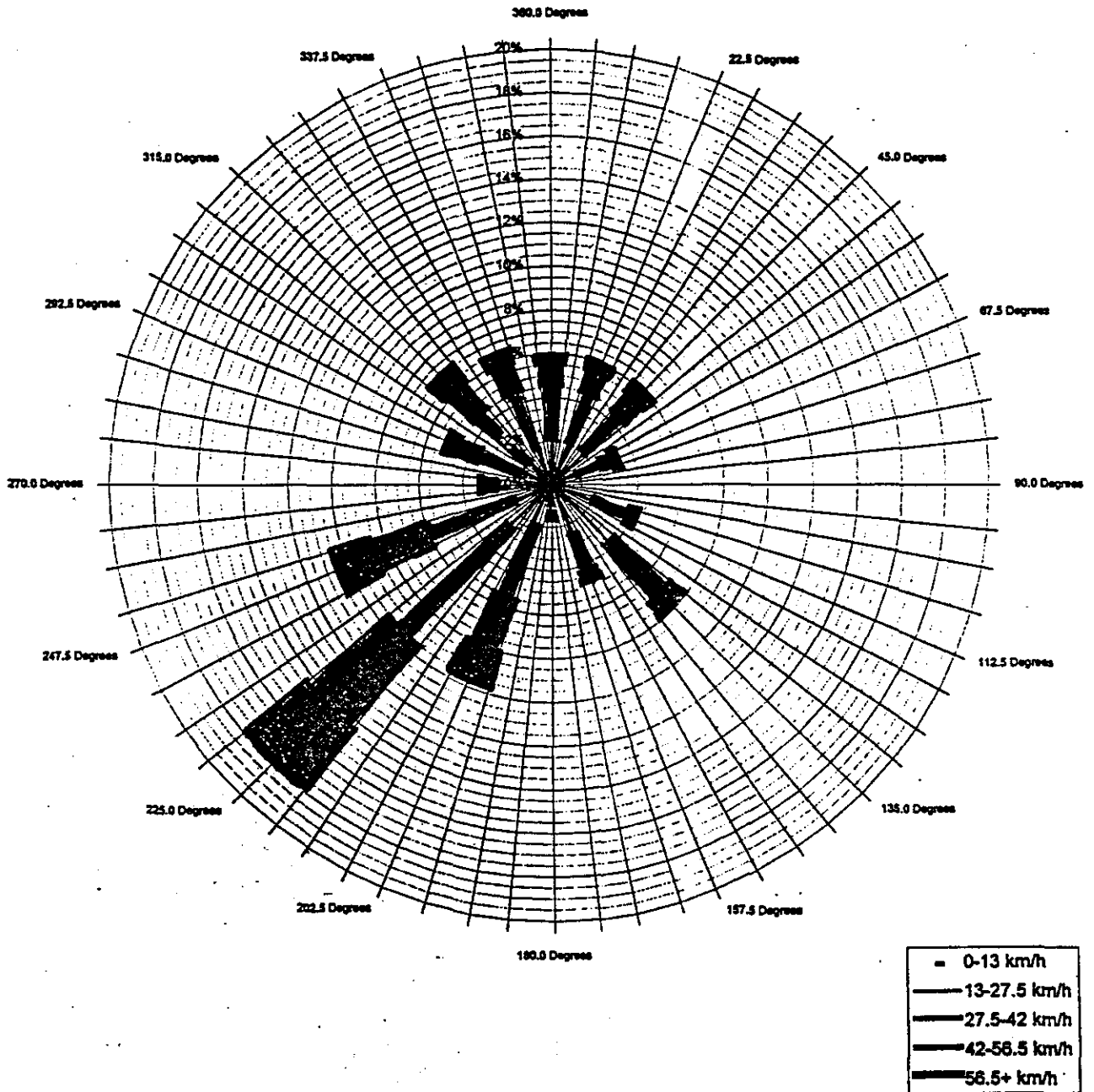


Figure 5 Wind frequency chart for Montreal (@ z=300 m) based on McGill Observatory data.

June 26, July 2, July 30 and August 7 of 1997. The wind speed on July 2nd was somewhat less than expected and as a result, the dilution measurements for this day were not similar to those obtained on the other days. However, the July 2nd results provide useful information on the influence of wind speed on plume behavior for this building geometry. Atmospheric conditions for the four Hall Building tests are shown in Table 1. The tests were carried out between the hours 10:30 to 16:40 EDT.

Table 1 Atmospheric conditions for the Hall Building tests (Test duration: ≥ 2 hrs)

Date	U (m/s)	Wind Dir. (deg)	σ_v/U	T (° C)
June 26, 1997	4.9	217	0.401	24.9
July 2, 1997	2.5	173	0.439	26.6
July 30, 1997	4.4*	210*		25.7
August 7, 1997	5.7	212	0.413	24.8

* Values estimated

Wind speed and wind direction were measured at a height of 7 m above the roof using a Gill sonic anemometer. The instrument measures the mean value and the standard deviation of two horizontal wind speed components (u_x , v_x) and the vertical wind speed (w_x) for the selected averaging time. The averaging time was set at 5 minutes for the June 26th and July 2nd tests and increased to 15 minutes for the August 7th test. Details of the sonic anemometer and wind data analysis procedures are provided in Appendix A.

Hourly wind data were also acquired by a meteorological station located on the roof of the Webster Library Building, which is a 10-storey building adjacent to the Hall Building, as shown in Figure 2. This station, operated by Professor David Frost of the Geography Department of Concordia University, has a Young propeller anemometer mounted at a height of 3 m above the roof. Due to the low measurement height, wind data from this anemometer are affected by the flow patterns generated by the Webster Building and nearby tall buildings. Nevertheless, hourly wind speed data from the station can be used to supplement the sonic anemometer data by applying a height correction factor, $U_{\text{Hall}}/U_{\text{Web}}$. Based on data obtained on June 26 and August 7, this correction factor is approximately 1.8 when the wind direction is southwesterly.

In this regard, it should be noted that wind data were not recorded by the sonic anemometer on July 30. As a result, wind speed data from the Webster anemometer, adjusted for the difference in height, have been used in the analysis. Likewise, wind direction data for July 30 were estimated using the Webster Library data. The Webster data were adjusted based on a comparison of Hall and Webster data for June 26 and August 7.

Average values of along-wind turbulence intensity, σ_v/U , for the Hall Building tests are shown in Table 1, where σ_u is the standard deviation of along-wind velocity fluctuations. The cross-wind turbulence intensity, σ_w/U , where σ_v is the standard deviation of cross-wind velocity fluctuations, was estimated by assuming that $\sigma_w/U \sim 0.8\sigma_u$ [Ogawa et al. (1983a), Oikawa and Meng (1997)]. The average value of σ_v/U for the Hall Bldg. tests is estimated to be approximately 0.33. Details regarding the calculation of turbulence statistics are provided in Appendix A.

Note that the standard deviation of wind direction, σ_{θ} , which is the turbulence parameter specified in the WL minimum dilution model was not measured in the study. According to Wilson and Lamb (1994), $\sigma_{\theta} \sim \sigma_{\sqrt{U}}$ when RMS turbulence intensity less than 0.3, where σ_{θ} is measured in radians. Assuming this approximation is valid for the Hall Bldg. tests, $\sigma_{\theta} \sim 0.33$ rad, or approximately 20° . Thus, substituting $\sigma_{\theta} = 20^{\circ}$ into Eq. 6 gives a distance dilution parameter, B_1 , of 0.069.

Locations of the stack and samplers are shown in Figure 6. A fume hood stack(#32A) on the southwest side of the roof was chosen for the tests as this allowed a significant portion of the roof to be sampled. Exhaust parameters are shown in Table 2. The stack was approximately 0.5 m in height and had a square cross-section with a width, d_s , of 0.585 m. The exhaust velocity, w_s , was checked with a TSI Velocicalc anemometer during the tests and varied between 13.6 m/s on June 26 to 15.4 m/s on August 7. Stack No.32A is part of a bank of seven fume hood stacks which were connected to a number of fume hoods in a chemistry laboratory on the 11th floor of the building. For the most part, the tests were performed with the adjacent stacks closed to prevent any influence on the plume of 32A.

A total of fifteen air samplers were used in the study; samplers 1-13 were placed on the roof and samplers 14 and 15 were located on the 12th floor level on the northeast side of the building.

Note that sampler No. 3 was placed upwind of the stack for the August 7 test after a smoke test revealed that the plume frequently travels upwind. It should also be noted that samplers 1-10 were located in a recessed part of the roof, approximately 2.5 m below the top of the stack.

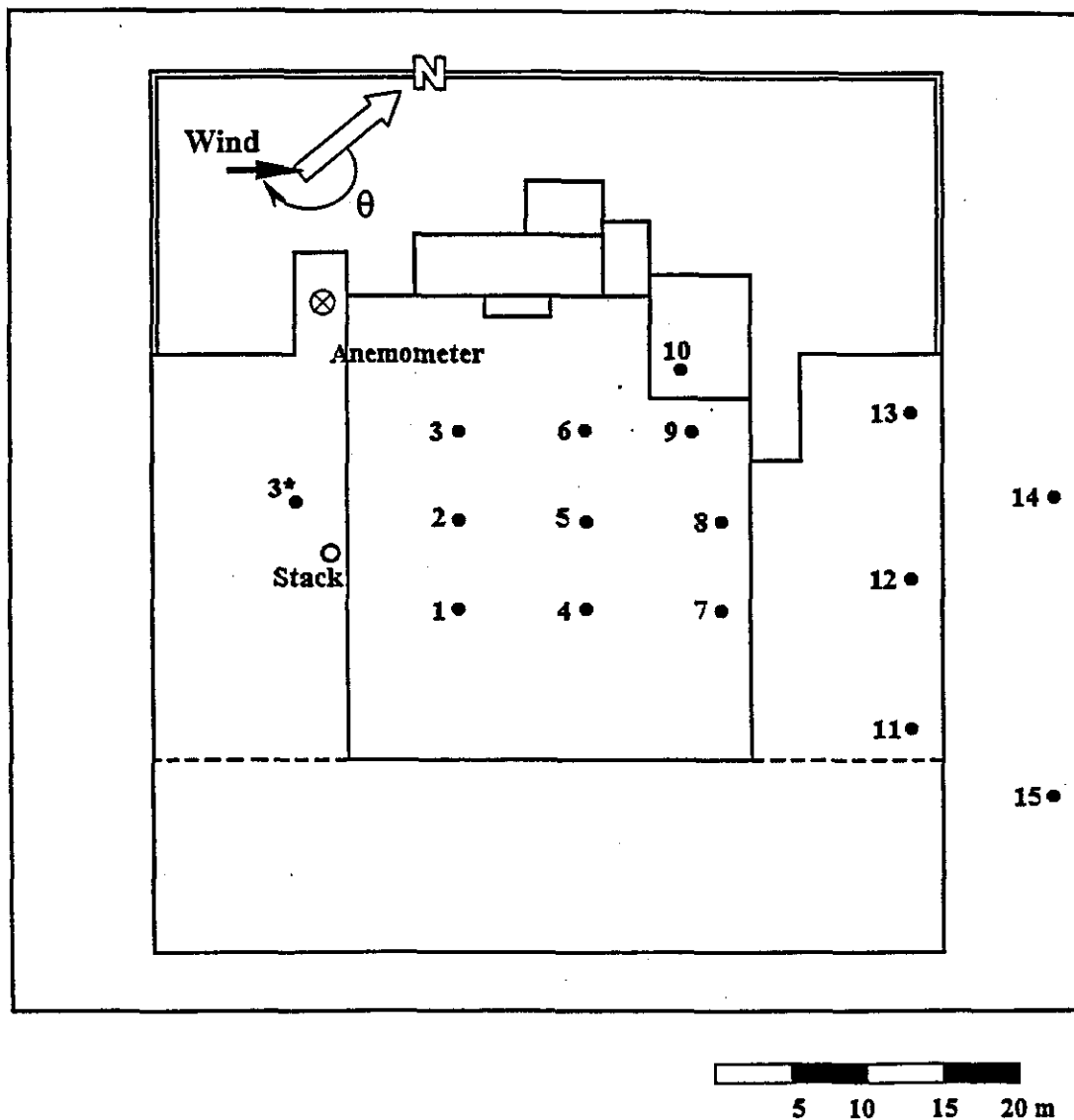


Figure 6 Plan view of Hall Building roof showing locations of the stack, samplers and the anemometer. (Samplers 1-13 are at the 14th storey level, samplers 14 and 15 are at the 12th storey level).

Table 2 Exhaust parameters for Stack No. 32A (Hall Building)

Stack Parameter	
Height (h_s)	0.50 m
Width (d_s)	0.59 m
Area (A_s)	0.34 m ²
Velocity (w_s)	14.7 m s ⁻¹
Flow Rate	5.0 m ³ s ⁻¹

The samplers contained an automated sampling module, designed and built at IRSST, that could provide up to 10 air samples over a specified time interval. The samples were collected with 1-litre bags (Cali-5-Bond). Details of the sampling system are provided in Appendix B.

The sampling period per bag was set at 15 minutes, which should allow comparison with mean concentrations obtained in the wind tunnel. The ASHRAE (1997) minimum dilution model predictions generally correspond to an averaging time of 10-minutes. However, if stacks and receptors are located in the same flow recirculation zone (as in the present study), dilution data are not very sensitive to averaging time. In such cases, ASHRAE (1997) suggests that D_{min} for a 3-min average corresponds to averaging times of 3 to 60 minutes. In the present study, it was not practical to use a 3-min. averaging time since this would have required many more sampling bags. It was decided that a 15-min. averaging time would be acceptable for wind tunnel comparisons and would also allow sampling to continue for more than 2 hours..

In most tests, ten 15-minute samples were obtained by each sampler. Thus the total sampling time

was usually 2.5 hours. In some cases, fewer samples were taken due to various technical problems, such as improper connection of sampler bags, depletion of SF₆, and problems with sampler batteries.

The tracer gas, sulfur hexafluoride (SF₆), was emitted into a fume hood in a chemistry laboratory on the 11th floor of the Hall Building. The concentration of SF₆ was monitored continuously using a Bruel and Kjaer gas analyzer located in the mechanical room on the 13th floor. The outlet concentration was usually set at approximately 10 ppm. An exception was the test performed on July 30 in which the outlet concentration varied between 5.55 ppm and 9.22 ppm over the test period of 2 hours. It should be noted, however, that the outlet concentration during each 15 minute period on July 30 was relatively stable.

After completion of each test, the sample bags were brought to the Building Aerodynamics Lab at the Centre for Building Studies for analysis. Two gas chromatographs (GC), one made by Varian and the other by Lagus Applied Technology, were used to measure the SF₆ concentration of the air samples. Generally, the Lagus GC was used for low concentration samples (C < 25 ppb). Periodically, a bag was analyzed using both instruments to check the measurement procedure. Concentrations obtained with the two instruments showed very good agreement; deviations in C were usually within $\pm 10\%$.

3.2.2 The BE Building

The BE Building is located approximately two blocks south of the Hall Building, as shown in

Figure 2. It is a 3-storey building that houses the Centre for Building Studies of Concordia University and several small businesses. A photograph of the BE Building and its surroundings is shown in Figure 7. Several high-rise structures are within 100 m of the BE building and these may strongly influence the wind flow over the building, depending on the wind direction. Most significant is the Faubourg Tower, a 12-storey building located across the street from the BE building on the southwest side.

The BE building was chosen for the study because, in preliminary tests, it was determined that exhaust from the fume hood stack was being reingested into the building for certain wind directions. Smoke tests showed that for westerly and northwesterly winds, the plume makes direct contact with the fresh air intake located on the penthouse. It was determined that the BE building would provide an interesting test case for assessment of the accuracy of wind tunnel modelling as well as that of empirical dilution models.

As previously discussed, it was decided that it would be preferable to carry out the field experiments on days with similar conditions so that firm conclusions could be made regarding the data. The wind conditions chosen for the BE Building tests were westerly or northwesterly winds with wind speeds greater than 5 m/s measured at Dorval Airport. Tests were performed on three days: October 1st, October 10th and December 2nd, 1997. Mean wind data and ambient temperatures for these tests are shown in Table 3. The fume hood stack on the BE building was manufactured by Strobic Inc. and is shown in Figure 8. The stack was approximately 3 m in height and had an outlet diameter, d_s , of 1.1 m. The stack parameters are shown in Table 4.



Figure 7 The BE Building viewed from the west

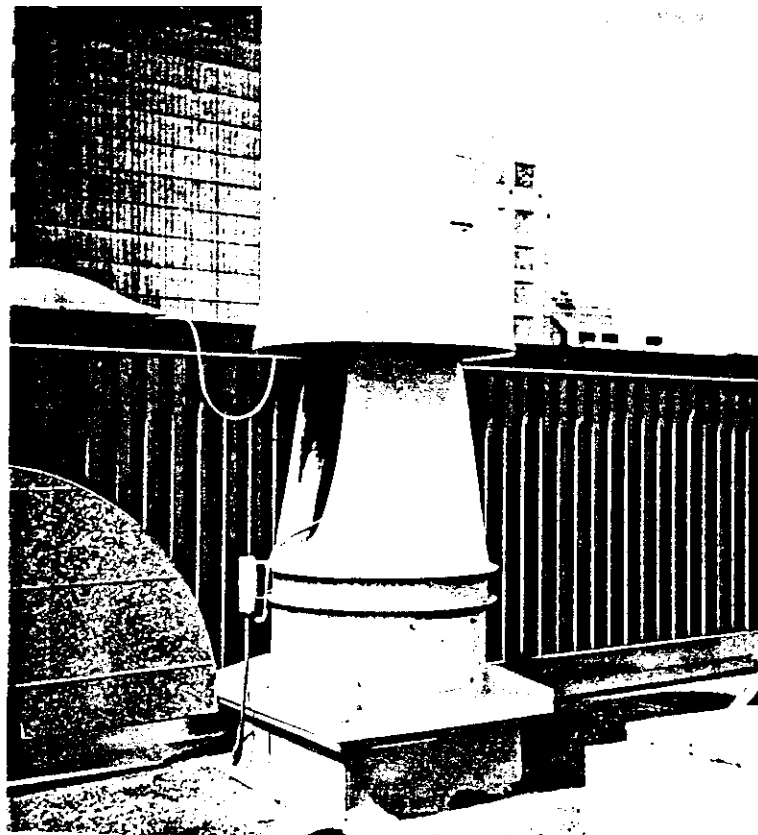


Figure 8a Photo of the test stack on the BE building.

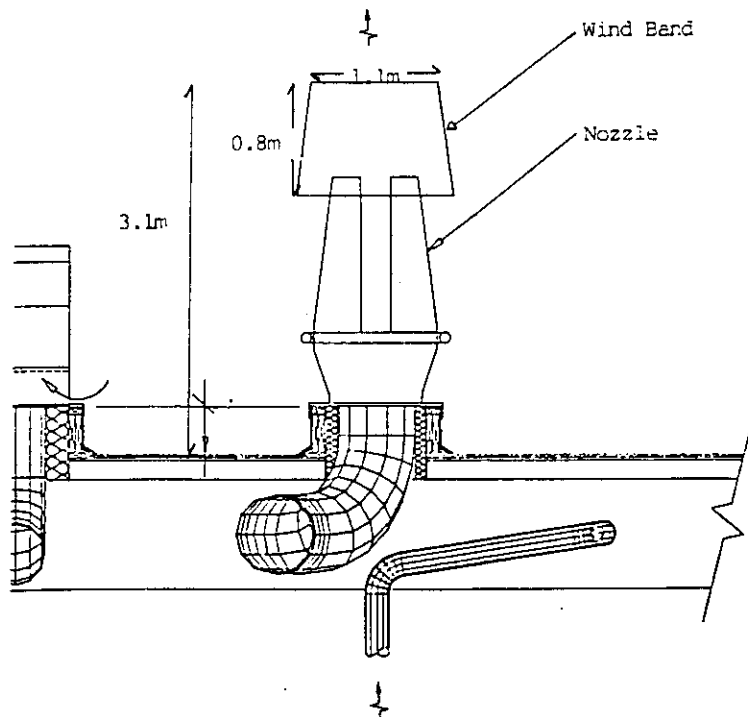


Figure 8b Dimensions of the BE Bldg. test stack

Table 3 Average wind conditions during field tests at the BE Building (test duration ≥ 2 hrs)

Date	U (m s ⁻¹)	Wind Direction (deg)	σ_v/U	T (° C)
Oct. 1, 1997	2	300		5.5
Oct. 10, 1997	4.5	270	0.6	16
Dec. 2, 1997	3.1	270	0.76	-0.5

It is important to note that the exhaust is emitted from two nozzles located only 0.76 m from the top of the stack (see Figure 8b). As a result, the exhaust velocity distribution at the outlet is not uniform, as shown in Figure 9.

In order to use the WC and WL dilution models, the mean exhaust velocity must be estimated. In this case, evaluation of w_e was difficult because of the nonuniform velocity profile. It could be argued that the mean velocity measured over the total stack area at the top of the wind band ($A_{top} = 0.95 \text{ m}^2$) be used. However, w_e obtained with this method is approximately 6 m s^{-1} -- much less than w_e measured in the core of the plume (see Fig. 9). This would produce an unrealistic value of M which would lead to inaccurate estimation of D_o and D_a (Eqs, 3,4 and 7).

An alternative method, which was used in the present study, is to evaluate the exhaust velocity in the core of the plume rather than over the total stack area. The plume was assumed to have an effective diameter of 0.9 m, based on the velocity distributions shown in Figure 9. The effective exhaust velocity was determined by taking the average of the velocity measurements obtained within this diameter. With this method, w_e was found to be approximately 8.1 m s^{-1} , which gives an effective flow rate of $5.2 \text{ m}^3/\text{s}$.

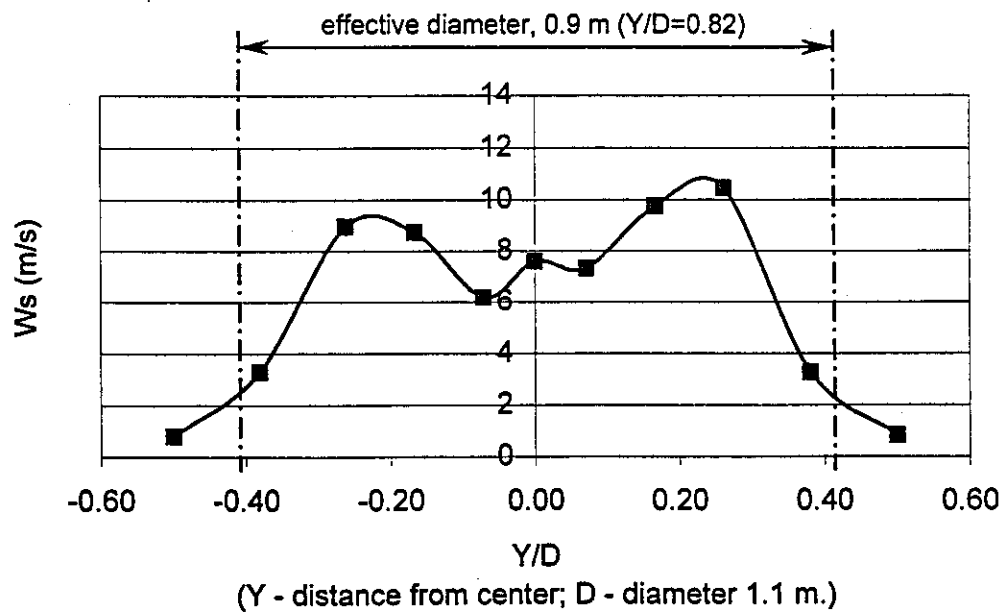
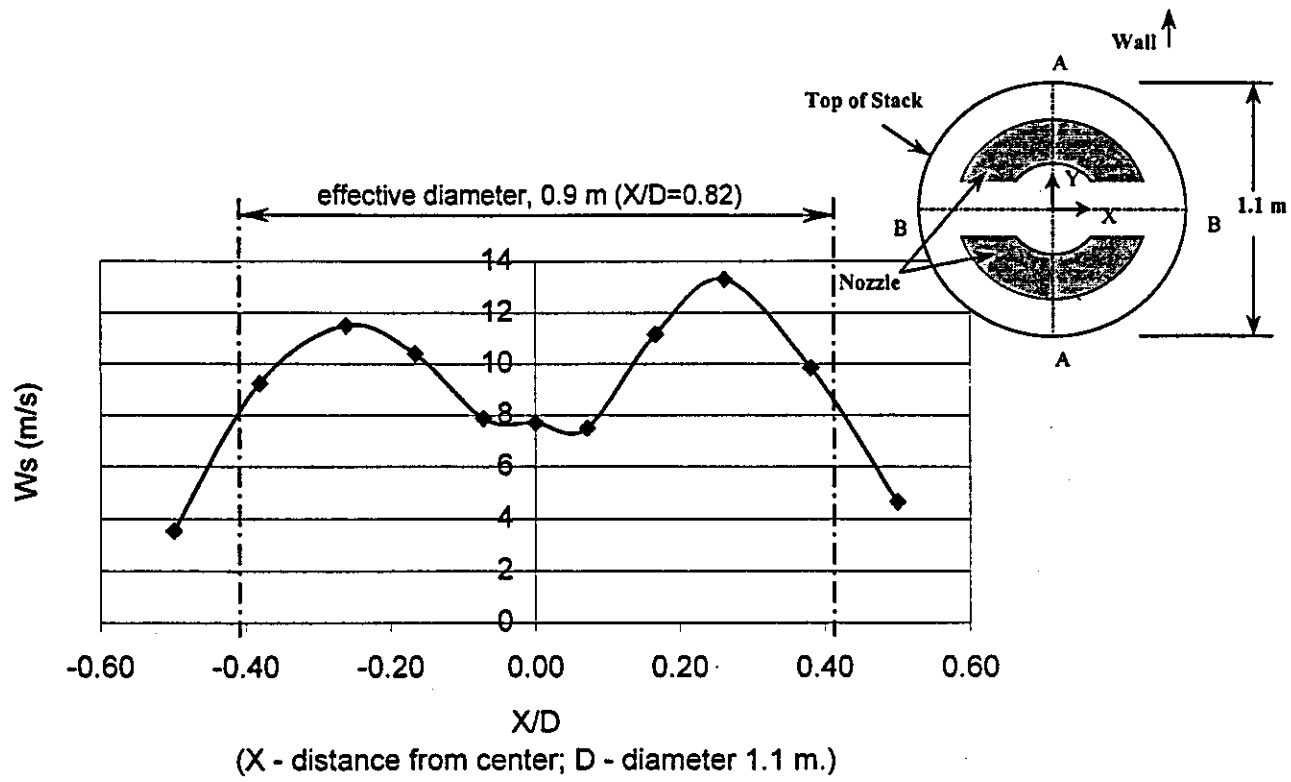


Figure 9 Exhaust velocity distribution at outlet of the BE Bldg. Stack.

Table 4 Exhaust parameters for Strobic Stack (BE Building)

Stack Parameter	
Height (h_s)	3.0 m
Outlet Diameter (d_s)	1.1 m
Effective Diameter	0.9 m
Effective Area (A_s)	0.64 m ²
Velocity (w_s)	8.1 m s ⁻¹
Flow Rate	5.2 m ³ s ⁻¹

As in the Hall Building tests, fifteen air samplers were used on the BE building. Locations of the stack and samplers are shown in Figure 10a; the relative heights of the stack and the rooftop structures are shown in Figure 10b. Due to variations in wind direction, the positions of the samplers were changed for each test and thus more than 15 sampler locations are indicated in Figure 10a. For example, smoke tests carried out before the 2nd test commenced showed that the plume was frequently brought down to the roof very close to the stack. Consequently, several samplers were relocated between the penthouse and the stack, as well as on the roof of the adjacent building to the northeast. The sampler numbers shown in Figure 10a do not correspond to the field samplers but instead indicate the locations of tappings on the wind tunnel model.

Usually, ten 15-minute samples were obtained at each location. However, in some cases, the bags did not fill due to improper connections with the pump. Also, some samplers did not work properly during the 3rd test due to cold temperatures ($T = -0.5$ °C).

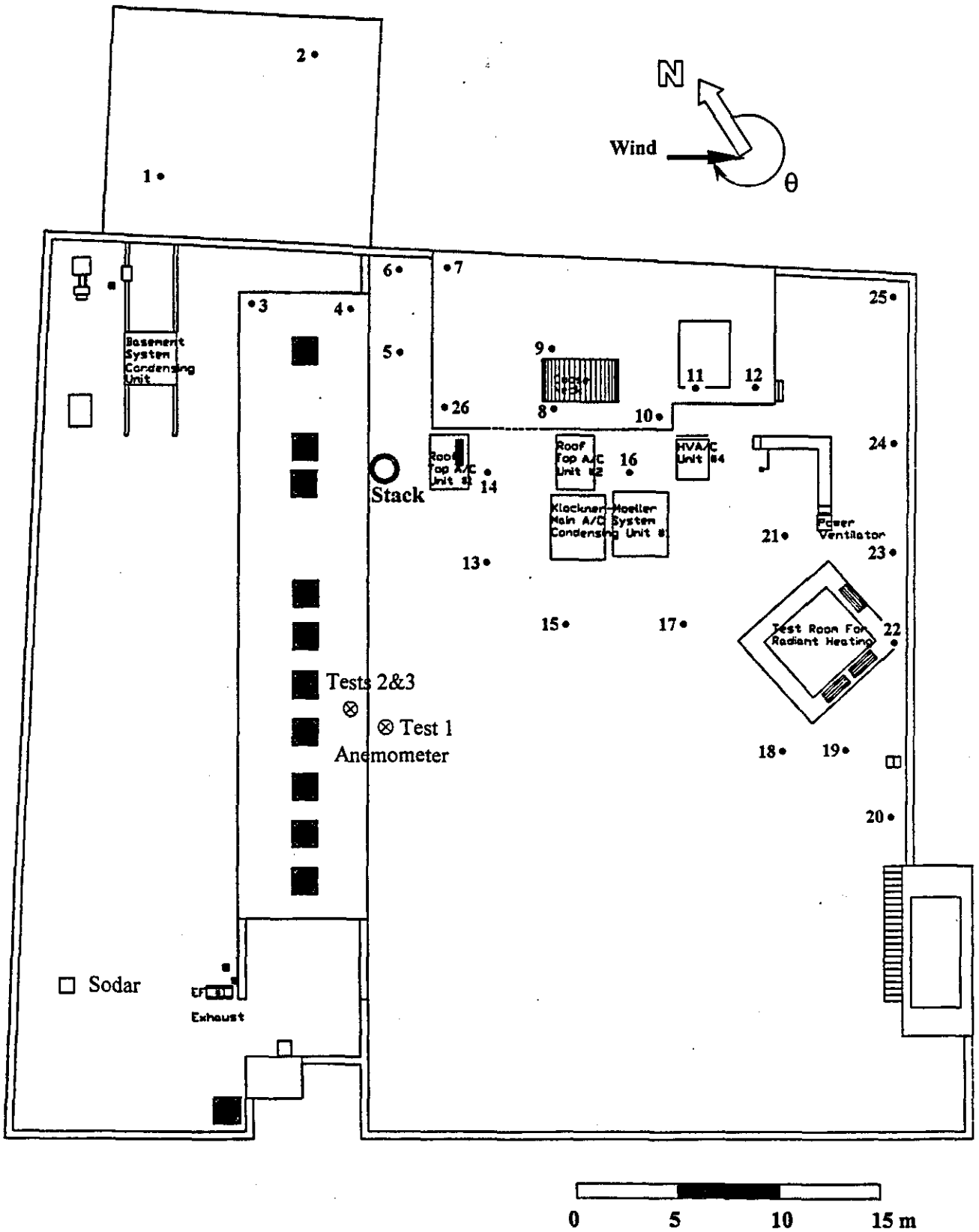


Figure 10a Plan view of BE Building showing locations of the stack, anemometer and sampling locations (numbers indicate wind tunnel model tappings)

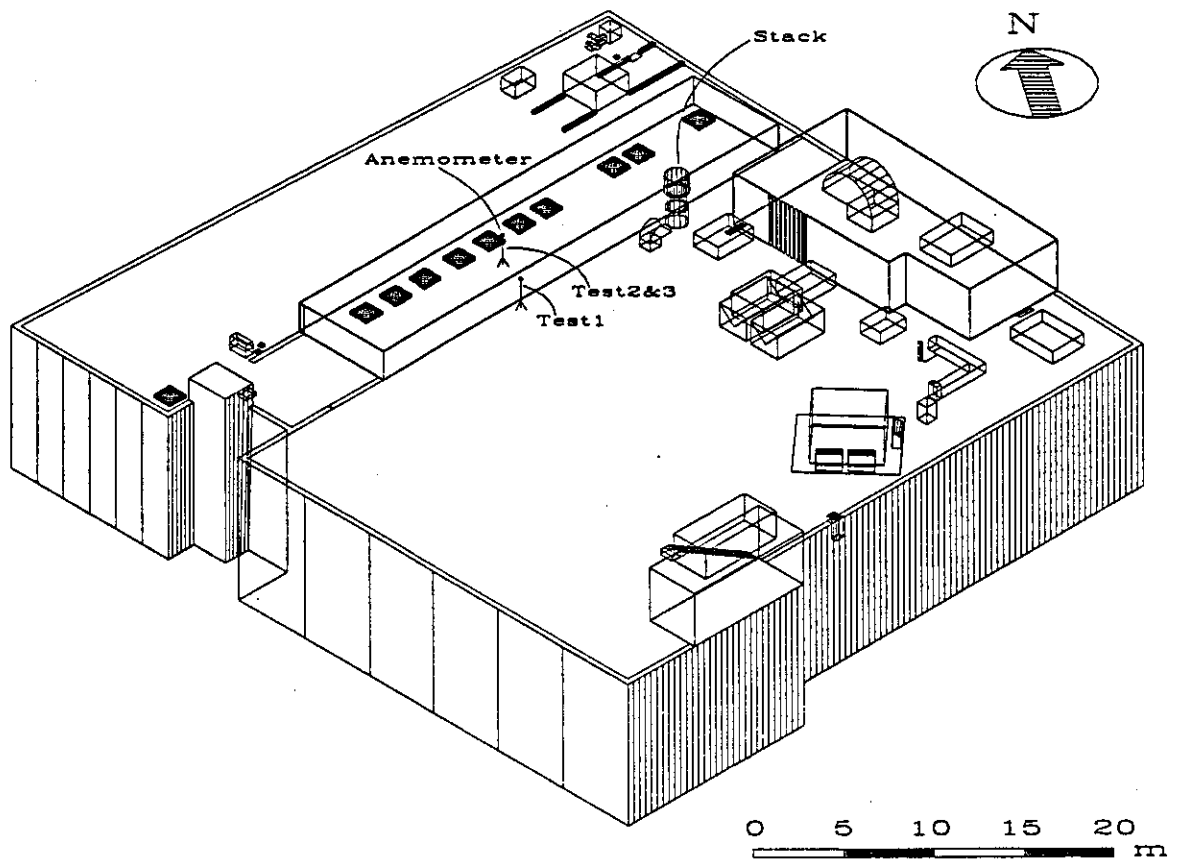


Figure 10b Perspective view of the BE Building showing relative heights of the stack and rooftop structures.

Sulfur hexafluoride was emitted into a fume hood in Building Aerodynamics Laboratory on the 2nd floor of the BE building. The concentration of SF₆ was monitored continuously using a Bruel and Kjaer gas analyzer through a sampling tube mounted on the stack. The outlet concentration was kept relatively constant throughout each test.

Wind speed and wind direction were measured with the Gill sonic anemometer. During the Oct. 1st test, it was mounted on a portable tower, approximately 4 m above the main roof. For the other two tests, it was placed nearby on a 3m stand on the skylight roof section. The location of the anemometer is shown in Figure 10a. During the October 1st test, wind data were also obtained with an acoustic wind profiler (sodar). The sodar was located on the northwest side of the building, as shown in Figure 10a.

3.3 Wind Tunnel Tests

3.3.1 Wind Tunnel Modelling Criteria

The boundary layer wind tunnel is ideal for evaluating near-field dilution of building exhaust. In general, exhaust from rooftop stacks is non-buoyant, so Froude number scaling is not necessary. Furthermore, critical plume concentrations tend to be associated with moderate to strong winds, since plume rise is usually minimal under these conditions. As a result, simulation of the neutrally stable atmospheric surface layer ASL is sufficient. With the above simplifications, the following criteria are important for wind tunnel modelling of near-field plume dilution [ASHRAE (1997)]:

- Geometric Similarity
- Similarity of wind tunnel flow with the ASL

- Building Reynolds number ($Re_b = UD/\nu$) $> 11,000$.
- Stack Reynolds number ($Re_s = w_s d_s/\nu$) > 2000 [to ensure turbulent exhaust]
- Equivalent stack momentum ratio ($M=w_s/U$)

where ν is kinematic viscosity of the air, D is the nominal building dimension and d_s is the stack diameter. The Reynolds number criteria may, in fact, be overly conservative. Castro and Robins (1977) found that the flow over a cubical model was independent of Reynolds No. for $Re_b > 4000$. Regarding the stack Reynolds number, Wilson and Chui (1985) note that the effect of a laminar exhaust flow on the dilution process is difficult to quantify. It is worth noting that minimum dilution models developed by Wilson and Chui (1987,1995) are based on wind tunnel experiments in which the exhaust flows were laminar.

As previously discussed, the accuracy of wind tunnel modelling of near-field dispersion of exhaust from rooftop sources has not been thoroughly investigated. One factor that must be considered when comparing field and wind tunnel data is the effect of averaging time on the field data.

As full-scale averaging time increases, mean concentration tends to decrease due to plume meander caused by turbulence and fluctuations in wind direction. Wind tunnels are only capable of modelling plume meander associated with small-scale turbulence since the walls constrain the flow in the lateral direction. Mean concentrations obtained in the wind tunnel are usually assumed to correspond to a full-scale averaging time of approximately 10 minutes [ASHRAE (1997)]. However, Wilson (1995) notes that this approximation is applicable for wind tunnels with a cross-wind dimension that is 10 times as large as the boundary layer thickness. Most wind

tunnels do not meet this criterion and thus may only be capable of simulating a full-scale averaging time of 1 to 5 minutes.

A recent comparison of wind tunnel data with field samples having an averaging time of 5 minutes showed that the wind tunnel may produce less plume dispersion than the atmosphere even for very short averaging times [Higson et al. (1994)]. Maximum wind tunnel concentrations obtained in this study were higher than those for the test building. Minimum wind tunnel concentrations, on the other hand, were lower than the field concentrations at corresponding locations. This indicates that the wind tunnel plume is more narrow than that produced in the atmosphere.

When the source and receptor are in the same recirculation region, as in the present study, the effects of averaging time are expected to diminish. ASHRAE (1993,1997) suggests that, in this case, dilution values obtained using a 3-min averaging time are applicable to averaging times of up to 1 hour.

3.3.2 Experimental Methodology

Wind tunnel experiments were carried out in the boundary layer wind tunnel at the Centre for Building Studies, Concordia University. Models of the Hall Building, BE Building and the surrounding buildings within a radius of 450 m were constructed at a scale of 1:500. Photographs of the wind tunnel models of both buildings with their surroundings are shown in Figure 11.

Steel tappings, which had an outside diameter of 1.2 mm were placed in the models at the

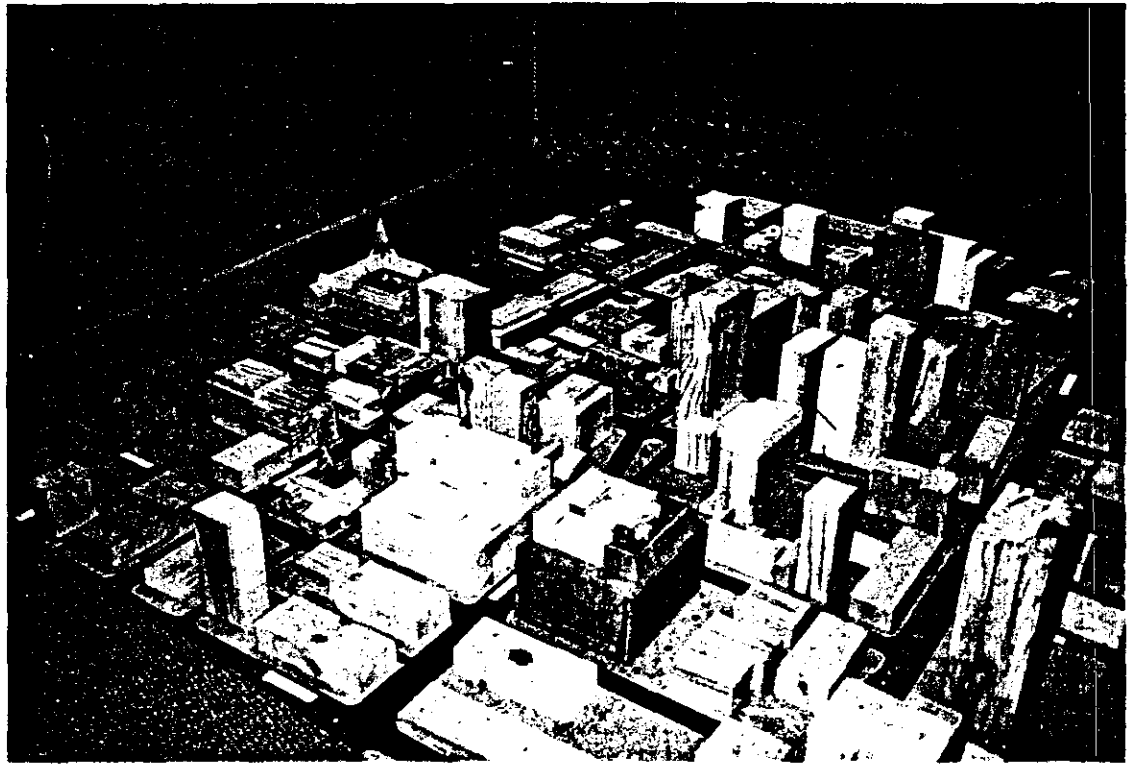


Figure 11a Wind tunnel model of the Hall Building.



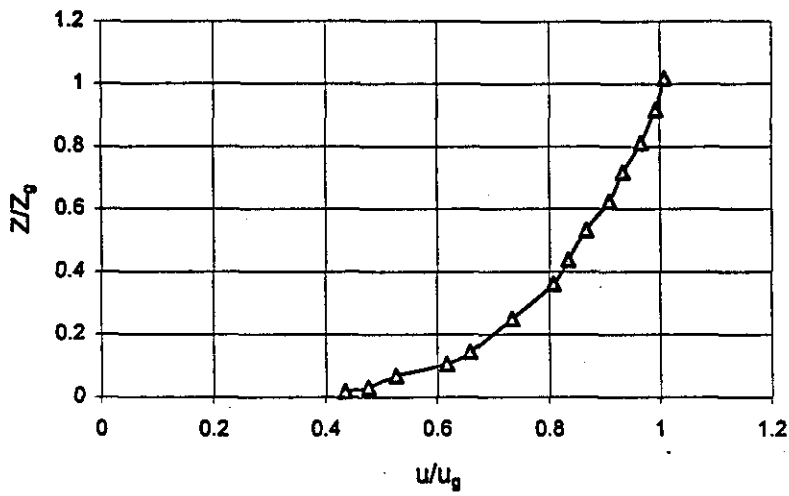
Figure 11b Wind tunnel model of the BE Building.

locations of the samplers in the field tests. The Hall Building model had 16 tappings; the BE model had 26 tappings. Locations of tappings on the Hall and BE Buildings are shown in Figure 6 and Figure 10a, respectively.

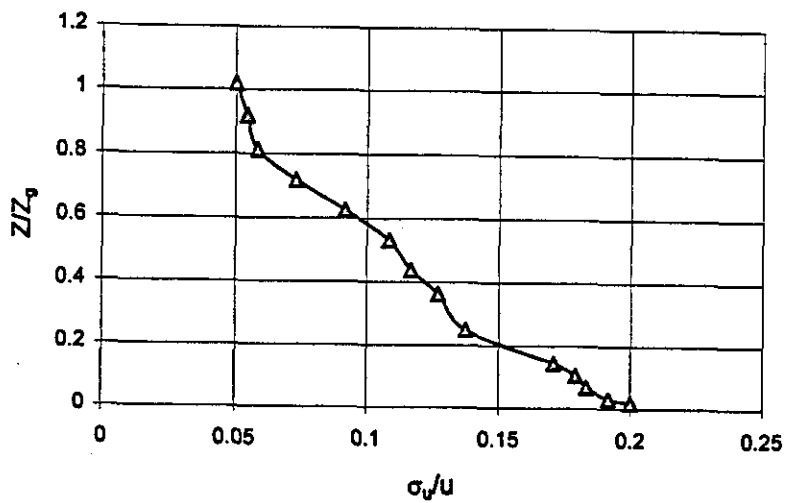
A suburban exposure, with a power law exponent (α) of 0.25, was used to simulate the atmospheric boundary layer that exists far upwind of the test section. The transition to an urban type boundary layer at the test section is simulated using the models of the surrounding buildings. Vertical profiles of mean velocity and turbulence intensity are shown in Figure 12. It should be noted that the boundary layer simulation corresponds to neutral atmospheric stability.

No attempt was made to model the influence of Mt. Royal on the results because of the difficulties in constructing the hill profile for a variety of wind directions. The hill is not expected to have a significant influence on the results obtained with either test building. Regarding the Hall Building tests, the hill was not upwind and so its effects should be minimal. The terrain effects may be more significant for the BE Building since the hill was upwind for these tests. However, it is assumed that the tall buildings near the BE building will have a much greater influence than the hill on plume behavior.

A key parameter for modelling plume rise is the exhaust momentum factor, M , which is the ratio of exhaust speed to wind speed. The experiments were carried out by adjusting the exhaust flow rate and wind speed to match the value of M obtained in the field study. The reference wind speed, U_{br} , was measured at the location of the anemometer on each test building. Since this



a) mean wind velocity profile



b) turbulence intensity

Figure 12 Vertical profiles of mean wind velocity and turbulence intensity obtained with a suburban exposure in the CBS boundary layer wind tunnel.

location is above the height of the exhaust stacks, the reference wind speed may have been higher than the wind speed at stack height. This was especially true for the Hall Building stack, which was located in the flow recirculation zone. Likewise, turbulence intensity measured at the reference height was probably lower than the value near the stacks.

Sulfur hexafluoride (SF_6) was used as the tracer gas for the wind tunnel experiments. A certified mixture of SF_6 and nitrogen was emitted from a model stack and the mean concentration of SF_6 at air intakes was measured using a Varian gas chromatograph. Samples of air were collected via plastic tubes which were attached to steel tappings on the model surfaces. At each tapping, five samples were collected over a period of 2 minutes to obtain stable estimates of mean concentration. The measurements were generally repeatable to within $\pm 10\%$. Tracer gas concentrations were obtained at receptors on the roof of the building model.

Mean wind speed and turbulence intensity were measured with a TSI hot film anemometer. The values of w_s and M were varied by precisely controlling the flow emitted from the stack. Because of the small diameters of the model stacks (d_s), the stack Reynolds number, usually did not exceed the critical value of 2000 required to ensure turbulent flow. Values of Re_s depend on the value of M , which was varied from 1.0 to 3.0 for the Hall tests and from 2.0 to 4.0 for the BE Bldg. Furthermore, for a given M value, the exhaust velocity will vary depending on the wind direction. For the Hall Building tests, stack Reynolds number varied from 400 to 1800 compared to the full-scale value of 5.7×10^5 . For the BE Building tests, Re_s varied between 500 and 1900 compared to the full-scale value of 5.5×10^5 . In the present study, relaxation of the Reynolds number criterion

is not expected to affect the results since the plumes should be dominated by building-generated and atmospheric turbulence even very close to the stacks.

4. Results

Results of the Hall Building and the BE Building studies will be presented separately. In each case, data obtained in the field tests will be discussed and compared with the previously described dispersion models. Comparison of the field data with wind tunnel results will follow.

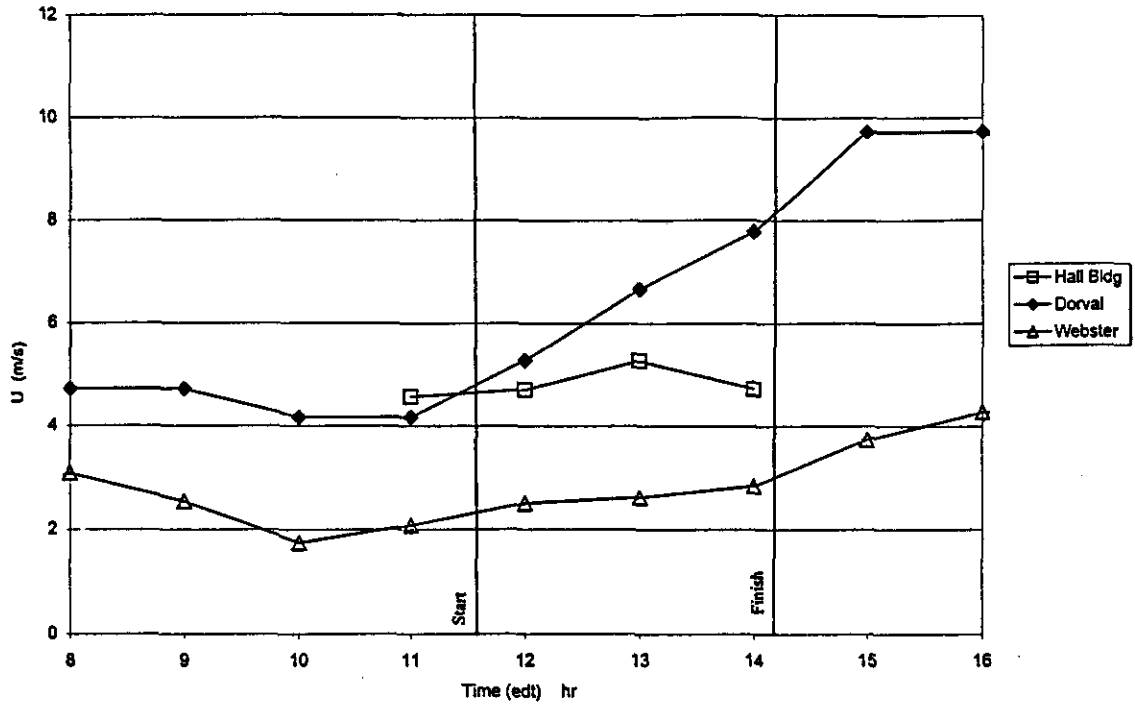
4.1 Hall Building

4.1.1 Field Study

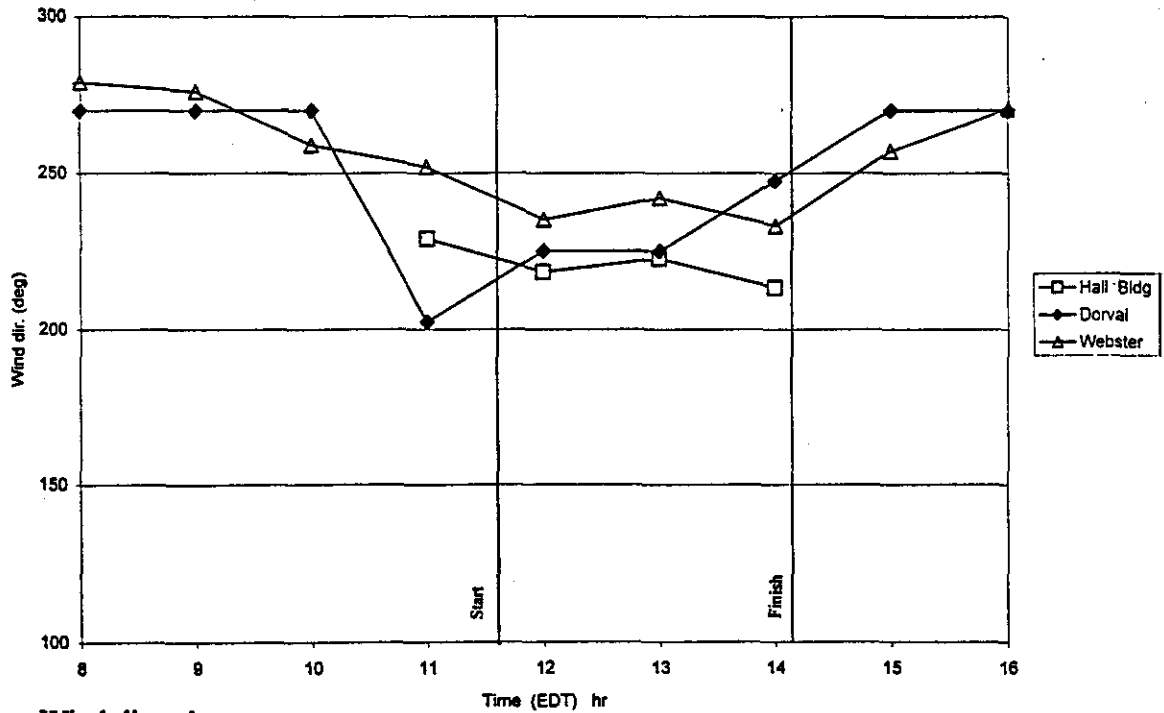
As discussed previously, field tests were carried out on June 26, July 2, July 30 and August 7, 1998; except for the July 2 test, the experiments were carried out in similar wind conditions.

Figures 13-16 show wind speed and direction data obtained on the roof of the building during tests 1 to 4, respectively. Also shown are data obtained at Dorval Airport and by the Webster Library anemometer.

Assuming the Hall anemometer is not influenced by nearby buildings or topography, differences between Hall wind speeds and Dorval speeds are due to differences in upstream roughness and measurement height at the two locations. Wind speeds generally increase with height in the boundary layer; an increase in upwind roughness, on the other hand, will reduce the wind speed at a given height. Thus, by taking into account these two factors, the Dorval data can be used to estimate wind speeds at the height of the Hall anemometer. The correction factor to apply to the

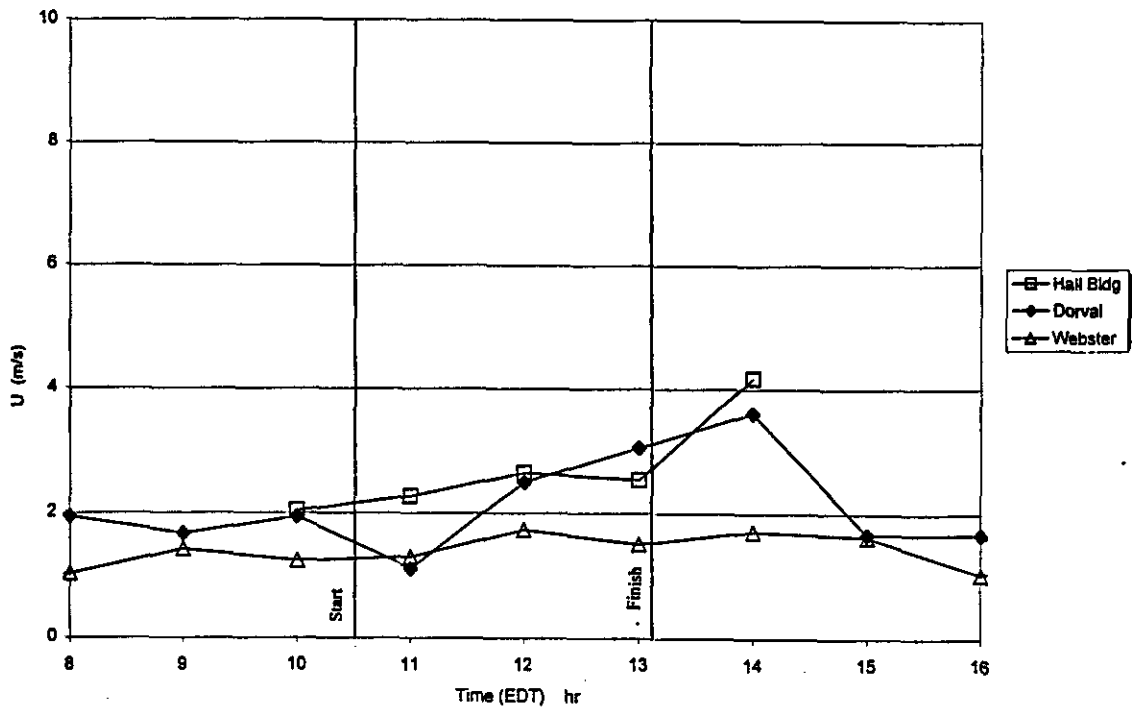


a) Wind speed

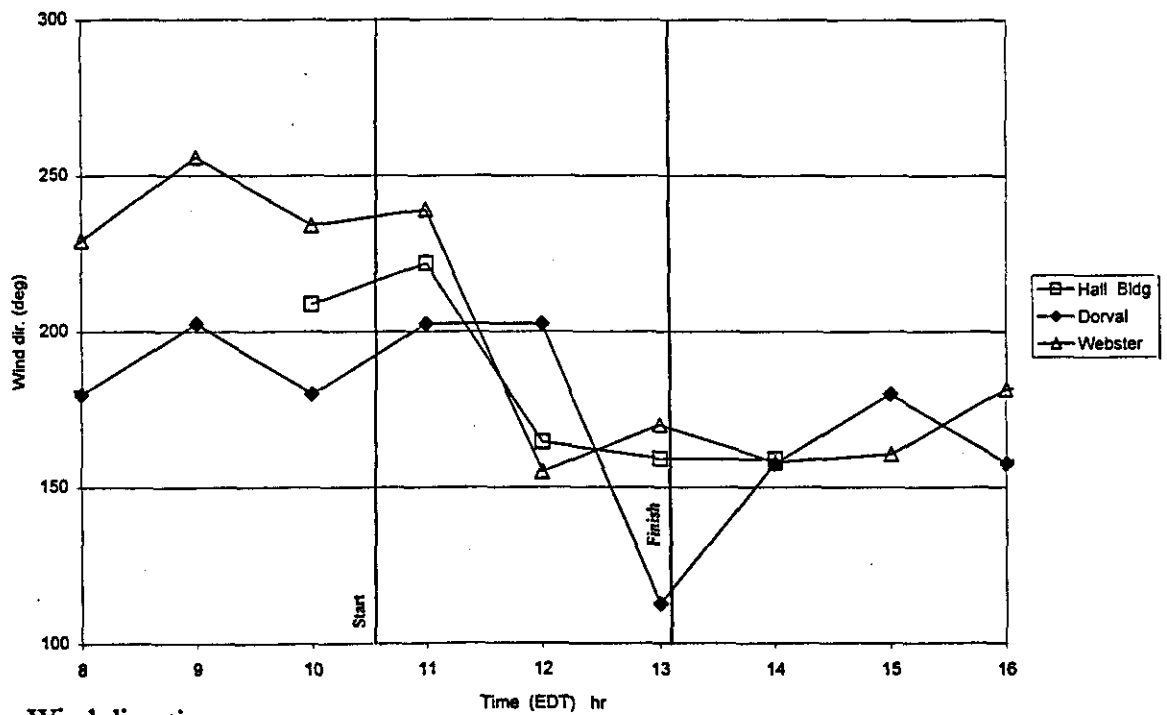


b) Wind direction

Figure 13 Wind data obtained during Hall Building Test No. 1 (June 26, 1997).

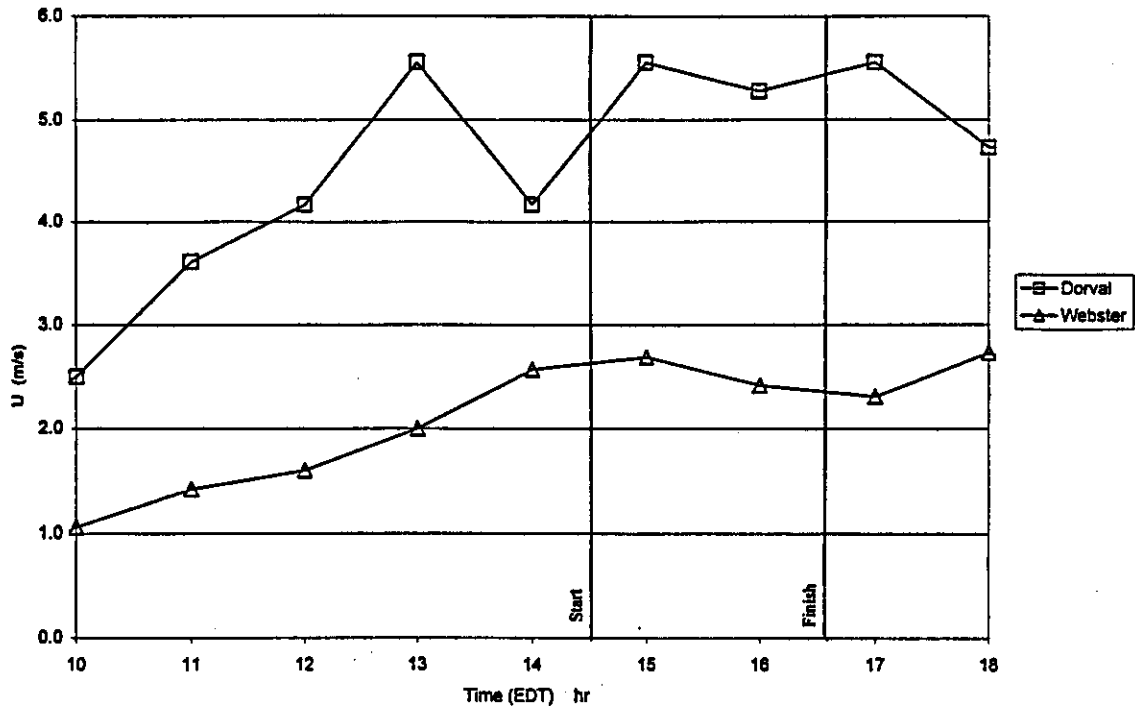


a) Wind speed

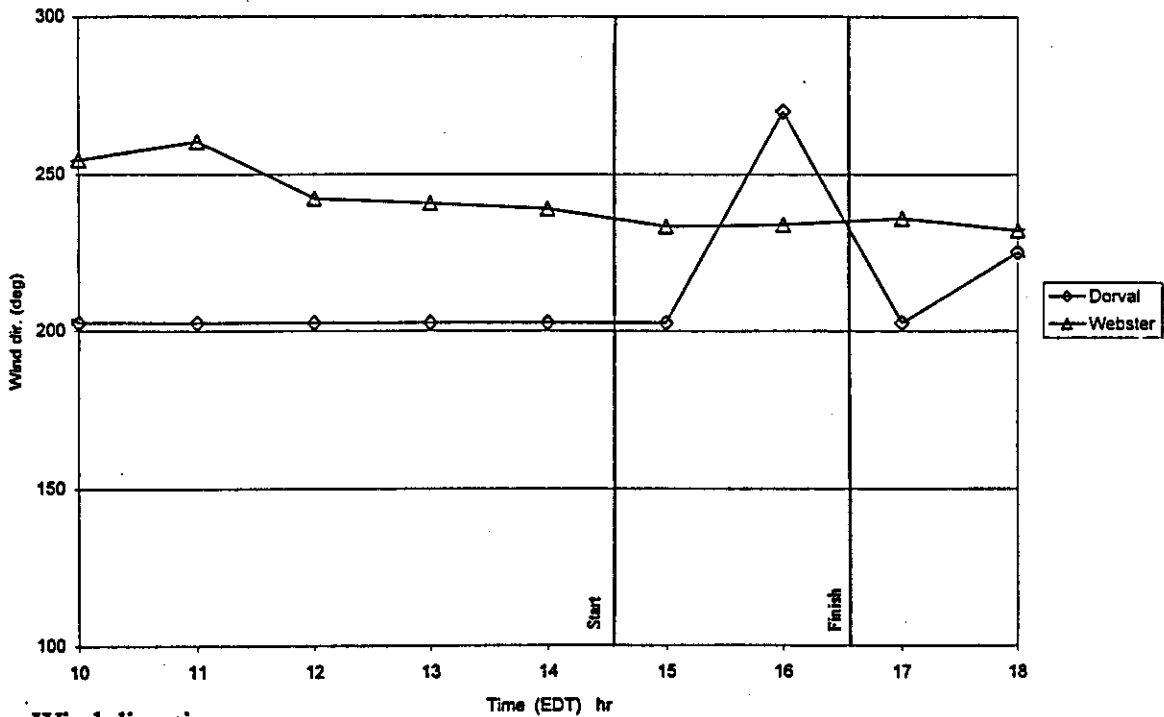


b) Wind direction

Figure 14 Wind data obtained during Hall Building Test No.2 (July 2, 1997).

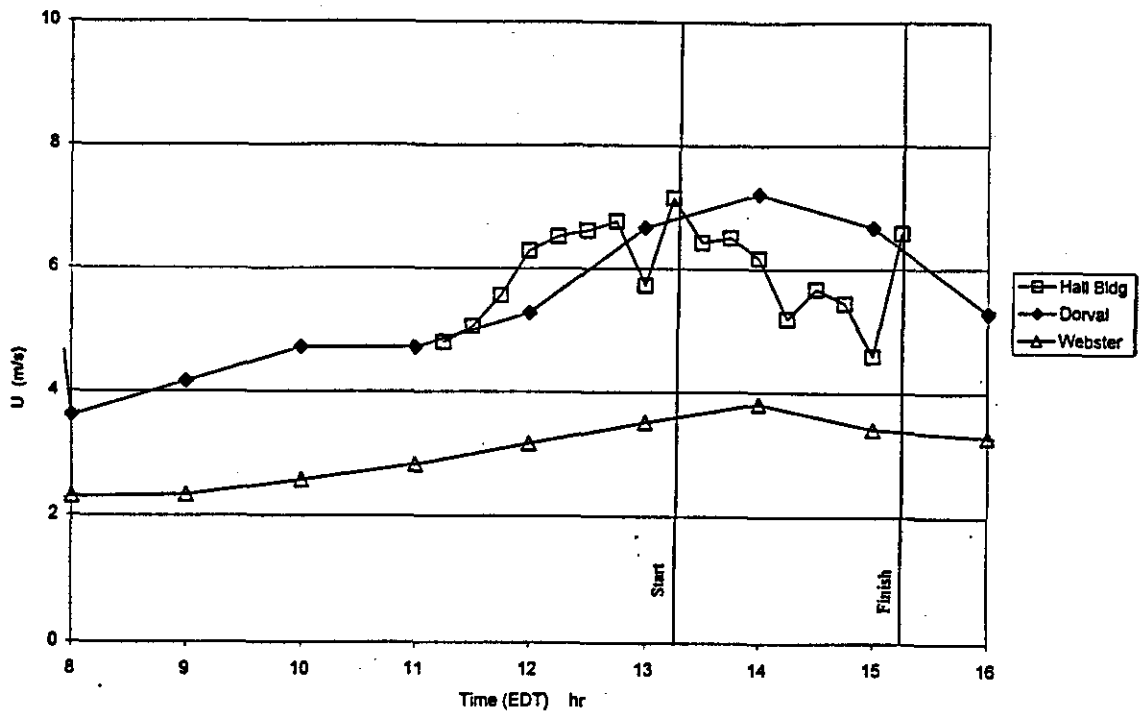


a) Wind speed

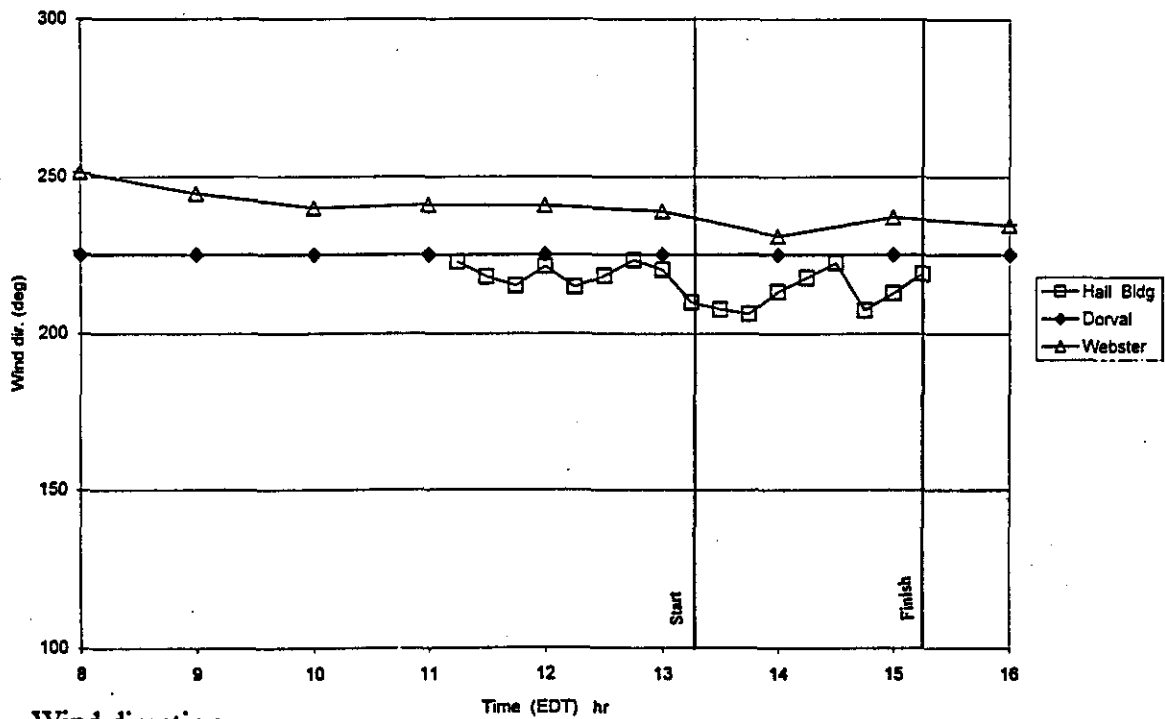


b) Wind direction

Figure 15 Wind data obtained during Hall Building Test No. 3 (July 30, 1997).



a) Wind speed



b) Wind direction

Figure 16 Wind data obtained during Hall Building Test No. 4 (August 7, 1997).

Dorval data is:

$$U_{\text{Hall}}/U_{\text{Dorval}} = (Z_{\text{goc}}/Z_{\text{Dorval}})^{0.15} (Z_{\text{Hall}}/Z_{\text{gurb}})^{0.28}$$

$$U_{\text{Hall}}/U_{\text{Dorval}} = (300/10)^{0.15} (70/500)^{0.28} = 0.96$$

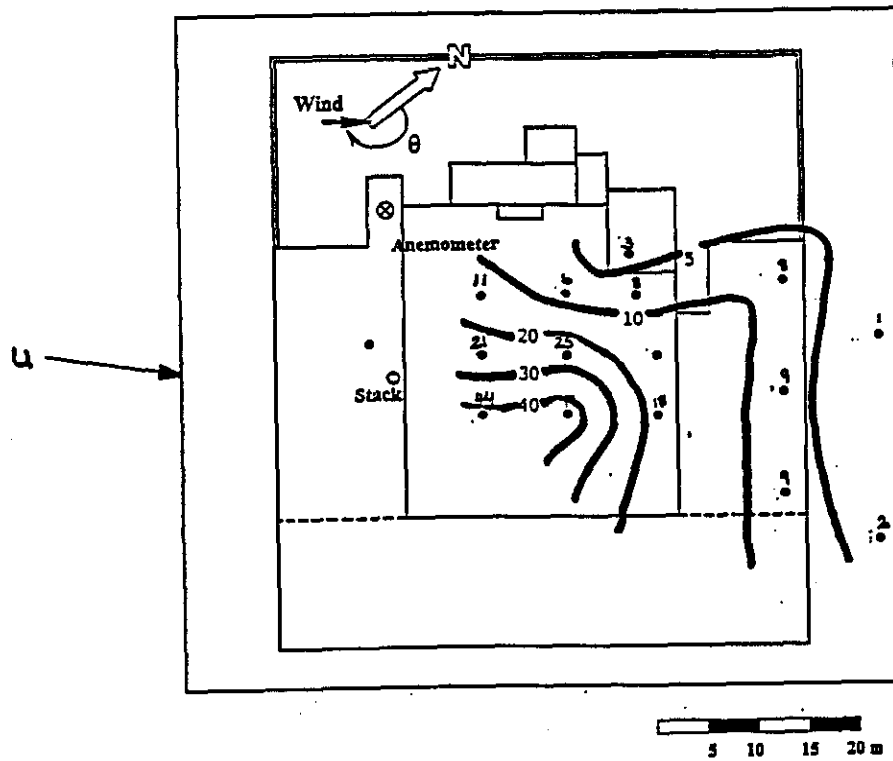
where Z_{goc} is the height of the atmospheric boundary layer (ABL) for open country terrain and Z_{gurb} is the ABL height for urban terrain. Thus, wind speeds at the Hall Bldg. should be approximately equivalent to Dorval wind speeds and the data generally confirm this. However, it should be noted that this is true only when no nearby large obstructions exist upwind. The data obtained on June 26 indicated that the wind speed increased at Dorval when the direction shifted from SW to W. The Hall Building anemometer did not record an increase in U during this period, probably due to the presence of Mt. Royal upwind.

The wind speed at the Webster Library is lower than expected for an elevation of 51 m. In the unobstructed flow, the wind speed should be $0.88U_{\text{Dorval}}$ at this elevation. However, the actual ratio of U_{Web} to U_{Dorval} is only 0.5 approximately. This is largely due to the low height of the anemometer above the roof (3 m) and the presence of upstream buildings.

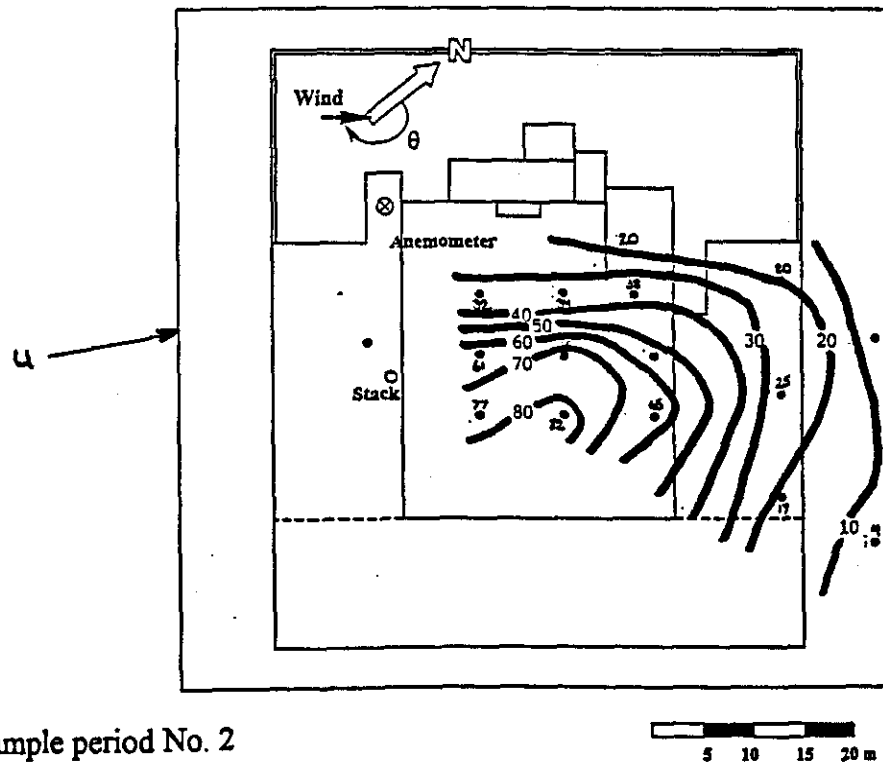
Concentration data are usually converted to dilution values to allow comparison between tests.

However, if the outlet concentration remains constant, the sampler data can be compared directly.

Concentration distributions for two typical sample periods, No. 1 and No. 2 on June 26, are shown in Figure 17. Values of C obtained in sampling period No. 2 were approximately 3 times higher than those obtained in sampling period No. 1, at all rooftop locations. For example, at tapping 5, in the center of the roof, C increased from 25 ppb for sample 1 (Fig. 17a) to 75.5 ppb



a) Sample period No. 1



b) Sample period No. 2

Figure 17 Concentrations (ppb) obtained in sample periods 1 and 2 of Hall Test No. 1.

for sample 2 (Fig. 17b). The higher concentrations obtained in sampling period No. 2 may be due to an increase in stack momentum ratio, M . As will be discussed, slight variations in M can produce large changes in concentration at rooftop receptors.

High correlation between samplers is evident, suggesting that fluctuations in the 15-min. average concentration are due mainly to variations in the frequency of wind gusts during the sampling period. A gust brings the plume down to roof level and thus, increases the instantaneous concentration at each location. The mean concentration will tend to increase with the frequency of gusts. Smoke tests carried out during another test showed that the plume trajectory varies significantly over the 15-min sampling period. The plume rise varied from 1 m to more than 10 m and the plume made frequent excursions upwind.

It is convenient to express the tracer gas concentrations in terms of dilution, $D=C_r/C$, since design formulas provide estimates of D . Dilution data obtained during Test 1 (June 26) are plotted in Figure 18 as a function of distance from the stack. Also plotted are minimum dilution curves obtained using the H, WC and WL models. For the H model (Eq. 1), the parameter α was set equal to 2.0, as recommended for rooftop receptors [ASHRAE (1993), Halitsky (1990)]. For the WL model, the value of B_1 depends on the level of atmospheric turbulence, σ_θ , at the building height. Based on the turbulence measurements during the tests 1, 2 and 4, σ_θ is assumed to be approximately 20° . Thus, from Eq. 6, a value of $B_1 = 0.069$ is used for the WL model.

The exhaust momentum ratio, M , is required as input to the WC and WL dilution models to

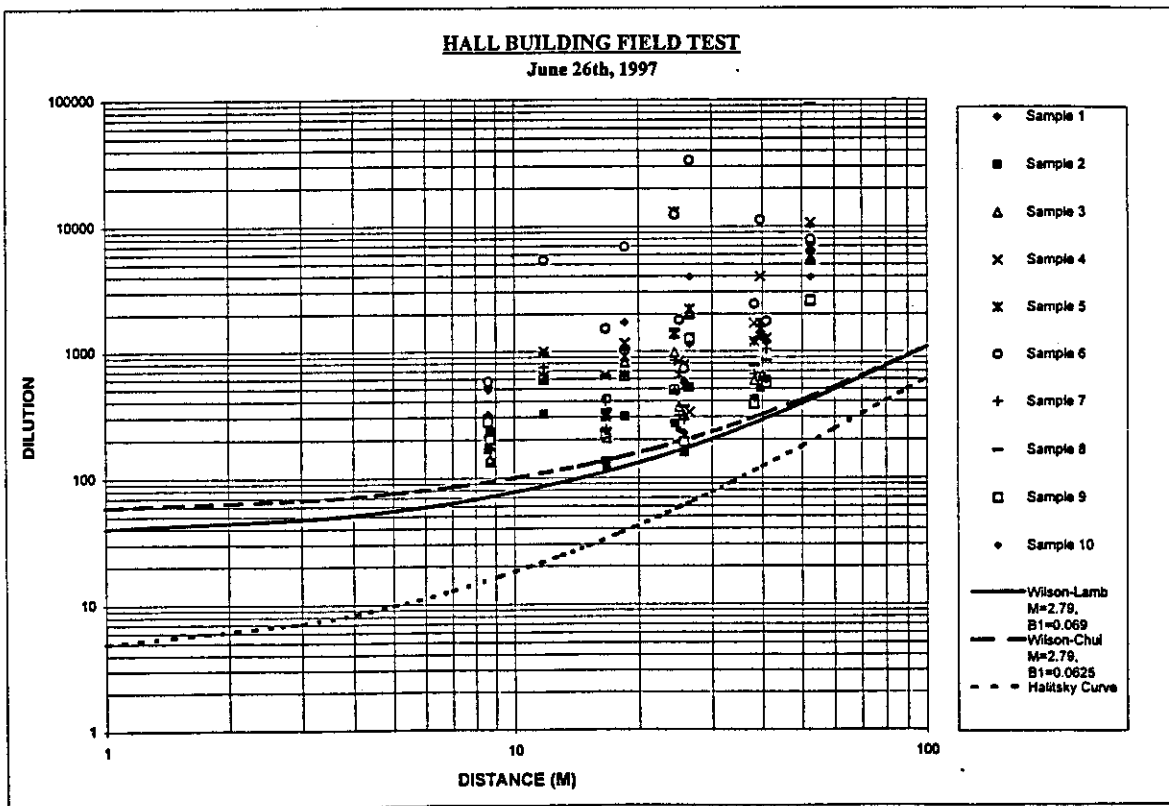


Figure 18 Dilution data obtained at all samplers during Hall Test No. 1 compared with ASHRAE minimum dilution curves.

obtain the initial dilution and distance dilution (see Eqs. 3, 4 and 7). In this case, the average M value for the entire test period ($M=2.79$) was used to plot the D_{\min} curves in Figure 18. Note, however, that M values for the 15-min samples varied from 2.43 to 3.24.

Figure 18 shows that both the WC and WL models predict D_{\min} well for Test 1, as most of the measured dilutions are above the model predictions. In comparison, the H model is conservative since it underpredicts D_{\min} at rooftop locations by factors of 2.5 to 8. The H model could provide more accurate prediction of D_{\min} if α was increased from the recommended value of 2.0 – see Section 2.1.1 – to a value of 5.0, say. However, a building designer will generally not have a priori knowledge of the “correct” value of α .

Dilution data obtained during Test 4 (August 7) are shown in Figure 19 and are generally similar to data for Test 1. The WC and WL models provide accurate estimates of D_{\min} while the H model underpredicts minimum dilution values by at least a factor of 3. The similarity in results of Test 1 and Test 4 may be due to similar M values. The exhaust momentum ratio in Test 4 varied between 2.41 and 3.35 and the average value of M of 2.72 was almost identical to that in Test 1.

It should be noted that Test 4 was carried out with sampler No. 3 approximately 4.5 m upwind of the stack, as shown in Figure 6. The sampler was moved to this location at the start of the test after a smoke test revealed that the plume made frequent excursions in the upwind direction. The low values of D obtained with sampler No. 3 ($170 < D < 280$) show that, for this building geometry, reingestion of stack exhaust may be significant even if the air intake is upwind.

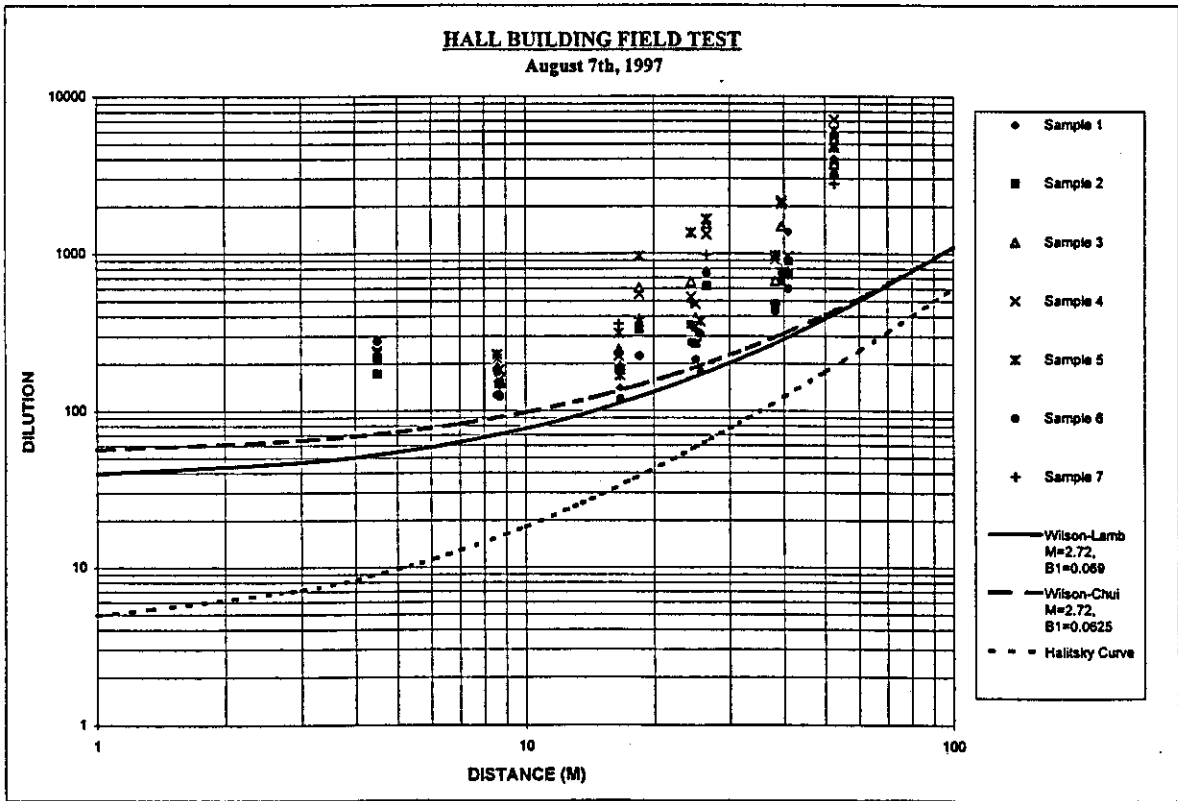


Figure 19 Dilution data obtained at all samplers during Hall Test No. 4 compared with ASHRAE minimum dilution curves.

Dilution data for Test 2 (July 2), obtained during low wind conditions, are shown in Figure 20.

The momentum ratio varied between 4.42 and 9.5; the average M value of 6.46 was used to plot the WC and WL D_{\min} curves. In this case, minimum dilution estimates obtained with the WL and H models are well below the measured values, with the H model being always more conservative. On the other hand, some of the dilution data fall below the WC D_{\min} curve.

The overprediction of dilution by the WC model is due to the high M -value, which produces an unrealistically high value for initial dilution. Note that the initial dilution obtained from Eq. 3 is 293, which is very close to dilutions obtained at a significant distance ($S = 37$ m) from the stack. Considering that distance dilution should be relatively large for $S > 30$ m, it is clear that the WC model overestimates the D_0 component of total dilution when M is large.

It should also be noted that, for all three models, the discrepancies between measured and predicted D may be partly due to large changes in wind direction that occurred during Test 2. During some sample periods, the wind direction deviated significantly from the critical direction.

Minimum dilution data obtained during Test 3 (July 30) were lower by a factor of 2 than data obtained during the other tests. Dilution measurements for this test are shown in Figure 21 along with the minimum dilution curves obtained with the three models. In this case, the WC and WL models tend to overpredict D_{\min} by a factor of two while the H model is moderately conservative. The reason for the low dilution measurements is not clear, although wind tunnel results to be discussed in the next section, suggest that the wind direction and/or momentum ratio may have

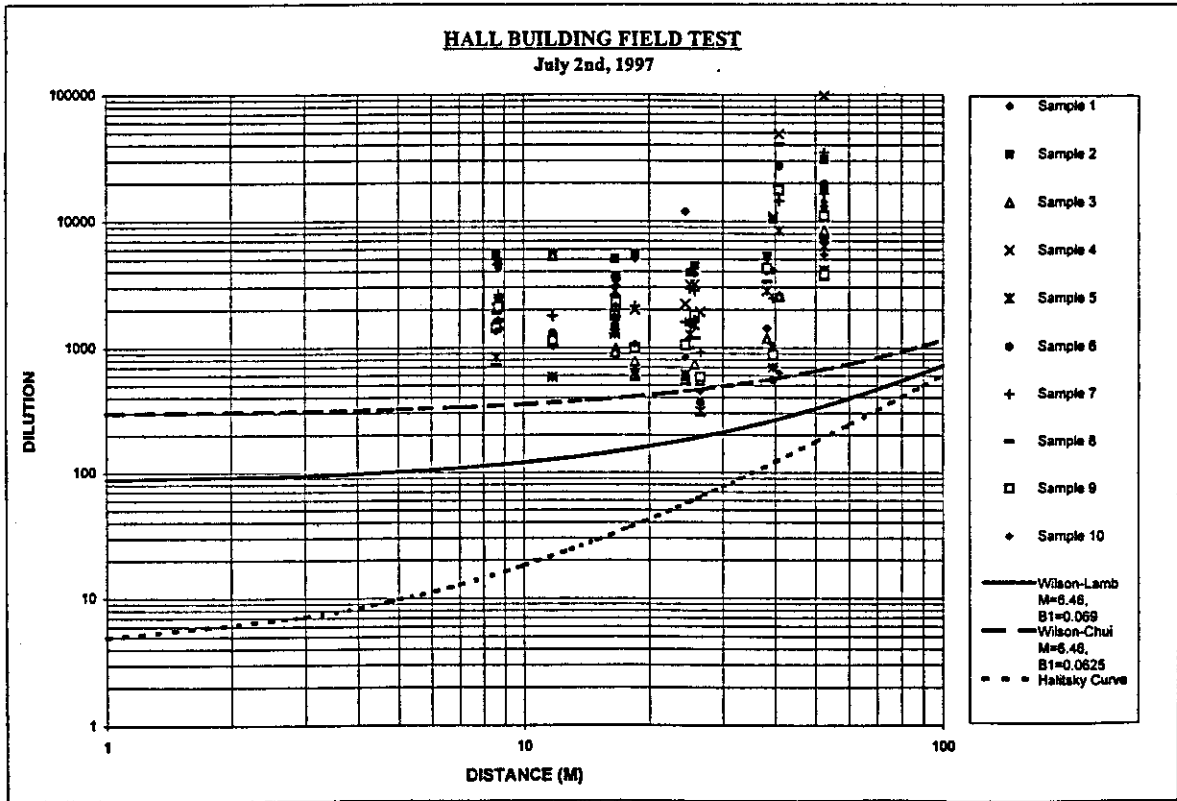


Figure 20 Dilution data obtained at all samplers during Hall Test No. 2 compared with ASHRAE minimum dilution curves.

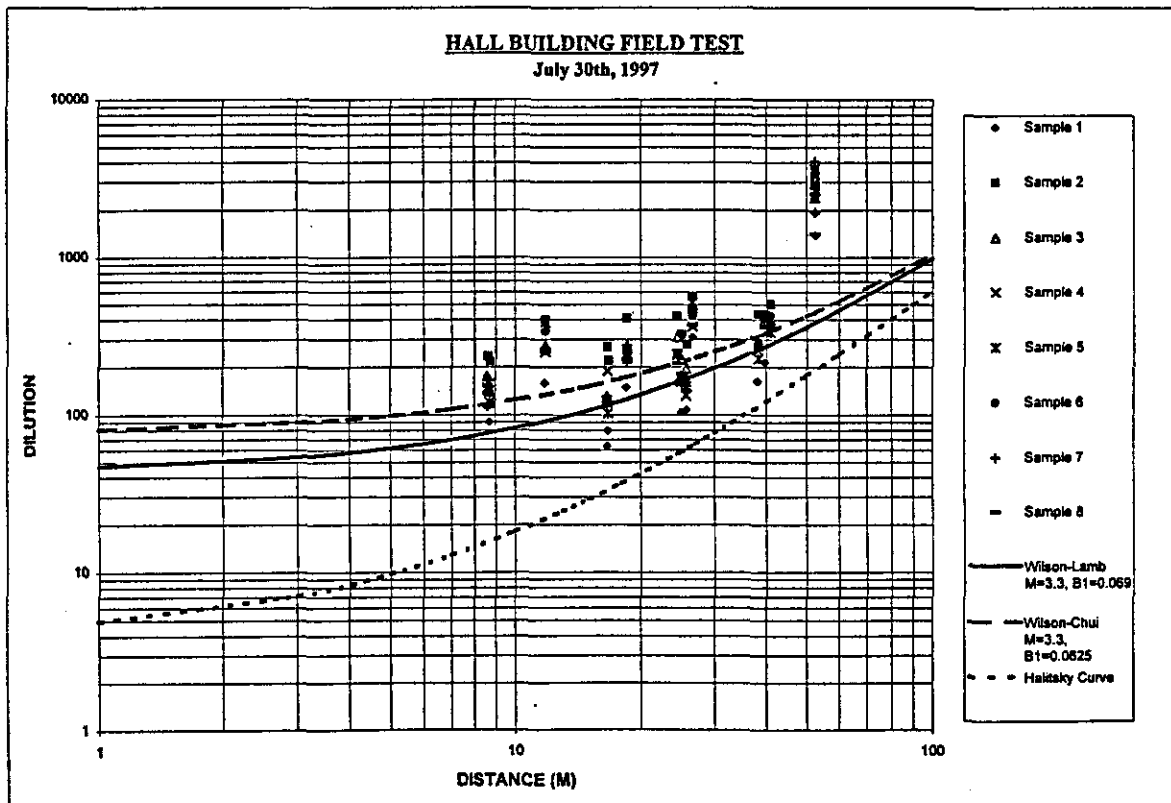


Figure 21 Dilution data obtained at all samplers during Hall Test No. 3 compared with ASHRAE minimum dilution curves.

been critical in this case. Although wind data was not available from the Hall Building anemometer, data from Dorval Airport indicate that winds were from SSW at the beginning of the test when the lowest dilution values were obtained. On the other hand, winds were generally from the SW during the other high wind tests (Tests 1 and 4).

Prior to discussing the wind tunnel data, a brief description of the time variation of the full-scale data may be beneficial. Dilution time series obtained with each sampler during the four tests are shown in Figures 22 to 25. One of the most striking characteristics of the time series plots, in general, is that the correlation between samplers is very high. Low dilution values at a particular sampler tend to coincide with low dilution at most of the other samplers, regardless of location. For example, Figure 22 shows that in Test 1, a minimum was recorded at most locations in sample period no. 2. Likewise, Fig 24 shows that in Test 3, low dilution values for the 1st sample were followed by higher D values for the 2nd sample at each location. Thus, it appears that variations in plume trajectory (e.g. plume rise, % of time plume travels downwind, etc.) tend to affect all downwind locations in a similar way.

More evidence of this is provided in Figure 25 which shows dilution data for Test 4. In this test, sampler no. 3 was moved upwind of the stack and thus, it may be expected that data for this sampler would show a negative correlation with data from the other samplers. Although dilution values were relatively stable throughout the test, a minimum occurred in period no. 6 at most locations. However, at location no. 3, the **maximum** dilution was recorded during period no. 6, indicating the plume made fewer excursions upwind during this 15-min interval.

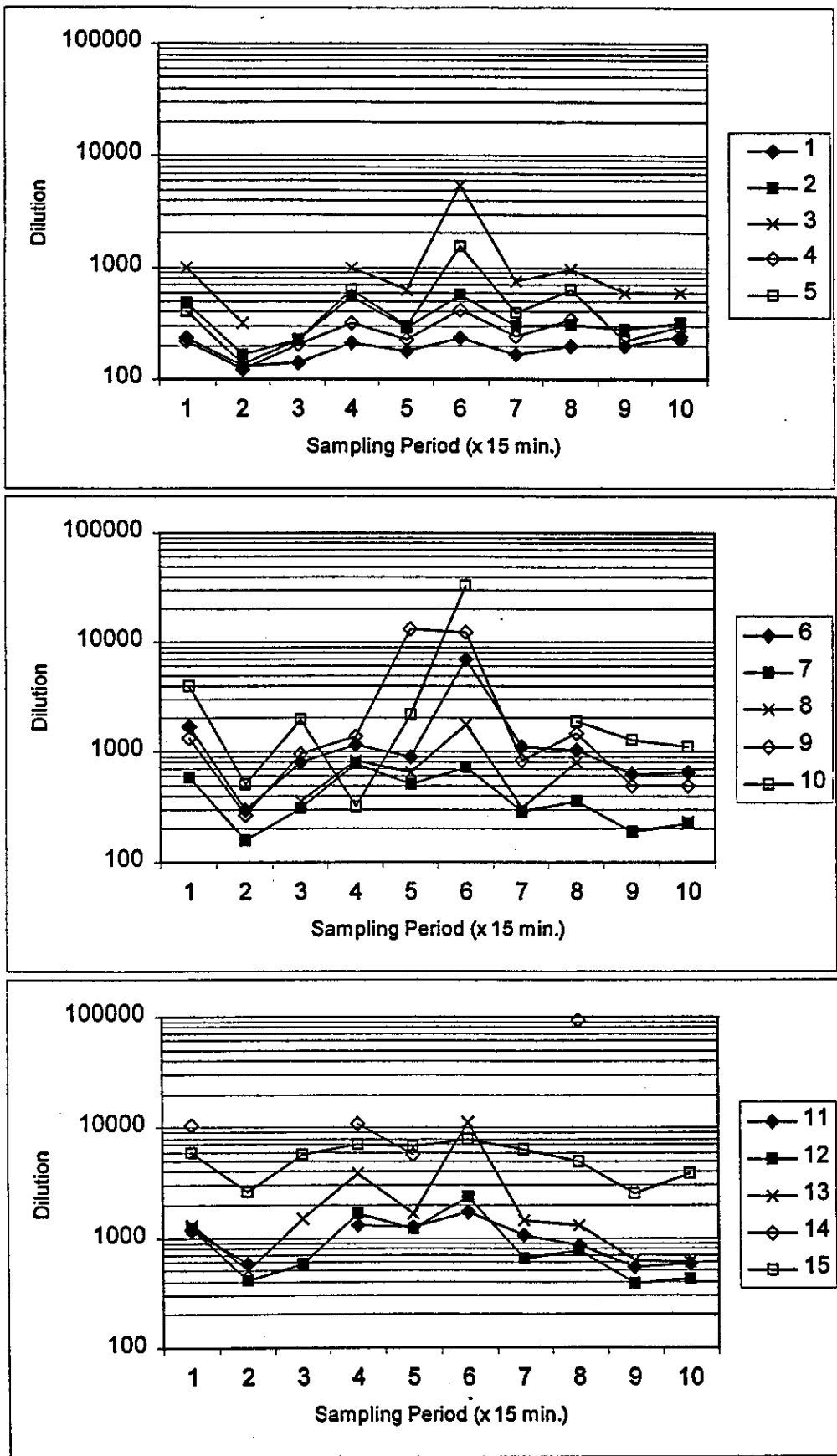


Figure 22 Variation of dilution with time during Hall Test No. 1, June 26th 1997

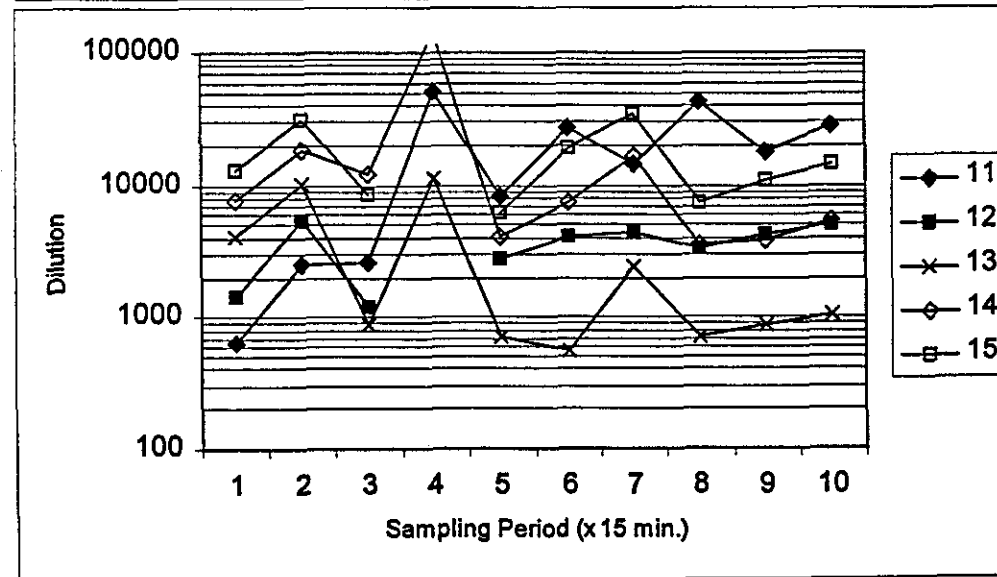
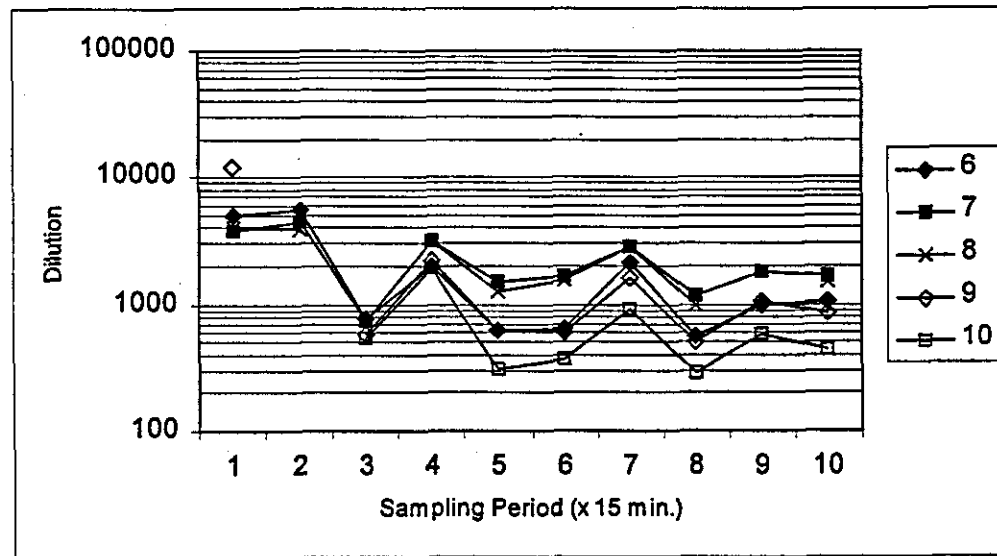
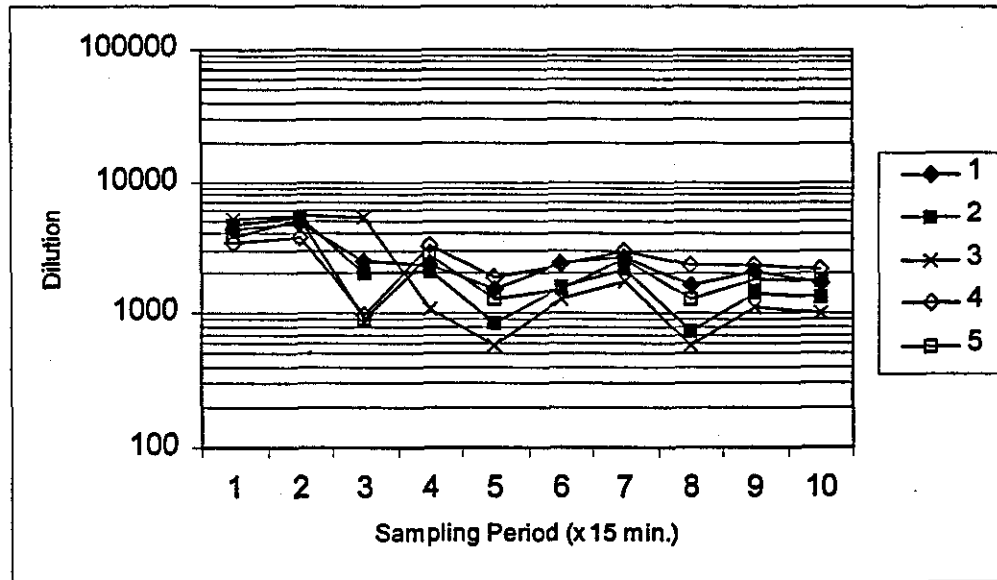


Figure 23 Variation of dilution with time during Hall Test No. 2, July 2nd 1997

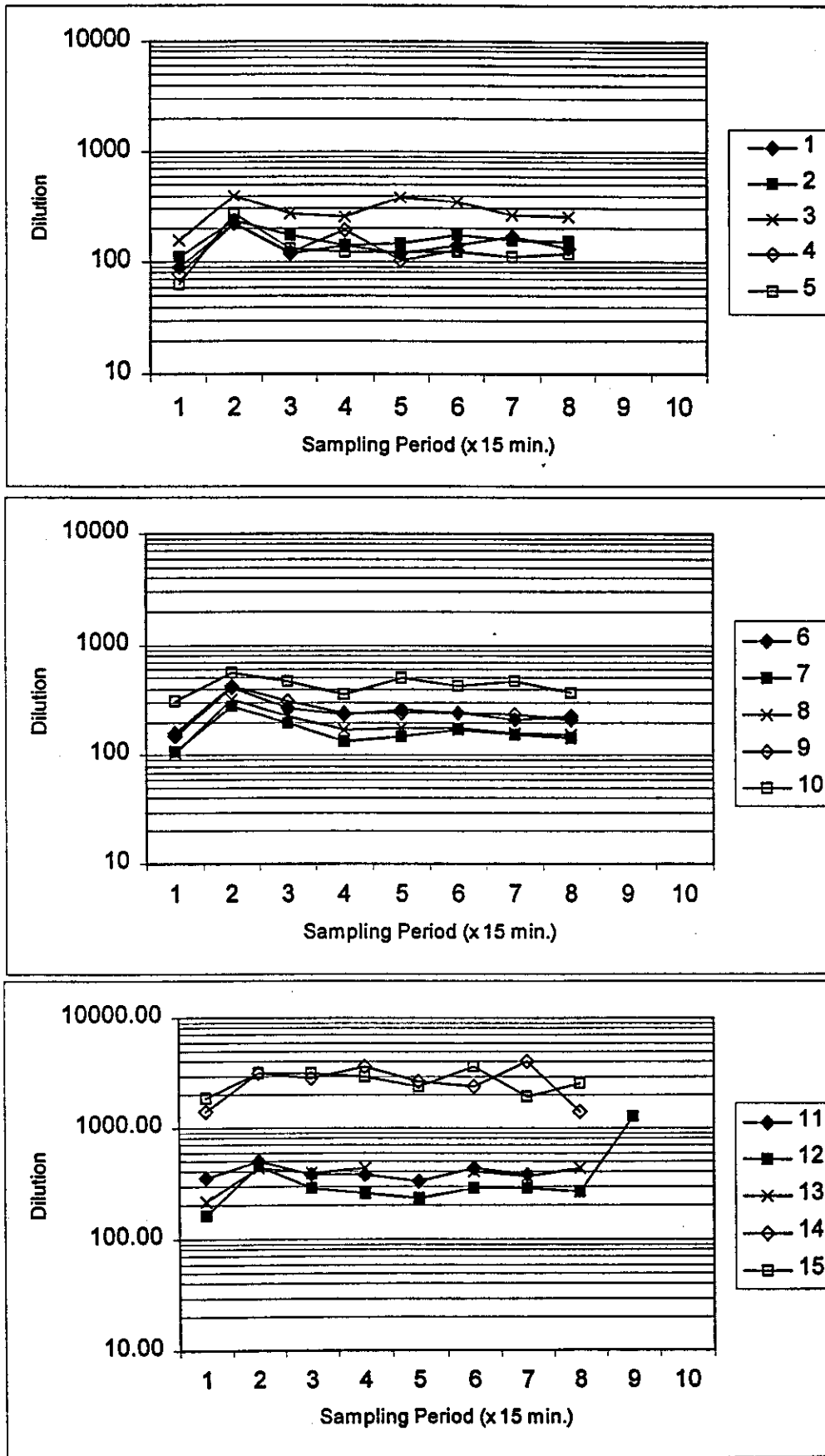


Figure 24 Variation of dilution with time during Hall Test No. 3, July 30th 1997

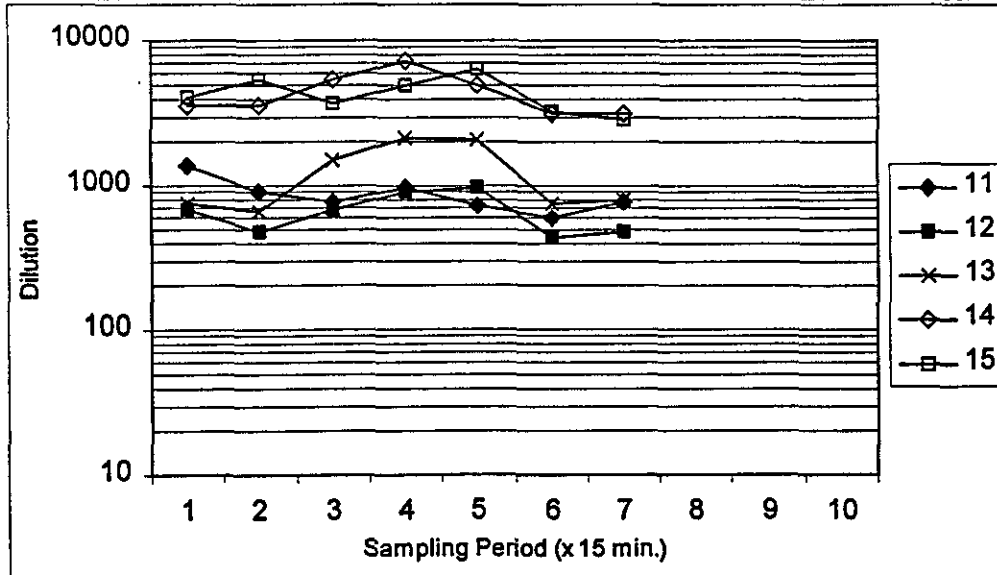
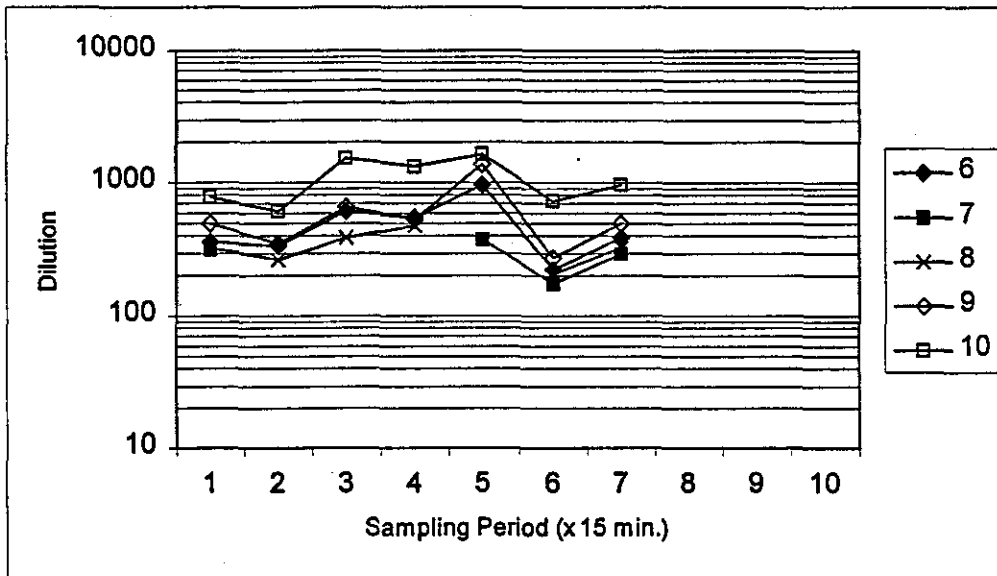
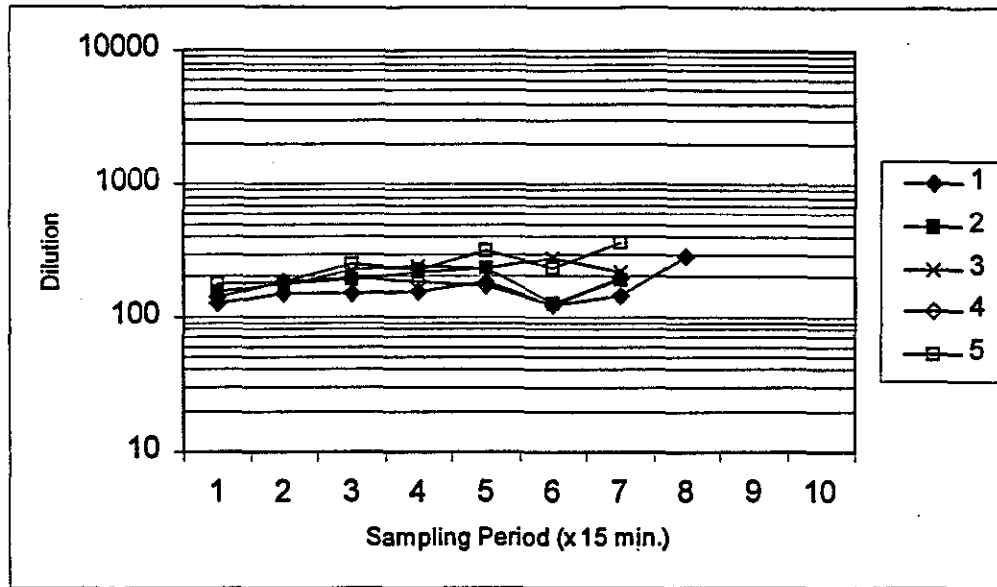


Figure 25 Variation of dilution with time during Hall Test No. 4, August 7th 1997

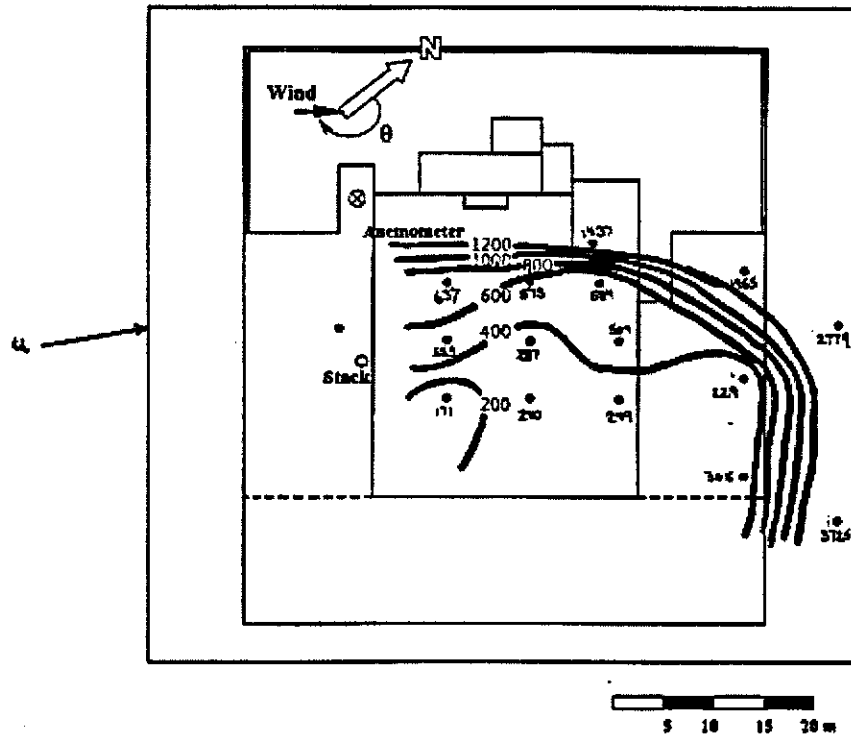
Another significant aspect of the time series plots is the degree of variability in the data over the entire test period. Fig. 24 shows that in test 3, data at all locations did not vary significantly after the 1st sample period. Values of D generally varied by less than a factor of three. On the other hand, significant variation with time is evident in the other tests, especially Nos. 1 and 2. This is not surprising for test 2, which was associated with large variations in wind direction. In test 1, however, wind direction was relatively constant. Nevertheless, values of D varied by more than a factor of ten at some locations during test 1.

4.1.2 Wind Tunnel Study

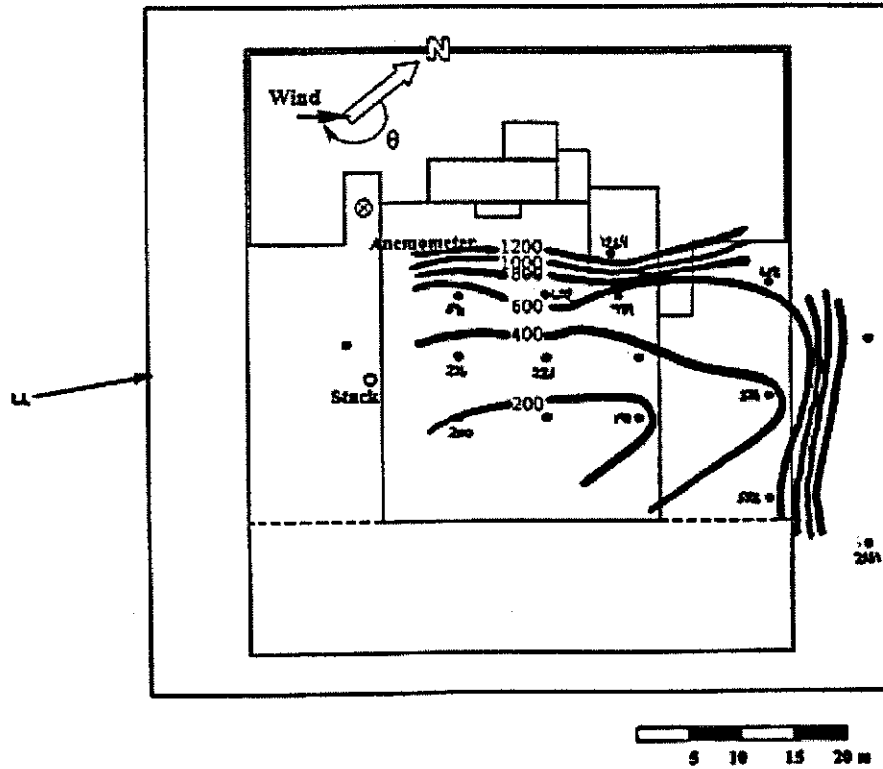
Numerous wind tunnel experiments have been carried out with the 1:500-scale model of the Hall Building. The results of these tests have been very useful in understanding the field data, but also raise additional questions.

Distributions of wind tunnel and field dilutions obtained with $M \sim 3.0$ are shown in Figures 26 and 27 for $\theta \sim 205^\circ$ and $\theta \sim 215^\circ$, respectively. It should be noted that the uncertainty of the 15-min. average values of θ obtained in the field study is expected to be $\pm 5^\circ$. (5-min average values of θ varied by more than 20° during the sampling periods). Both sets of field data were obtained during Test 1 (June 26).

Figure 26 shows that for $\theta \sim 205^\circ$, the wind tunnel data compare well with the field results; at most locations, the field dilution, D_{field} , is within a factor of two of the wind tunnel dilution, D_{wt} . In most cases, D_{field} was less than D_{wt} . The largest discrepancy occurred at location 13 where the

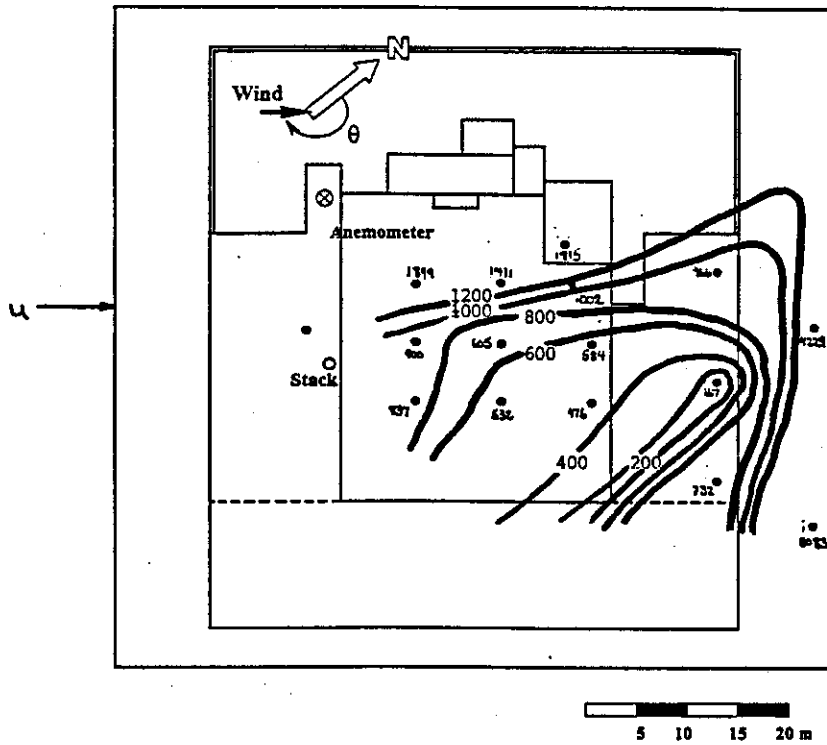


a) wind tunnel data

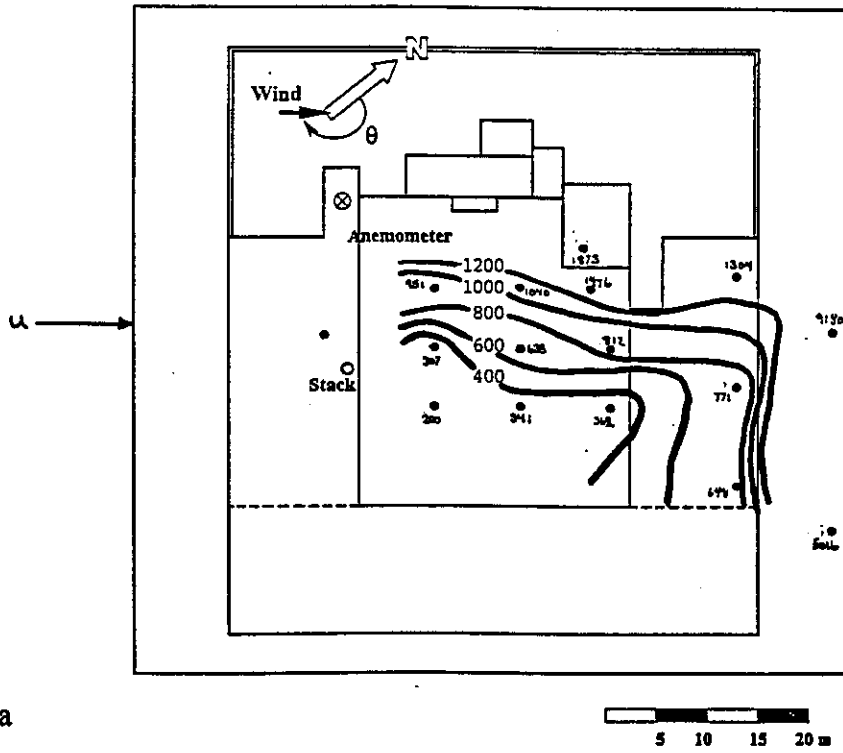


b) field data

Figure 26 Distributions of wind tunnel and field dilution obtained with $M=3$ for $\theta=205^\circ$.



a) wind tunnel data



b) field data

Figure 27 Distributions of wind tunnel and field dilution obtained with $M=3$ for $\theta \sim 215^\circ$.

wind tunnel dilution is approximately three times the field value ($D_{\text{field}}=618$, $D_{\text{wt}}=1955$).

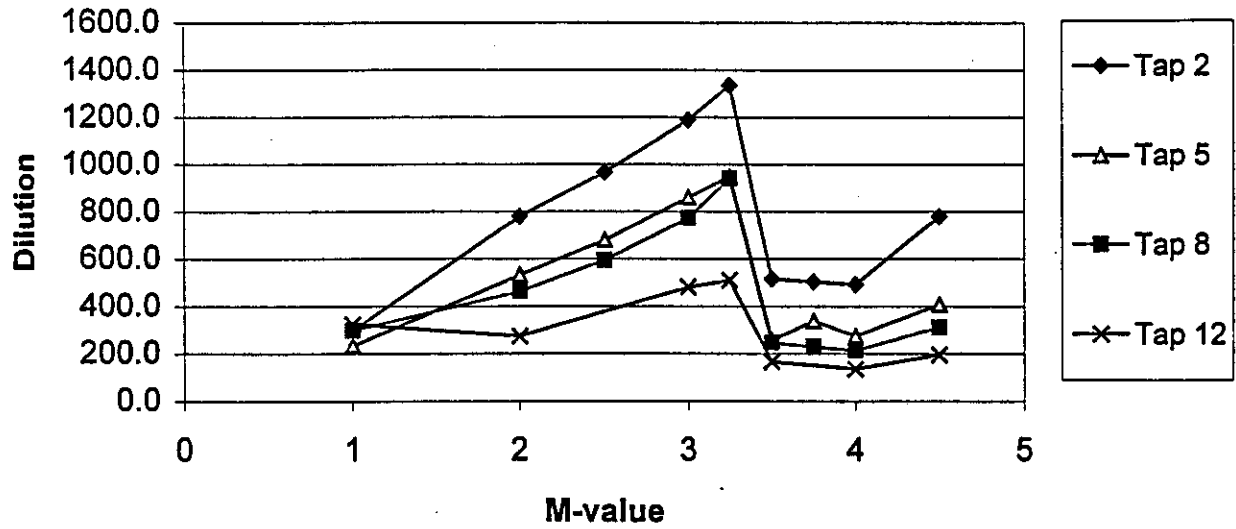
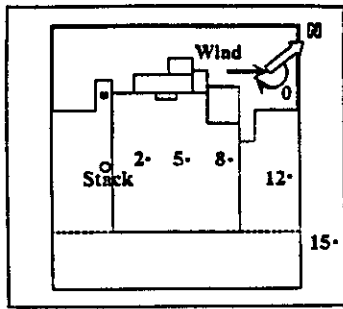
Figure 27 shows that with the wind direction approximately normal to the SW face of the building ($\theta \sim 215^\circ$), the wind tunnel data generally compare well with the field data for $s > 10$ m. However, at locations closest to the stack (Nos. 1, 2 and 3), D_{wt} is greater than D_{field} by as much as a factor of four. On the other hand, D_{field} exceeds D_{wt} by a factor of 2 at location 12 near the downwind edge of the roof and at locations 14 and 15 on the 12th floor level.

Effect of M on D_{min}

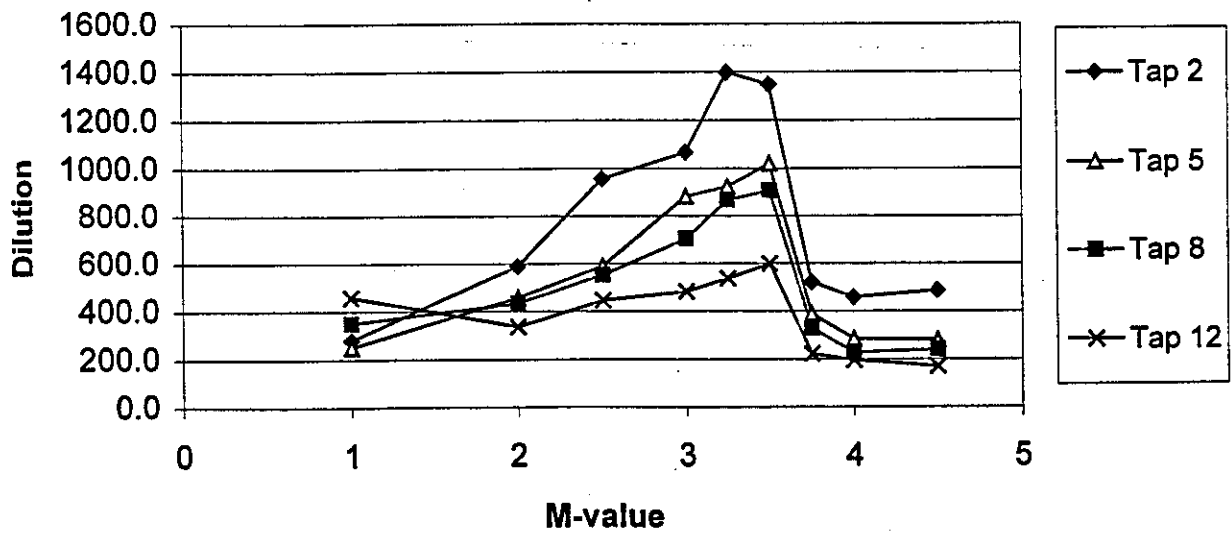
Wind tunnel experiments were performed to evaluate the influence of M on dilution measured at selected tappings. The variation of D_{wt} with M at tappings 2, 5, 8 and 12 is shown in Figure 28 for $\theta = 210^\circ$ and $\theta = 215^\circ$. At $\theta = 210^\circ$, dilution increases with exhaust momentum when $1 < M < 3.25$ but drops significantly for $M > 3.5$. Similar results were obtained for $\theta = 215^\circ$, although D remained high until M reached 3.75.

The magnitude of the reduction in D at high M depends on tapping location, with intermediate tappings being most strongly affected. For example, at $\theta = 210^\circ$, dilution is reduced by a factor of four at intermediate tappings 5 and 8 when M is increased from 3.25 to 3.5. On the other hand, the reduction factor is only 2.5, approximately, for tappings nearest the stack (Tap 2) and farthest from the stack (Tap 12).

The critical M value, M_{crit} , at which the dilution decreases appears to vary with wind direction. It



a) $\theta = 210^\circ$



b) $\theta = 215^\circ$

Figure 28 Variation of D_{wt} with M at tappings 2, 5, 8 and 12.

should be noted, however, that the uncertainty of M values is relatively high since the estimate of M is based on the reference wind speed which is highly dependent on measurement location and wind direction. In addition, the flow out of the model stack is laminar and this produces some uncertainty in the estimated value of exhaust velocity, w_e . Additional tests should be performed to determine whether M_{crit} varies significantly with θ . Furthermore, stack location and stack height may also affect M_{crit} ; the influence of these parameters will be investigated in the future.

The variation of D with M shown in Figure 28 is probably typical of buildings with small aspect ratio, L/H , where L is the building dimension in the flow direction. For this building geometry, the flow separation region covers the entire roof when the wind direction is approximately normal to the front face. As a result, the trajectory of a plume from a rooftop stack can vary significantly depending on the plume momentum. For example, if M is small (<0.5), the plume will make frequent excursions upwind. As M increases, however, the plume will more often travel downwind although upwind excursions still occur.

For large aspect ratio buildings, on the other hand, the flow reattaches near the leading edge and thus, the flow circulation region is small. This case is associated with a decrease in D at locations far downwind of the stack as M increases.

The effects of wind direction and exhaust momentum on wind tunnel dilution values, D_{wb} are shown in Figure 29 for five selected locations (Nos. 2, 5, 8, 12 and 15). Tappings 2, 5, 8 and 12 are located on the roof, roughly along a line that extends from near the stack (tap 2, $S=8.6$ m) to

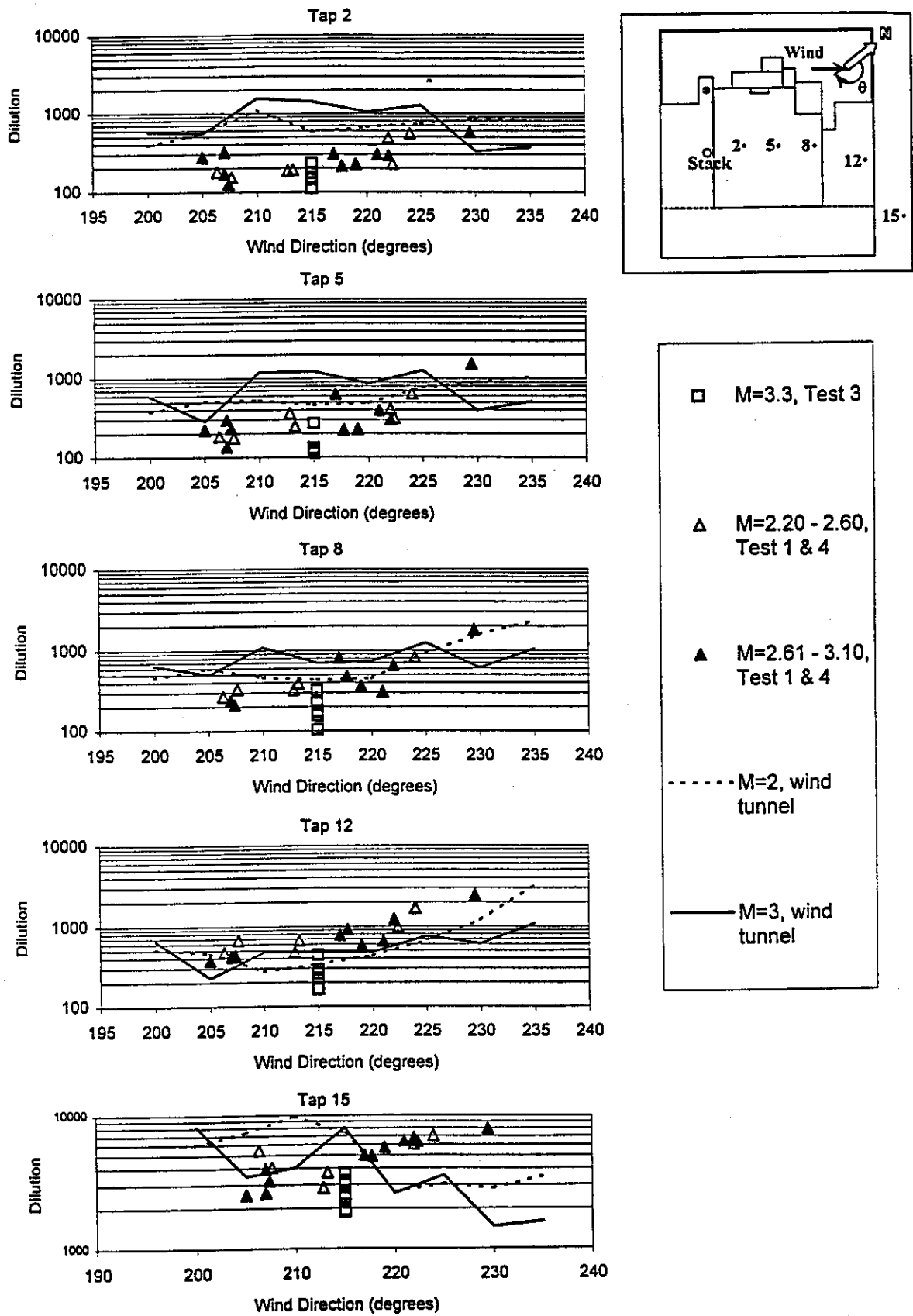


Figure 29 Effect of wind direction on wind tunnel and field dilution measured at locations 2, 5, 8, 12, and 15.

the trailing edge of the building (tap 12, $S=38.2$ m). These tapings are expected to be representative of the other rooftop tapings. Tapping 15 is located on the leeward side of the building at the 12-storey level. Results obtained at this tapping should be similar to those obtained at Tapping 14.

For comparison, Figure 29 also shows D_{field} obtained at the five locations during Tests 1, 3 and 4. Field data obtained in Test 2 have not been included since dilution values for this test were large and hence are not relevant in the following discussion of minimum dilution. (Recall that the wind direction and M value associated with Test 3 data were estimated using wind data from Dorval Airport.)

The values of M specified in Figure 29 for the field data are average values for each 15-min sample period. However, wind speed measured at 5-min intervals during Test 1 exhibit significant low-frequency unsteadiness. Consequently, M values exhibit a similar unsteadiness. For example, in 15-min sample period 3 of Test 1, the 5-min avg. M values were 2.0, 2.27 and 3.4. The variability of M may explain the relatively large scatter of D_{field} values plotted in Figure 29. Although the average value of M in this example was only 2.43, M may have exceeded the critical value during much of the sample period and thus produced lower than expected dilution.

Wind tunnel dilution data obtained at the tapping nearest to the stack (Tap 2, $S=8.6$ m.) were generally larger than the field values. Values of D_{wt} obtained with $M=2$ and $M=3$ were approximately two to five times as large as D_{field} for $\theta \sim 200-225^\circ$. The amount of field data

obtained with $\theta > 225^\circ$ is too small to allow comparison with the wind tunnel values. However, it is interesting to note that for $\theta=230^\circ$ and $\theta=235^\circ$, D_{wt} values obtained with $M=3$ are significantly lower than those obtained with $M=2$. Clearly, the drop in D_{wt} at $M=3$ is an example of the critical M phenomenon illustrated in Figure 28. Although M_{crit} for $\theta > 230^\circ$ appears to be less than the values obtained for $\theta=210-215^\circ$, additional experiments are required to determine the influence of wind direction on M_{crit} .

Data for tappings 5, 8 and 12 shown in Figure 29 indicate that the wind tunnel predicts the field dilution better as distance from the stack increases. At tapping 5 ($S=16.6$ m), D_{wt} generally exceeds D_{field} . For example, the wind tunnel overestimated the field dilution by a factor of two for θ between 215° and 225° , although good agreement is evident when the critical M value was reached. Data for tappings 12 and 8 are in better agreement with the field data – in fact, at the farthest tapping (T12), the wind tunnel generally provides conservative estimates of dilution. The field data for Test 3 appear to be an exception, as they tend to be lower than D_{wt} at this location. However, the low values of D for this test may be associated with high M values.

4.1.3 Summary of Findings from the Hall Building Study

The field and wind tunnel experiments with the Hall Building have provided a significant amount of data regarding the dispersion of exhaust from the roof of a cubic-shaped building in an urban environment. The major findings of the study are:

1. The Halitsky model gives highly conservative predictions of minimum dilution.
The accuracy of the model can be improved by adjusting the parameter, α .

However, the magnitude of the adjustment may be difficult to determine since it depends on various factors (e.g. building shape, stack height, exhaust momentum ratio and locations of receptors.)

2. The minimum dilution models of Wilson-Lamb and Wilson-Chui generally provide reasonable lower bounds for D_{min} , although both models produced unconservative predictions of some of the field data.
3. The initial dilution formula of the Wilson-Chui model overestimates D_0 when M is large ($M > 4$). The Wilson-Lamb formula for D_0 provides better estimates of initial dilution when M is large.
4. The Wilson-Chui minimum dilution model with a revised formula for initial dilution is recommended because it is simpler than the Wilson-Lamb model and also more conservative for urban environments.
5. Dilution data obtained in the wind tunnel study are generally within a factor of two of the field data. The agreement between the wind tunnel and field data improves as distance from the stack increases.
6. Results of both the field study and the wind tunnel study indicate that the behavior of the plume is dramatically affected when the momentum ratio of the exhaust flow reaches a critical value of approximately 3.5. For $M > 3.5$, dilution is reduced significantly at all rooftop locations. This suggests that the use of high velocity stacks on cubical buildings may actually increase pollutant levels under certain wind conditions. Further experimental work will be carried out to investigate the influence of various parameters on this phenomenon.

4.2 BE Building

4.2.1 Field Study

The field tests on the BE Building were performed on three days in October and December of 1997 during periods of moderately strong winds. Unlike the Hall Building tests, the sampler locations were not the same for each test. Smoke tests carried out prior to Test No. 2 and Test No. 3 indicated that the wind direction was predominantly westerly during these tests, as opposed to west-northwesterly in Test 1. Consequently, the samplers were relocated in the latter two tests to ensure that some of the samplers would be near the center-line of the time-averaged plume.

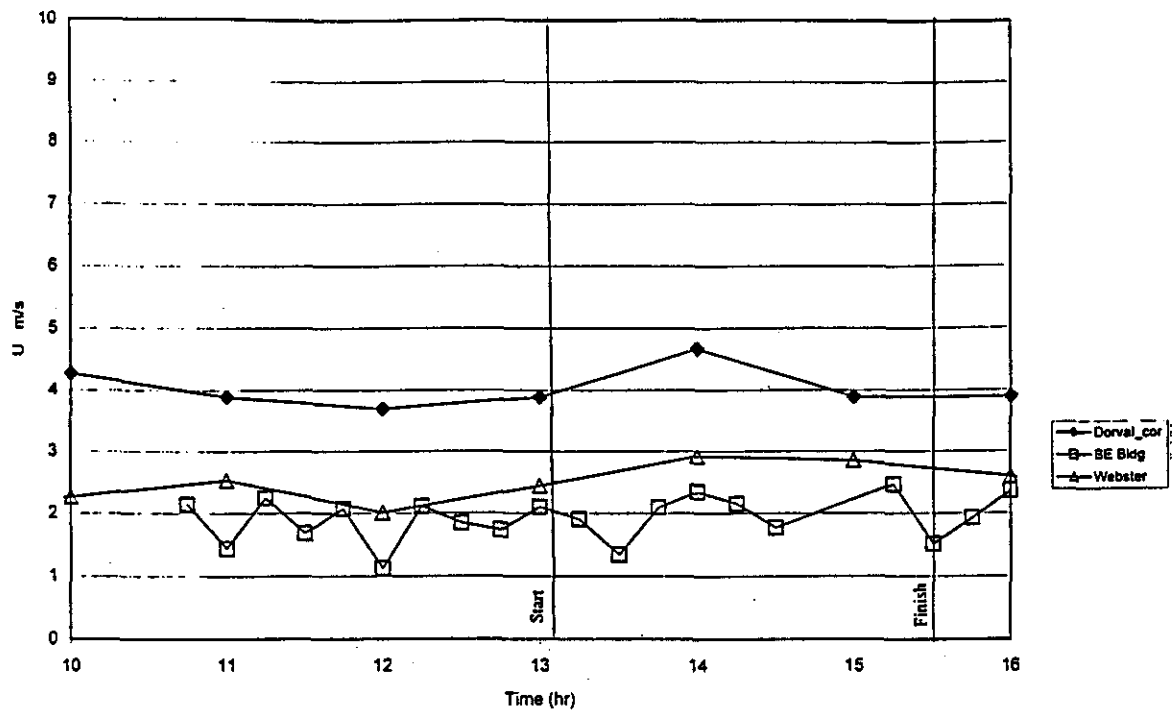
Field tests were carried out on October 1, October 10, and December 2, 1997. Figures 30-32 show wind speed and direction data obtained on the roof of the building during these tests. Also shown are data obtained on the library building and data obtained at Dorval Airport. Note that the raw wind speed data from Dorval have been modified to take into account the height of the BE Building and the increase in roughness associated with an urban exposure.

If it is assumed that differences between BE wind speeds and Dorval speeds are mainly due to differences in upstream roughness and measurement height, the correction factor to apply to the Dorval wind speed is:

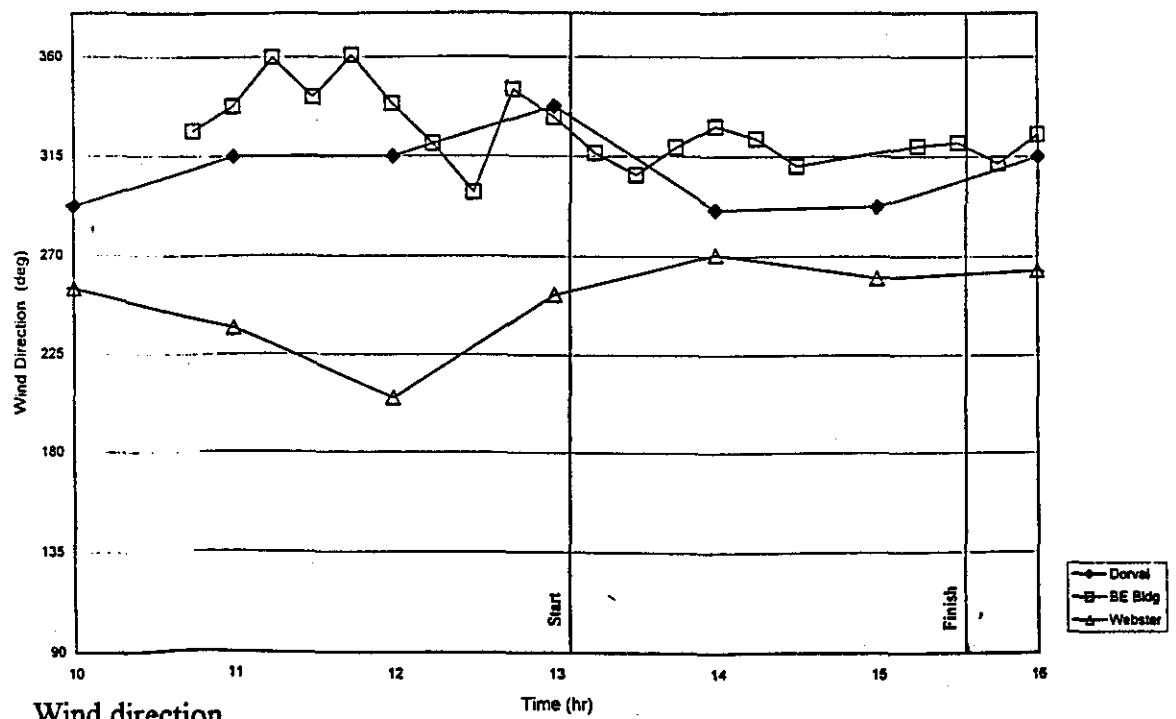
$$U_{BE}/U_{Dorval} = (Z_{goc}/Z_{Dorval})^{0.15} (Z_{BE}/Z_{gurb})^{0.28}$$

$$U_{BE}/U_{Dorval} = (300/10)^{0.15} (19/500)^{0.28} = 0.67$$

However, measured values of U_{BE}/U_{Dorval} during the three field tests varied between 0.33 and 0.50,

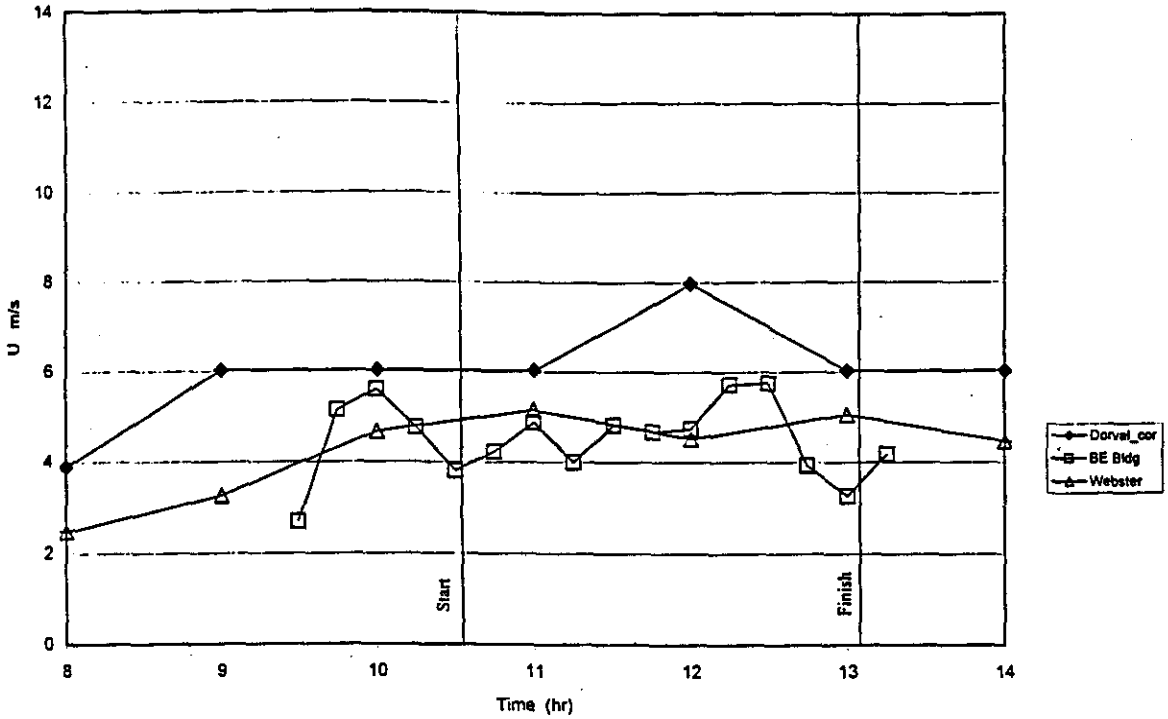


a) Wind speed

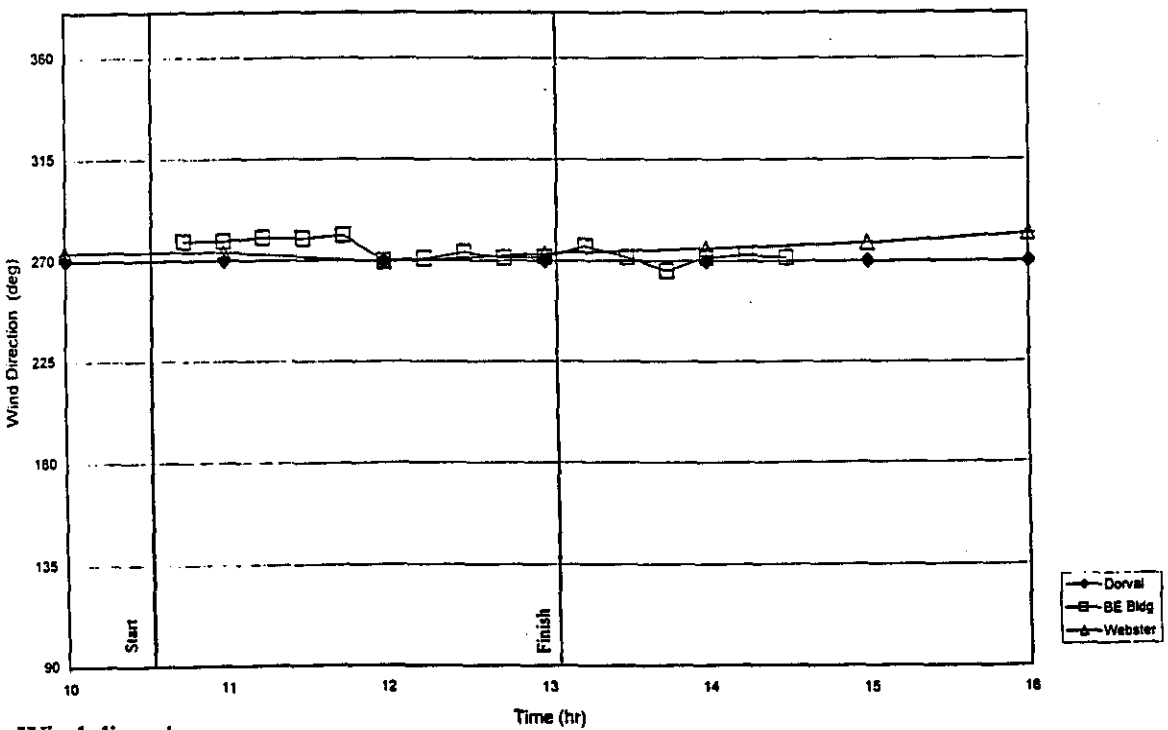


b) Wind direction

Figure 30 Wind data obtained during BE Building Test No. 1 (Oct. 1, 1997).

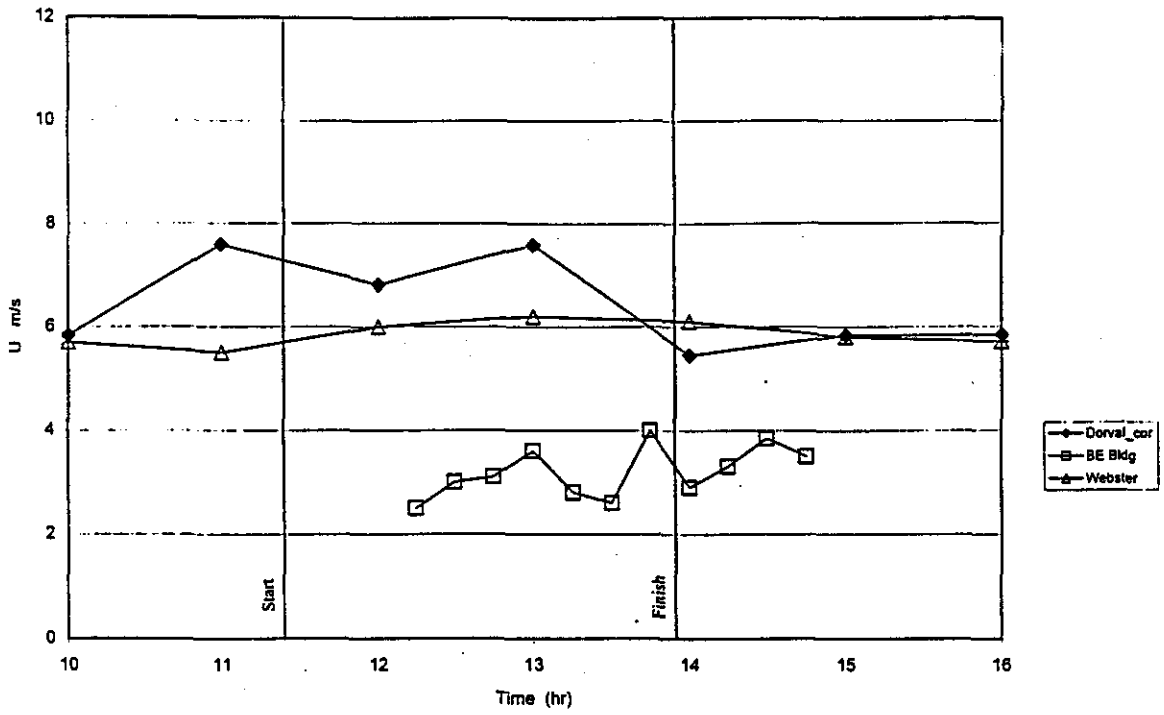


a) Wind speed

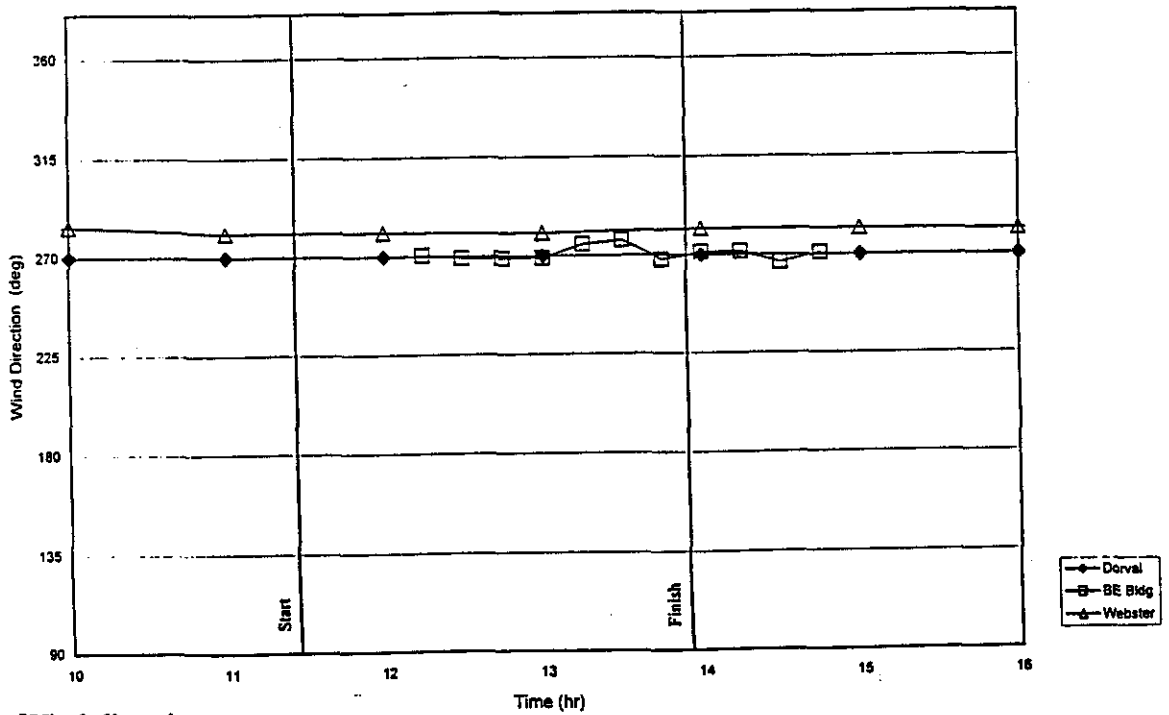


b) Wind direction

Figure 31 Wind data obtained during BE Building Test No. 2 (Oct. 10, 1997).



a) Wind speed



b) Wind direction

Figure 32 Wind data obtained during BE Building Test No. 3 (Dec. 2, 1997).

i.e. lower than predicted by the above equation. This is partially due to the presence of large buildings and the hill upwind. Furthermore, the anemometer was located at a height of only 2 m (Oct. 1st) or 3 m (Oct. 10th, Dec. 2nd) above the roof and was thus inside the separated flow region. Unfortunately, it was not feasible to install a higher tower on the roof of the BE Bldg.

During the Oct. 1st test, wind data were also obtained by an acoustic wind profiler (sodar). The sodar measures wind speed, wind direction and turbulence level at heights up to 300 m by recording the movement of temperature perturbations. Wind data obtained during two 15-min intervals at the end of the tracer gas test are shown in Figure 33. At a height of 40 m above the roof ($z=54$ m), the sodar wind speed was approximately 5.3 m/s. This compares reasonably well with the wind speed of 5.8 m/s obtained on the roof of the library building ($z=51$ m).

Wind direction measurements obtained with the sodar show significant variation with height. The average value of θ at a height of 20 m was approximately 278° ; this is somewhat lower than the value of 300° obtained with the sonic anemometer.

The time variation of dilution measured at all locations during the tests on Oct. 1st, Oct. 10th and Dec. 2nd are shown in Figures 34 to 36, respectively. (Note that not all of the 15 samplers were operational during each test.)

The dilution values generally exhibit remarkable consistency throughout the tests. The ratio of

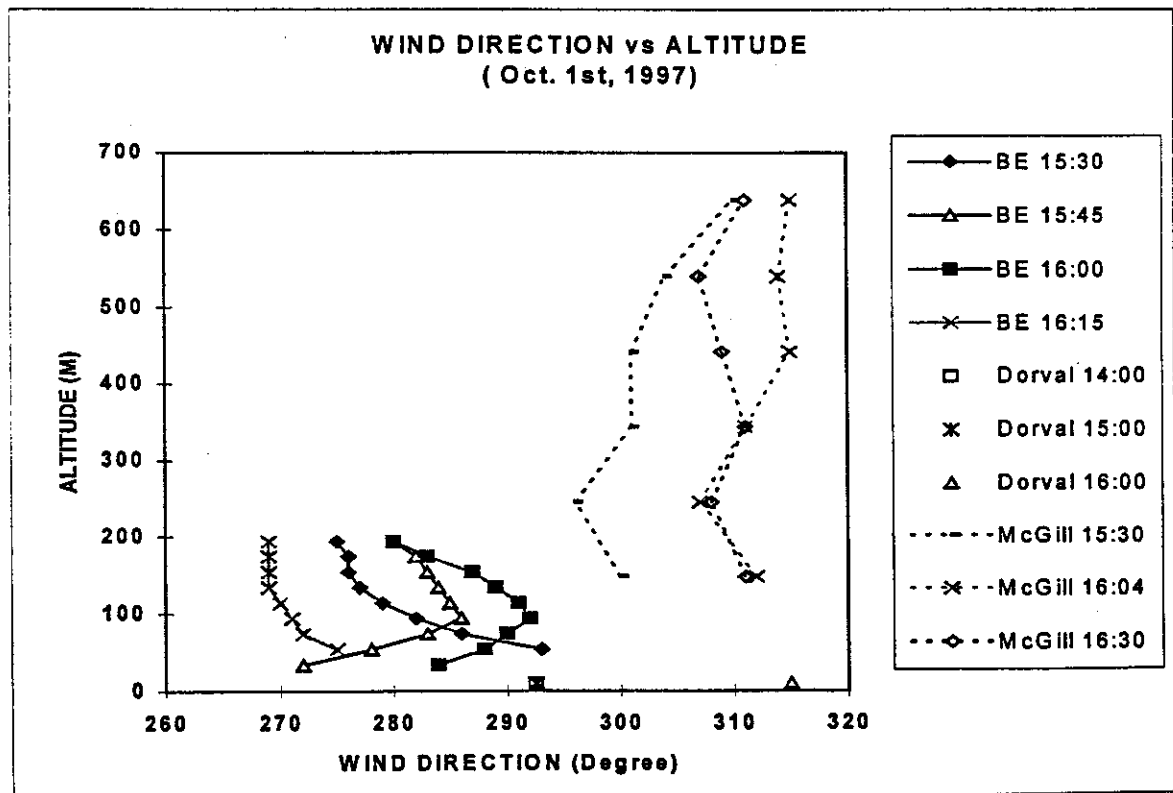
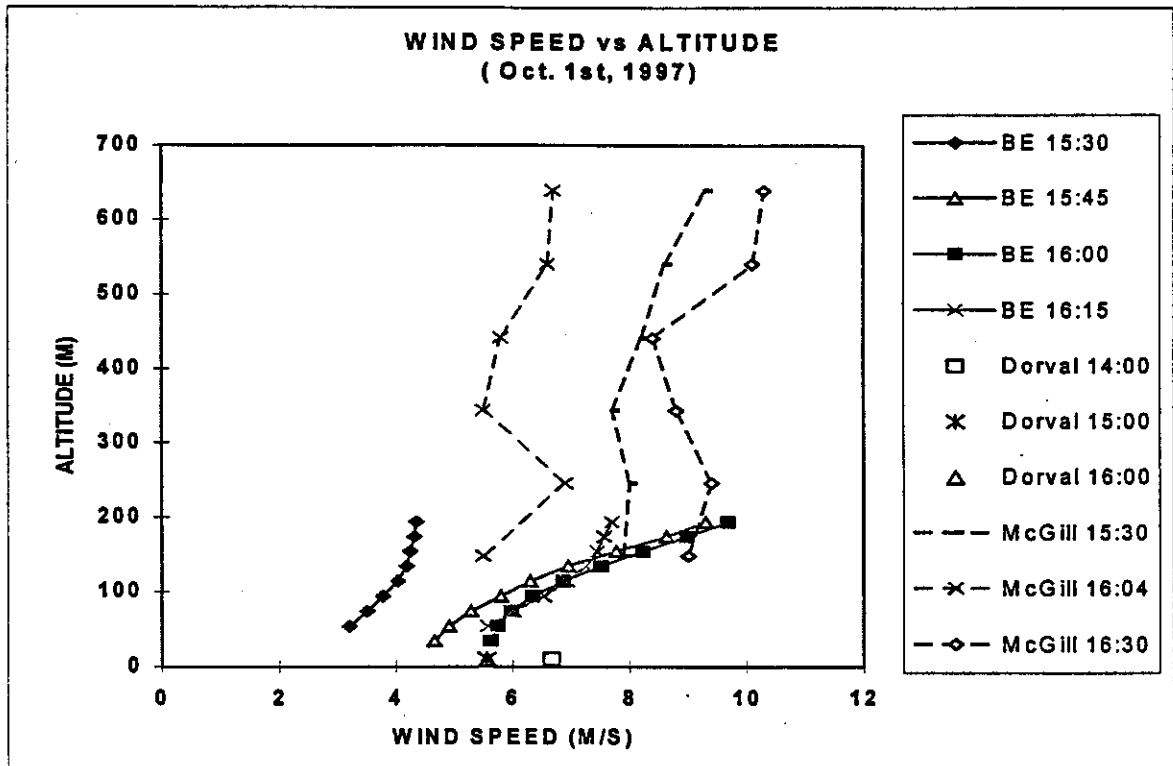


Figure 33 Wind profiles obtained by the sodar and the McGill radar during BE Test No. 1

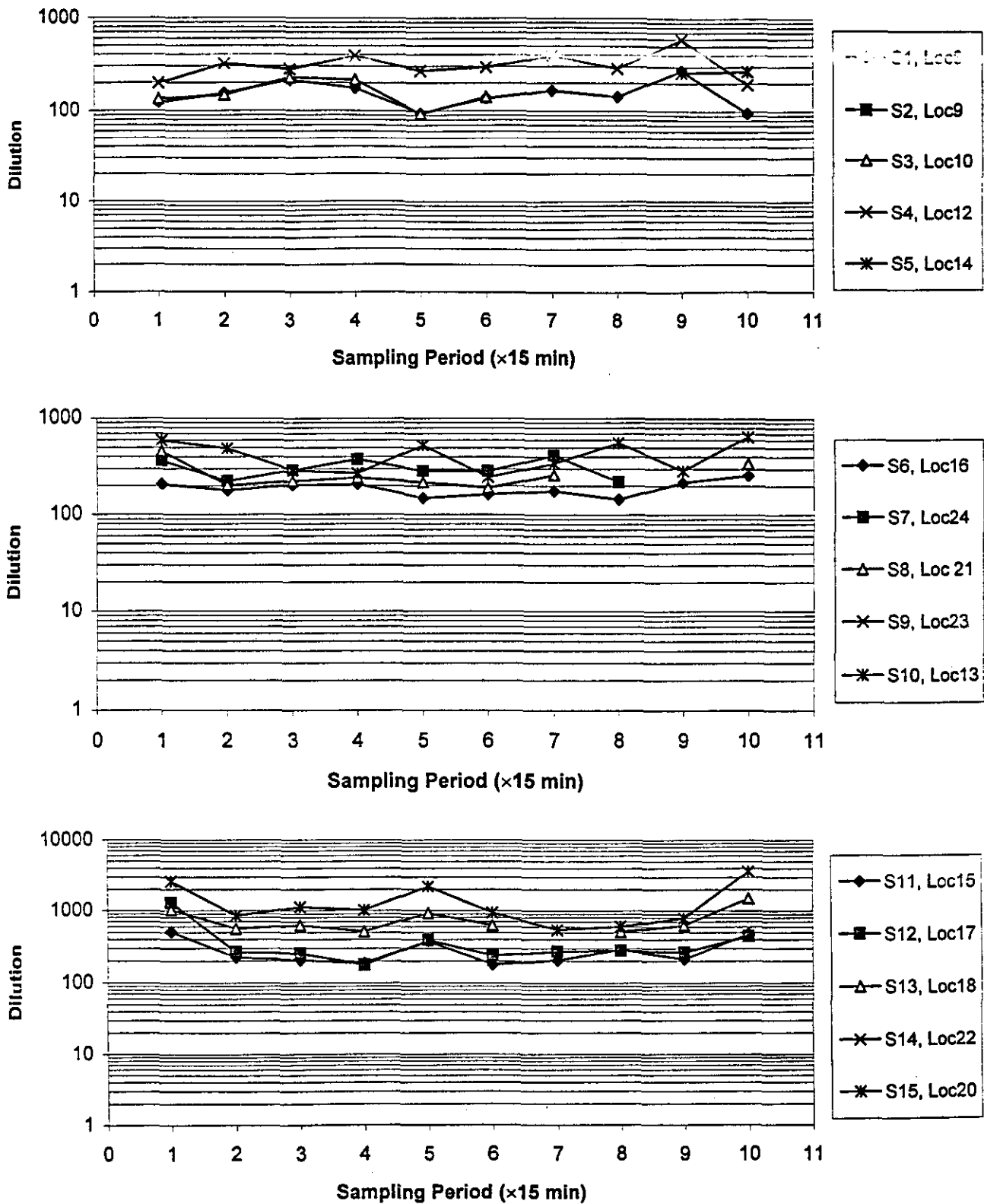


Figure 34 Variation of dilution with time during BE Test No. 1 (see Fig. 10 for sampler locations).

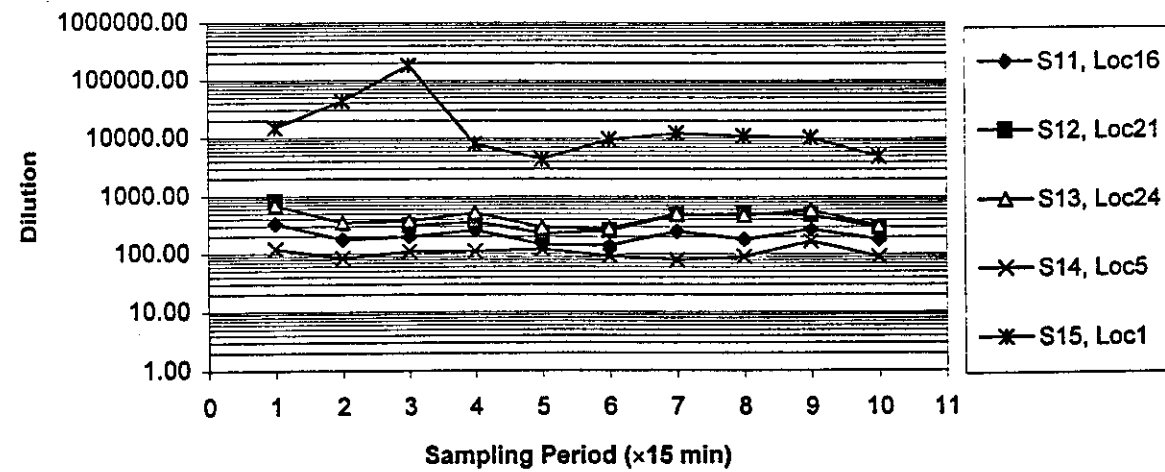
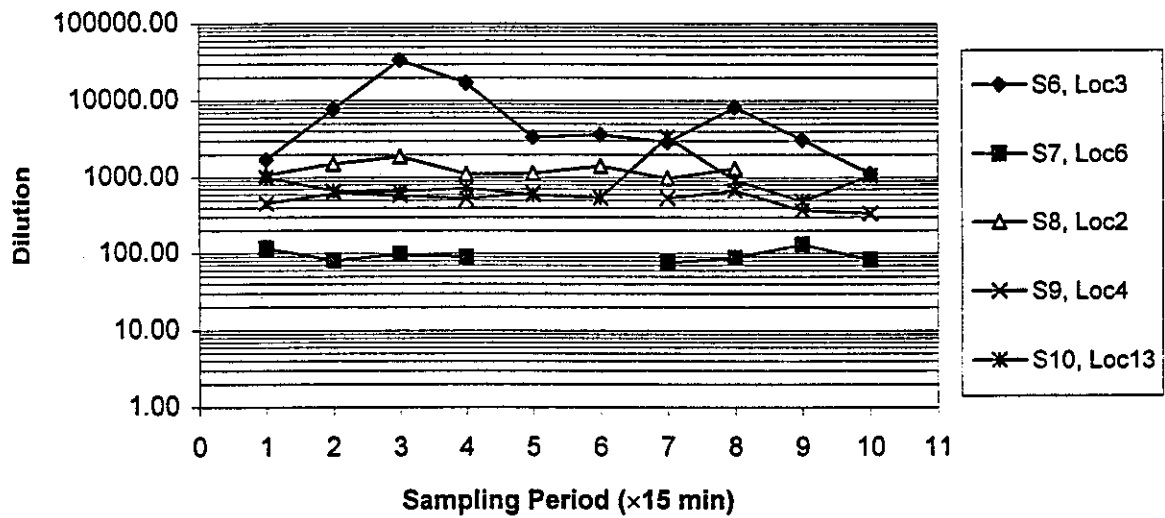
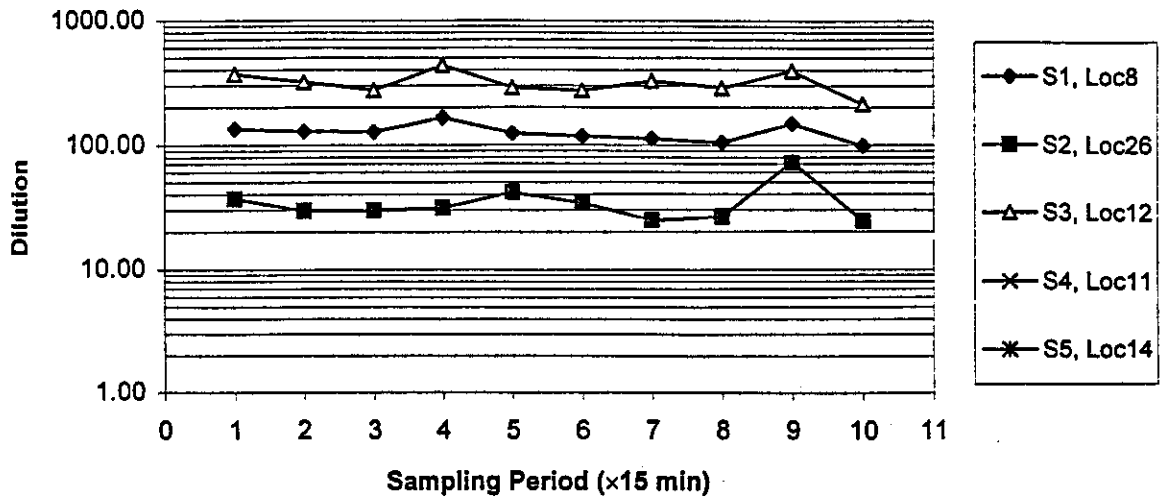


Figure 35 Variation of dilution with time during BE Test No. 2 (see Fig. 10 for sampler locations).

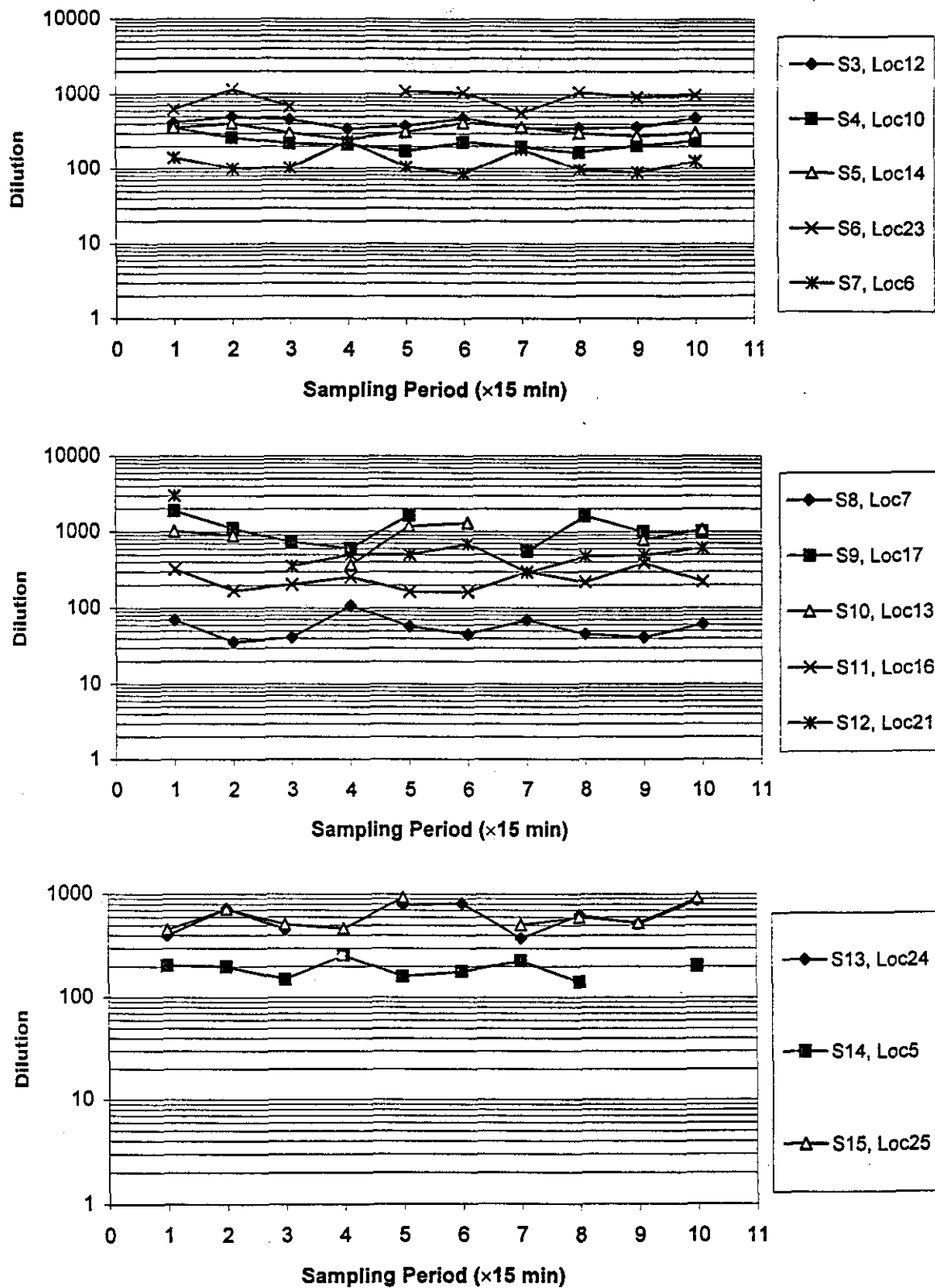


Figure 36 Variation of dilution with time during BE Test No. 3 (see Fig. 10 for sampler locations).

maximum to minimum dilution is approximately 2 at most locations. An exception occurred for sampler No. 6 on Oct. 10th which showed variations in D of more than a factor of 10. In this case the sampler was located relatively near the stack but well off the plume axis (at Location 3, Figure 10a) and thus the intermittency of concentration was high.

The BE Bldg. dilution data are plotted as a function of distance from the stack in Figures 37-39. Also plotted are minimum dilution curves obtained with the Halitsky (H), Wilson-Chui (WC) and Wilson-Lamb (WL) models. For the WL model, the distance dilution parameter was set at the maximum value of 0.09 since the turbulence levels were very high during all of the tests.

The WC and WL D_{min} curves were plotted using the average M value for the entire 2.5 hour sampling period of each test. Estimated values of M for individual 15-min samples for each test are shown in Table 5. The 15-min M values were generally within $\pm 20\%$ of the average value for the entire test. However, larger variation of M is evident for the Oct. 1st test.

When comparing measured and predicted dilution values, it is important to recall that the WC and WL models were developed for flush vents. The models are not strictly applicable to receptors on the main roof since the stack outlet was approximately 3 m above the roof. They are expected to give conservative predictions of minimum dilution for these locations. On the other hand, the models are more appropriate for the penthouse samplers since these are most likely to make direct contact with the plume.

CBS FIELD TEST
Day #1, Oct. 1, 1997

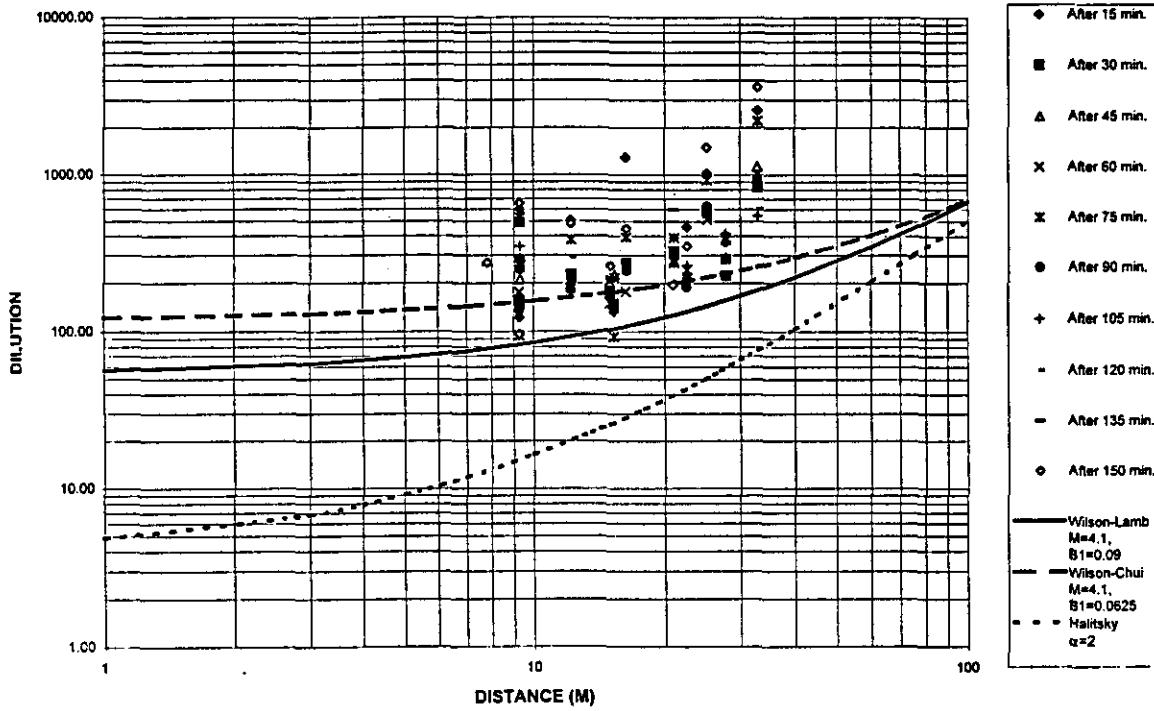


Figure 37 Dilution data obtained at all samplers during BE Test No. 1 compared with ASHRAE minimum dilution curves.

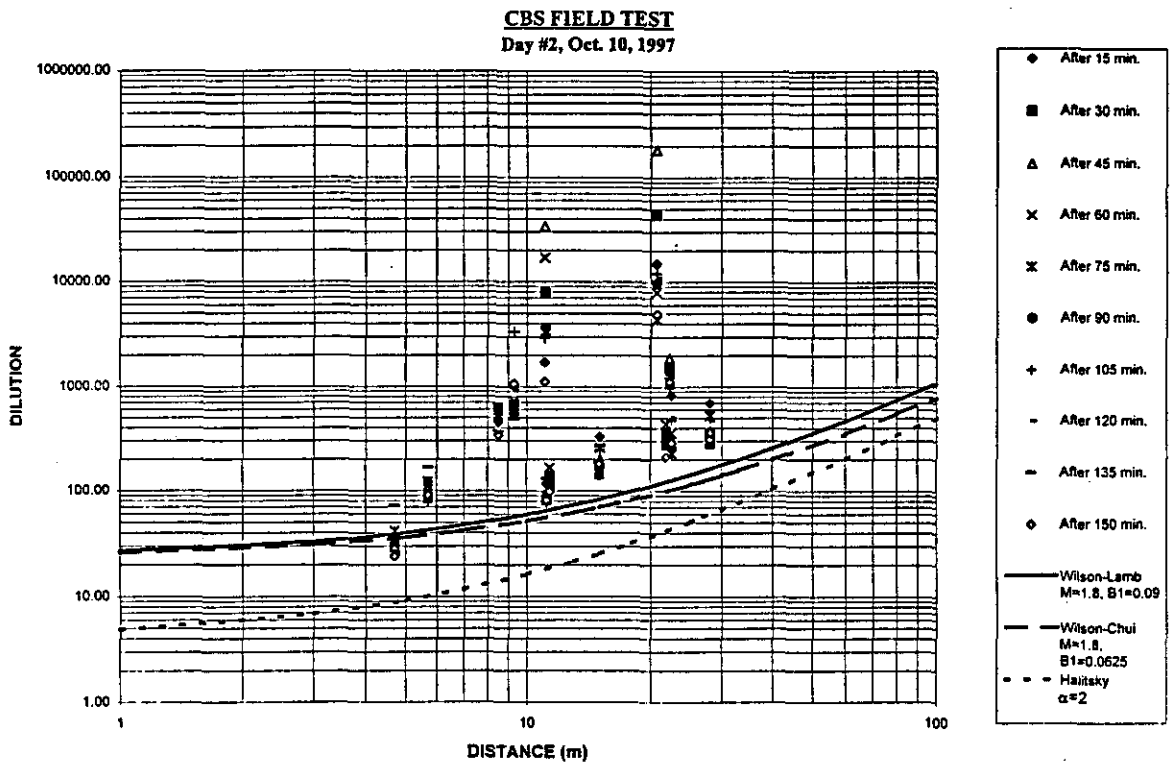


Figure 38 Dilution data obtained at all samplers during BE Test No. 2 compared with ASHRAE minimum dilution curves.

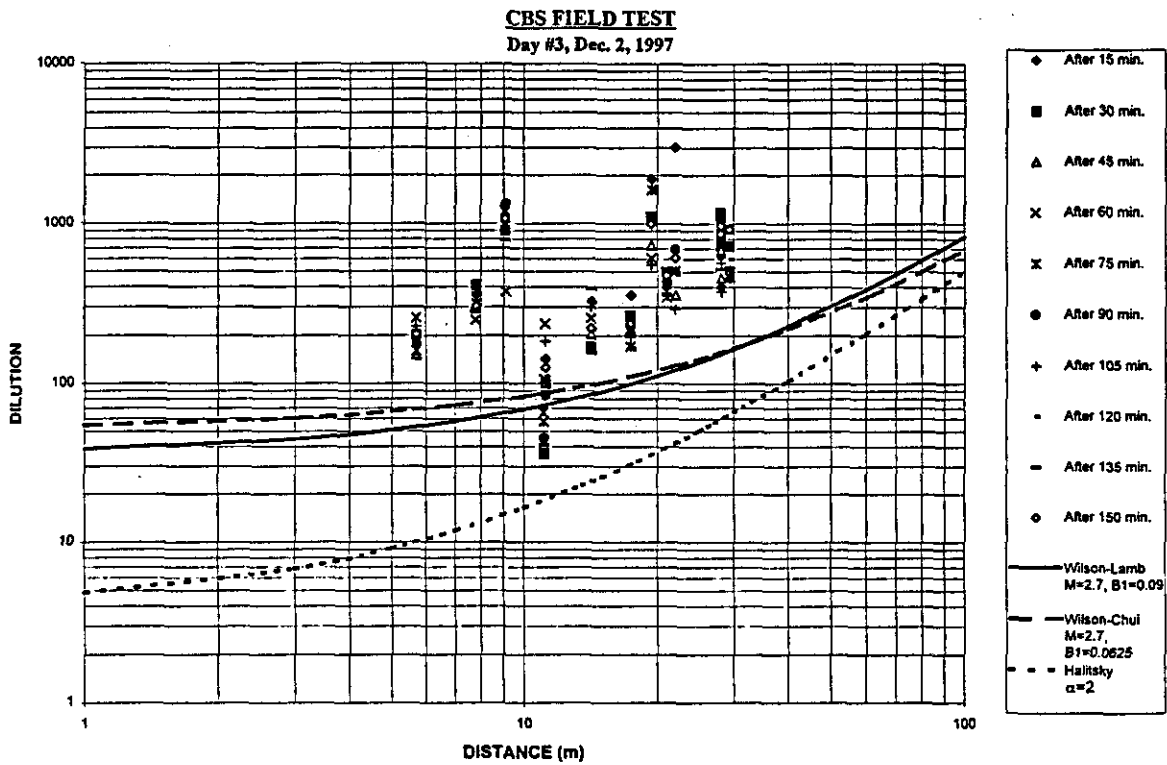


Figure 39 Dilution data obtained at all samplers during BE Test No. 3 compared with ASHRAE minimum dilution curves.

Table 5 Estimated M values for 15-min sampling periods (BE Bldg.)

Sample No.	Oct. 1 st	Oct. 10 th	Dec. 2 nd
1	4.3	1.9	
2	6.0	1.7	
3	3.9	2.0	3.2
4	3.5	1.7	2.7
5	3.8	1.7	2.6
6	4.6	1.7	2.3
7		1.4	2.9
8		1.4	3.1
9	3.3	2.1	2.0
10	5.4	2.5	2.8
Avg. M	4.3	1.8	2.7

In this regard, the Halitsky model parameter, α , was set equal to 2.0 as recommended for elevated plumes with rooftop receptors. However, for some of the penthouse receptors, it could be argued that α should be set equal to 1.0.

The measured dilution values for the Oct. 1st test ($M_{avg}=4.3$) are generally well above the WL D_{min} curve at most locations, as shown in Figure 37. Except for one sample obtained at S=15 m, minimum dilution measured at locations near the plume centre-line are approximately 1.5 times the predicted values. The under-prediction of D_{min} by the WL model is largely because the elevated plume did not make direct contact with the samplers, except instantaneously. In addition, the mean wind direction was not critical for most of the samplers.

The Halitsky model underestimates D_{\min} at all locations by at least a factor of 5. On the other hand, the WC curve exceeds the measured dilutions at several receptors by as much as 1.5 times. The differences between the WC and WL model predictions are due mostly to the different formulas used to calculate initial dilution, D_0 . Recall that $D_0 = 1 + 7M^2$ for the WC model and $D_0 = 1 + 13M$ for the WL model. For moderate exhaust momentum ($1 < M < 2.5$), the two formulas give similar values of D_0 . However, for high M ($M > 4$), the WC formula gives significantly higher initial dilution than the WL model.

For the Oct 1st test ($M=4.1$), D_0 obtained with the WC model is 119, approximately twice as large as the WL value of 54. The WC approximation of initial dilution appears to be too large in this case since measured dilutions near the stack are well below the WC D_{\min} curve in Figure 37.

Close to the stack, the initial dilution component of total dilution is much larger than the distance dilution component. Thus, the WC model's overestimation of measured dilutions at $S=9.3$ m and $S=15.3$ m (Locations 8 and 10, Fig. 10) is due to the overestimation of D_0 . On the other hand, the WL formula for D_0 appears to be a better approximation, at least for this data set, since most of the data lie above the WL D_{\min} curve.

Dilution data obtained on Oct. 10th ($M_{\text{avg}}=1.8$) are shown in Figure 38 with the WC, WL and H minimum dilution curves. In this case, little difference is observed between the WC and WL curves. Since M_{avg} is relatively small, both models give approximately the same initial dilution and thus similar values of D_{\min} near the stack. The WC model becomes slightly more conservative than the WL model as distance from the stack increases since the former uses a lower value of B_1 .

For the most part, all three models provided conservative estimates of the Oct. 10th minimum dilution data. As expected, the largest discrepancies were observed with the H model, which underestimated D_{\min} by at least a factor of three. The WC and WL models underpredicted D_{\min} by at least a factor of two at most receptors. An exception was the penthouse sampler closest to the stack (S=4.7 m), which obtained some dilution values that were slightly less than predicted by the WC and WL models. It is important to note, however, that the apparent conservatism of the models is somewhat misleading since the wind direction (WNW) was not critical for most of the samplers.

Dilution data and D_{\min} curves for the Dec. 2nd test ($M_{\text{avg}}=2.7$) are shown in Figure 39. As with the Oct. 10th test, the Halitsky curve underestimates the measured dilution at all locations, at least by a factor of three. Likewise, the WC and WL models underestimate the measured dilution at most locations due to the effects of plume height and/or wind direction. However, these models overpredict some dilution values obtained at sampler No. 8 (S=11 m) by a factor of 2, approximately. The discrepancy between measured and predicted dilution is slightly larger for the WC model because it assumes a larger initial dilution ($D_0=52$) than the WL model ($D_0=36$).

The over-prediction of D_{\min} at S=11 m by the WC and WL models suggests that both models overestimate the initial dilution of the plume. Another possible cause of the overprediction of dilution at this receptor is that the value of the distance dilution parameter, B_1 , used in each model is too large. However, considering that the lowest measured dilution at S=11 m ($D \sim 35$) is approximately equal to D_0 , extremely low values of B_1 would be required to fit the WL and WC

models to the data. A significant reduction in B_1 is not realistic since the high level of turbulence in the approaching flow ($\sigma_v/U > 50\%$) should enhance dispersion of the plume. Consequently, it is more likely that the initial dilution approximation of the models should be revised.

Additional data obtained near the stack on the plume centre-line would be required to obtain a better estimate of D_0 . Likewise, more samplers would be required at distances greater than 10 m in order to evaluate the adequacy of B_1 values that are assumed. Unfortunately, it was not possible to place samplers in the path of the plume at larger distances for the Dec. 2 test.

It should also be noted that the use of the average M value for the entire 2.5 hr sampling period as input to the models may have increased the discrepancy between predicted and actual dilution values. Each 15-minute sample, with its own specific M value, could have been used to evaluate the minimum dilution models. As shown in Table 5, the 15-min M values obtained in the Oct. 10th and Dec. 2nd tests were fairly consistent. However, the Oct. 1st data showed greater variability. Considering the uncertainties associated with the measurement of w_e and U_{10} , the use of 15-min M values is probably not warranted.

4.2.2 Results of BE Building Wind Tunnel Study

A series of wind tunnel experiments were carried out to evaluate the influence of wind direction and exhaust momentum on plume dilution at various rooftop locations on the BE Building.

A total of 26 tappings were placed on the model of the building as shown in Figure 10a. These

correspond to the locations of samplers during the field tests.

Before discussing the results of the wind tunnel study, it is important to note possible sources of uncertainty in the results. Firstly, high turbulence levels, of the order of 25%, at the reference height above the roof of the BE Bldg. model will cause the hot film anemometer to overestimate the mean wind velocity. Consequently, the M values may have been underestimated. No attempt was made to adjust the M values to account for the bias in measured wind speed due to other sources of uncertainty in the measurements. For example, wind velocity measurements are highly sensitive to the location of the hot film probe since large velocity gradients exist in the flow above the model roof.

The second major source of uncertainty concerns the effect of upstream terrain. Wind tunnel tests were carried out with a standard suburban boundary layer flow without modelling Mount Royal upwind since it was felt that the tall buildings in the vicinity of the BE Bldg would dominate the flow. However, the dispersion process may be affected by larger scale flow patterns produced by Mount Royal. The influence of the hill on the results may be the subject of a future study. It should be realized that the effect of the hill was assumed to be negligible in the Hall Building tests because the wind direction was southwesterly.

Finally, it should be noted that the stack diameter of the BE Bldg. model was based on the outlet diameter of the Strobic stack ($d_s=1.1$ m). However, after the wind tunnel experiments had been completed, it was determined that the effective diameter of the Strobic stack was somewhat less

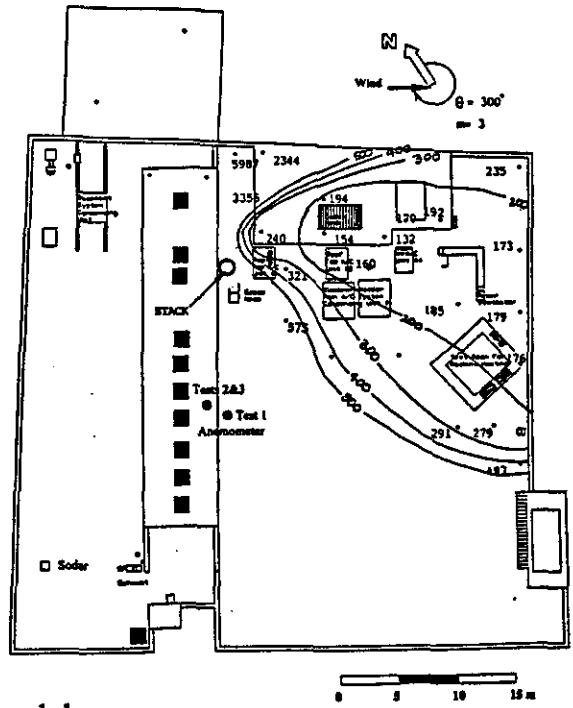
than the actual diameter because of the form of the velocity profile (see Fig. 9). The effect of this mismatch in model scale on dilution measurements is expected to be small since, for a given value of M , D_{\min} is relatively insensitive to variations in stack diameter. In addition, since the exhaust flow profile from the model stack was usually laminar, use of the correct model scale may not have been appropriate anyway.

Figure 40 shows contour plots of dilution obtained in the wind tunnel for $M=3$ when the wind direction was northwesterly ($\theta=300^\circ$). Also shown are typical field results obtained on Oct. 1 for approximately the same wind direction. The average M value measured during the field test was approximately 3.3. The field data are generally within a factor of 2 of the wind tunnel results for $M=3$.

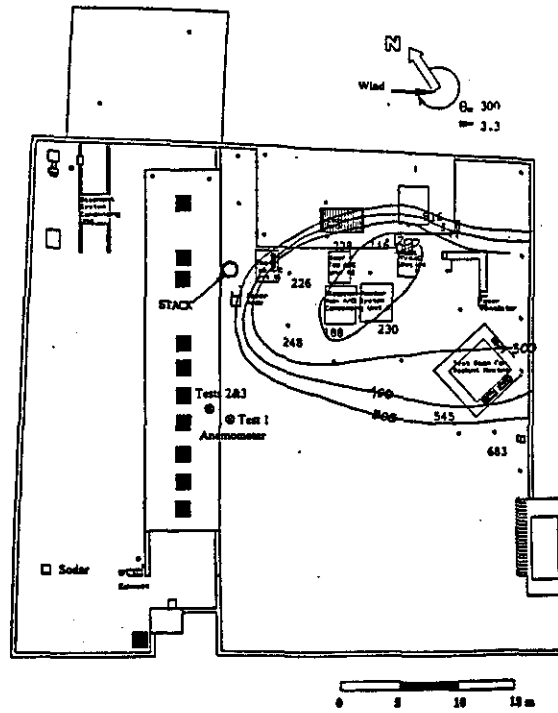
Figure 41a shows wind tunnel data obtained with a westerly wind ($\theta=270^\circ$) for $M=2$.

Field data obtained on Oct. 10 for approximately the same wind direction and $M\sim 1.8$ are shown in Figure 41b. The field data compare reasonably well with wind tunnel results for $M=2$, especially on the penthouse.

The influence of wind direction on wind tunnel and field dilution values for selected locations on the penthouse is shown in Figure 42; similar data are shown in Figure 43 for locations on the main roof. Wind tunnel dilution curves are plotted for $M=2$ and $M=3$ since much of the field data were obtained in this range. Considering the uncertainties in estimating M and θ for the field tests, the agreement between wind tunnel and field data is quite encouraging.

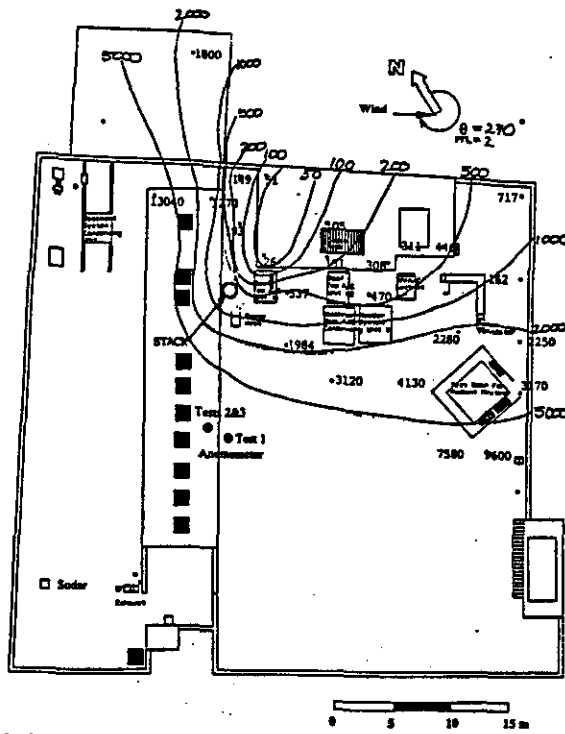


a) wind tunnel data

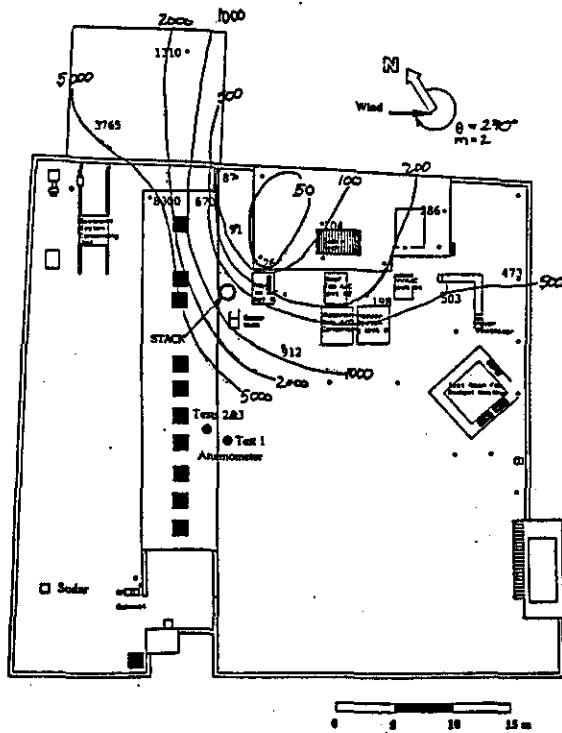


b) field data

Figure 40 Contour plots of wind tunnel and field dilution for the BE Building ($M=3, \theta=300^\circ$)



a) wind tunnel data



b) field data

Figure 41 Contour plots of wind tunnel and field dilution for the BE Building ($M=2, \theta=270^\circ$)

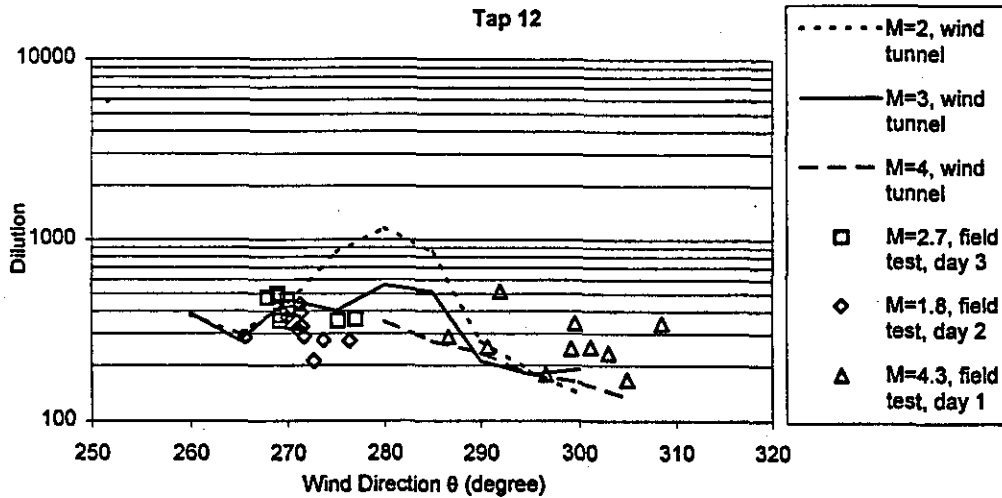
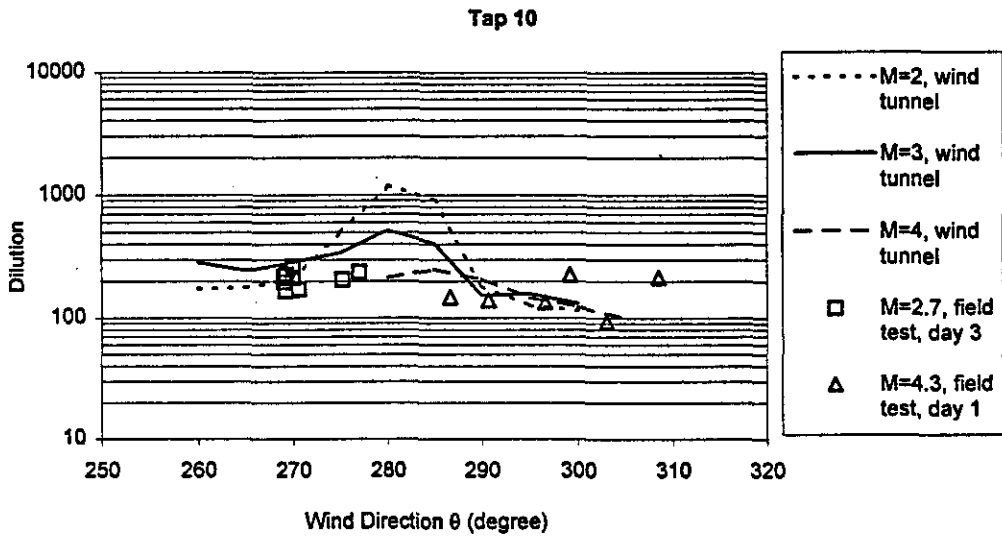
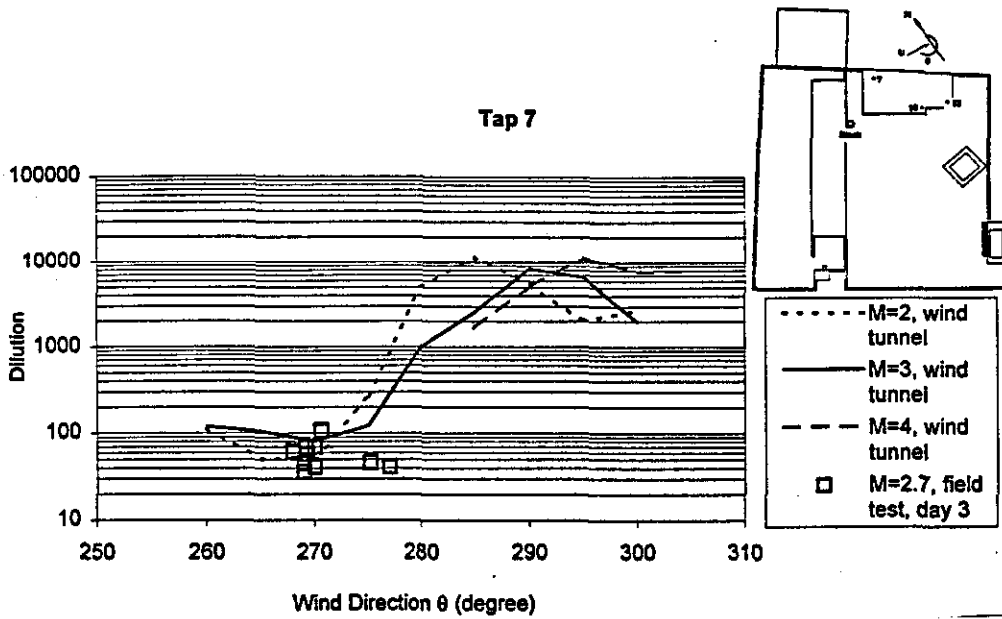


Figure 42 Effect of wind direction on wind tunnel and field dilution measured on the penthouse of the BE Building.

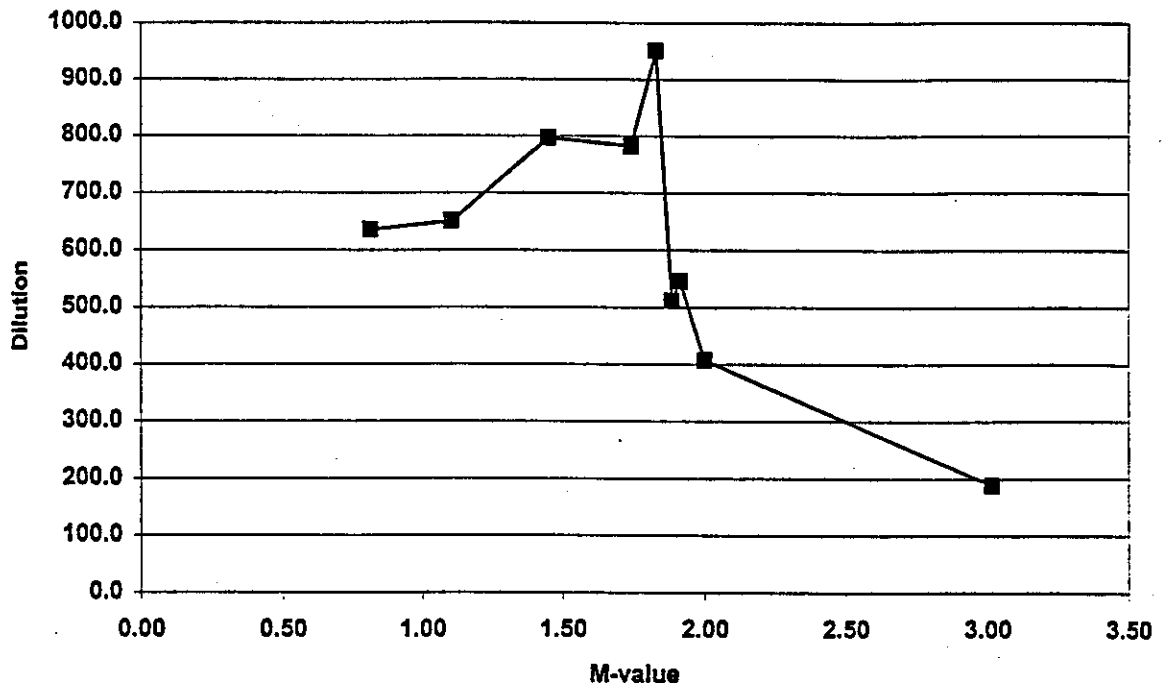


Figure 43 Variation of D_w with M at location 10 for $\theta=280$ deg.

At penthouse location 7, wind tunnel dilution curves for $M=2$ and $M=3$ show similar variation with 2 (Fig. 42a). Minimum dilution values of 50 to 100 occur for $260^\circ < \theta < 275^\circ$ but D increases significantly to a peak of 10000 as the wind shifts to west-northwesterly $285^\circ < \theta < 290^\circ$. Field data were obtained only for westerly winds during the Dec. 2nd test but these compare very well with the wind tunnel data. In general, the wind tunnel data are greater than the field values but the discrepancies are less than a factor of two.

Wind tunnel dilution curves obtained at locations 10 and 12 on the penthouse are similar in appearance, as shown in Figures 42b and 42c. For these receptors, dilution data for $M=2$ and $M=3$ tend to diverge when the wind direction is in the range of $275^\circ < \theta < 285^\circ$ with values at $M=2$ being three times as large as those at $M=3$. Results of the field study are inconclusive regarding the variation of D with M in this θ range because the number of samples was small, although several samples were obtained on Oct. 10th ($M \sim 1.8$) at location No. 12 for $270^\circ < \theta < 280^\circ$. These data do not compare well with the wind tunnel data obtained at $M=2$; the wind tunnel dilution values exceed the field values by a factor of four, in this case. Nevertheless, the field data obtained at $M \sim 2.7$ compare reasonably well with the $M=3$ wind tunnel data obtained at locations 10 and 12.

The reason for the four-fold increase in wind tunnel dilution at $M=2$ for $275^\circ < \theta < 285^\circ$ is not clear, but may be due to turbulence produced by several large buildings located approximately 150 m upwind of the BE Bldg. Additional experiments were carried out to determine the sensitivity of D to variations in M for this wind direction range. Figure 43 shows dilution at location 10 is

relatively high ($D \sim 800$) for $0.8 < M < 1.9$ but drops abruptly to 400 at $M=2$ and further to 200 at $M=3$. (Note the large discrepancy between $M=2$ dilutions at $\theta=280^\circ$ shown in Figures 42 and 43, which is due to the uncertainty in estimating M .)

Wind tunnel tests were carried out at $M=4$ for west-northwesterly winds to compare with field results obtained on Oct. 1st. At location 10, the wind tunnel data compare well with the field dilutions. At location 12, the field dilutions are slightly higher than the wind tunnel values when $\theta \sim 300^\circ$. At both locations 10 and 12, it is interesting to note the similarity of wind tunnel D curves obtained with $M=2$, $M=3$ and $M=4$ when $\theta > 290^\circ$ and the dissimilarity of the curves for $\theta < 290^\circ$.

Figure 44a shows dilution data obtained at location 6 on the main roof. The wind tunnel dilution curves for $M=2$ and $M=3$ are similar in appearance and resemble those obtained at location 7. Dilution reaches a minimum of 150 to 300 for westerly winds but increases significantly to a value of 10000 as θ increases to 285° . The field data for location 6 were obtained mainly for westerly winds and these generally agree well with the wind tunnel results. At $\theta=270^\circ$, D_{wt} exceeds D_{field} by up to a factor of three; larger discrepancies are observed for $\theta \sim 275^\circ$, however. The apparent increase in modelling error at $\theta \sim 275^\circ$ may not be real, considering the uncertainty of the field θ measurements. Clearly, additional field experiments are needed to conclusively determine the variability of dilution with wind direction.

Figures 44b and 44c show dilution data obtained at locations 16 and 24 on the main roof. The

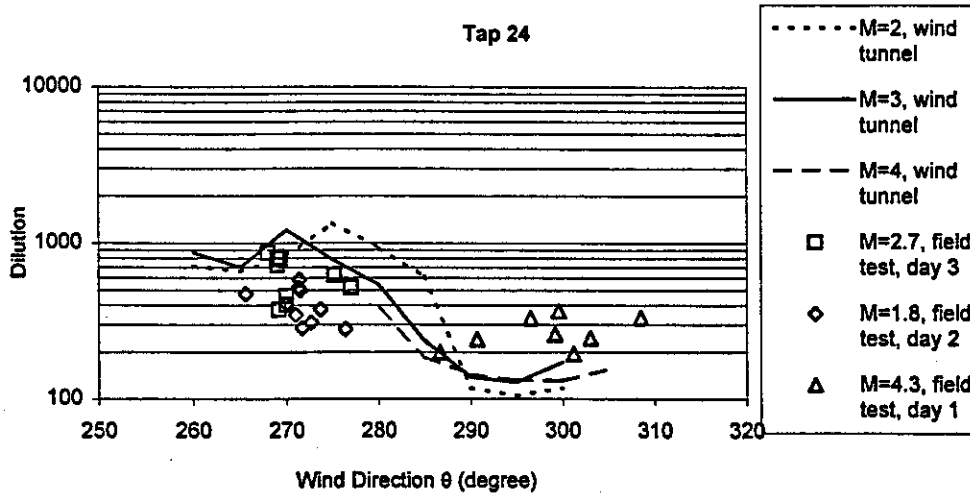
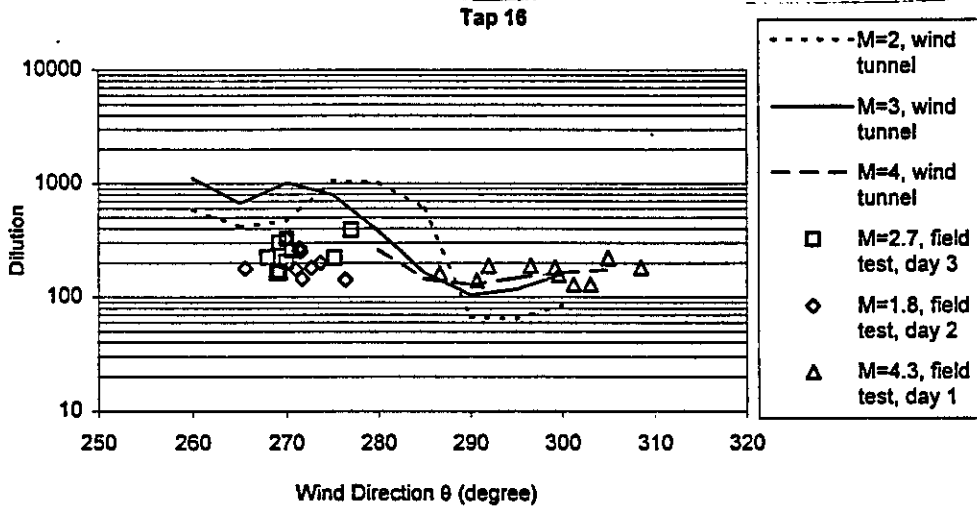
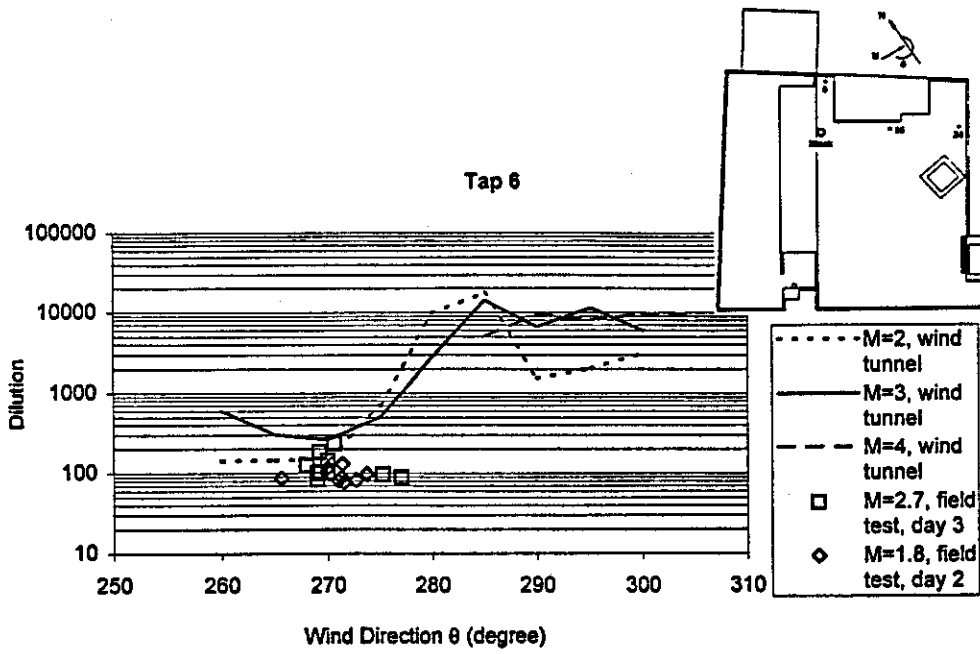


Figure 44 Effect of wind direction on wind tunnel and field dilution measured on the main roof of the BE Building.

wind tunnel dilution curves for $M=2$ and $M=3$ show a maximum of approximately 1500 for westerly winds ($270^\circ < \theta < 285^\circ$). Field data in the same M -range obtained during the Oct. 10th and Dec. 2nd tests for westerly winds show less sensitivity to wind direction. Also, the relatively low values of dilution obtained in the field tests for westerly winds is somewhat surprising since the samplers were not on the plume centre-line. It appears that lateral dispersion in the field tests was significantly greater than that simulated in the wind tunnel.

Minimum wind tunnel dilution at locations 16 and 24 occurred at a wind direction of 290° for $M=2$, $M=3$ and $M=4$. Field data obtained at location 16 for WNW winds (Oct. 1st, $M_{avg} = 4.3$) compare very well with wind tunnel dilutions obtained for $M=4$. On the other hand, field dilutions at location 24 are approximately twice as large as the wind tunnel values for WNW winds.

4.2.3 Summary of Findings from the BE Building Study

The field and wind tunnel experiments with the BE Building have provided a significant amount of data regarding the dispersion of exhaust from a 3-m stack on the roof of a low-rise building in an urban environment. Of particular importance were data from samplers near the stack on the adjacent penthouse which provide a good approximation of the initial dilution of the plume.

The major findings of the study are:

1. The Halitsky model gives highly conservative predictions of minimum dilution.
2. The minimum dilution models of Wilson-Lamb and Wilson-Chui provide reasonable lower bounds for D_{min} , although both models provide unconservative

predictions of some of the field data.

3. The Wilson-Chui formula for calculating initial dilution causes the WC model to significantly overestimate D_{\min} near the stack when the stack momentum ratio is large ($M > 4$).
4. The Wilson-Lamb initial dilution formula provides a more realistic approximation of initial dilution at large M than the WC formula. However, the WL formula also overestimates D_0 . This appears to be the main cause of occasional overestimates of D_{\min} by the WL model.
5. Tracer gas measurements and records of flow visualization obtained during the field tests showed that the plume was frequently brought down to the main roof very close to the stack, even though the exhaust momentum ratio was relatively large. This phenomenon, which was simulated well by the wind tunnel, may be due to the exceptionally high turbulence in the approaching wind or the flow patterns produced by the BE Bldg. itself. Future wind tunnel experiments can be carried out with an isolated model to investigate this topic.
6. Dilution data obtained in the wind tunnel study are generally within a factor of two of the field data. At most locations, wind tunnel dilution values tend to be slightly larger than the field measurements.

5.0 Guidelines for Design

The present study provides significant information regarding the dispersion of exhaust from rooftop stacks. However, the study also raises additional questions which must be investigated

before firm guidelines can be offered. Nevertheless, the following tentative design guidelines are provided.

1. Comparison of the ASHRAE models with the field results shows that the Halitsky model provides conservative estimates of dilution and is therefore applicable for cases involving toxic gases where a factor of safety is appropriate. The Wilson-Lamb model and the revised Wilson-Chui model (using the Wilson-Lamb initial dilution approximation) generally provide a reasonable lower bound to dilution values. The WC and WL models are suitable for situations involving nuisance odors. However, for situations involving toxic gases, a factor of safety should be used since both models may provide unconservative estimates of minimum dilution at some locations. The revised Wilson-Chui model is recommended because it is simpler to use.
2. For complex building geometries, a wind tunnel modelling study is preferred over the use of the ASHRAE formulas. It is recommended that a factor of safety of two be applied to the wind tunnel measurements.
3. Wind tunnel studies should include information regarding the sensitivity of the results to the exhaust speed/wind speed ratio, M .

6.0 Acknowledgments

The authors would like to gratefully acknowledge the contribution of Mr. Yves Beaudet and Mr. Claude Letourneau of IRSST for their excellent work regarding the collection of the field data. Likewise, the work of Mr. Po Te, who constructed the samplers is appreciated.

The following students in the Centre for Building Studies assisted with the field and wind tunnel experiments: Xuan Wei, Joanne Choubavlis, Anthony Caci, and Enrico Yu. Dr Hanqing Wu assisted with the data analysis. The authors are also grateful to Professor David Frost of Concordia University and Professor Rod Rogers of McGill University for supplying meteorological data. Finally, the authors are very appreciative of the comments of the reviewers. Many of the comments have been addressed in the final report.

7.0 REFERENCES

- Allwine, K., Meroney, R. and Peterka, J. (1980) "Rancho Seco building wake effects on atmospheric diffusion: Simulation in a meteorological wind tunnel," NUREG/CR-1286.
- ASHRAE (1993) Chapter 14, Airflow around buildings, *ASHRAE handbook--1993 fundamentals*, American Society of Heating, Refriger. and Air-Cond. Eng., Inc., Atlanta.
- ASHRAE (1997) Chapter 15, Airflow around buildings, *ASHRAE handbook--1997 fundamentals*, American Society of Heating, Refriger. and Air-Cond. Eng., Inc., Atlanta.
- Bachlin, W., Theurer, W. and Plate, E. J. (1991) "Wind field and dispersion in a built-up area – a comparison between field measurements and wind tunnel data," *Atmospheric Environment*, Vol. 25A, No. 7, pp. 1135-1142.
- Castro, I.P. and Robins, A.G. (1977) "The flow around a surface-mounted cube in uniform and turbulent streams," *Journal of Fluid Mechanics*, Vol. 79, pp. 307-335.
- Chui, E.H. and Wilson, D.J. (1988) "Effects of varying wind direction on exhaust gas dilution," *Journal of Wind Engineering and Ind. Aerodyn.*, Vol. 31, pp. 87-104.

- Georgakis, K., Smith, J., Goodfellow, H. and Pye, J. (1995) "Review and evaluation of models estimating the minimum atmospheric dilution of gases exhausted near buildings," *Journal of the Air & Waste Management Assoc.*, Vol. 45, pp. 722-729.
- Halitsky, J. (1963) "Gas diffusion near buildings," *ASHRAE Trans.* Vol. 69, pp. 464-484.
- Halitsky, J. (1990) "Calculation of minimum available atmospheric dilution downwind of building exhausts," *ASHRAE Trans.* Vol. 96, pp.46-51.
- Higson, H. L., Griffiths, R.F., Jones, C.D. and Hall, D.J. (1994) "Concentration measurements around an isolated building: a comparison between wind tunnel and field data," *Atmospheric Environment*, Vol. 28, No. 11, pp. 1827-1836.
- Higson, H.L., Griffiths, R.F., Jones, C.D. and Biltoft, C. (1995) "Effect of atmospheric stability on concentration fluctuations and wake retention times for dispersion in the vicinity of an isolated building," *Environmetrics*, Vol. 6, pp. 571-581.
- Lam, K.S., Kot, S.C., Fung, K.W. and Ma, R.Y.P., (1985) "A field validation of roof-top dispersion formula in an urban centre," *J. of Wind Engr. and Indust. Aerodyn.*, 21 pp.295-305.
- Lam, K.S. and Kot, S.C. (1993) "Field study of roof top dispersion in an urban area," 3rd Asia-Pacific Symposium on Wind Engineering, Dec. 13-15, Hong Kong.
- Lamb, B. and Cronn, D. (1986) "Fume hood exhaust reentry into a chemistry building," *Journal of the Am. Ind. Hyg. Assoc.*, Vol. 47 (2), pp. 115-123.
- Li, W.W. and Meroney, R.N. (1983) "Gas dispersion near a cubical model building," *Journal of Wind Engineering and Ind. Aerodynamics*, Vol. 12, pp. 15-23.
- Martin, J.E., (1965) "The correlation of wind tunnel and field measurements of gas diffusion using krypton-85 as a tracer," Ph.D. Thesis, Dept. of Health Sciences, Univ. of Michigan.
- Ogawa, Y., Oikawa, S. and Uehara, K., (1983a) "Field and wind tunnel study of the flow and diffusion around a model cube--I. Flow measurements, *Atmospheric Environment*, 17, 1145-1159.
- Ogawa, Y., Oikawa, S. and Uehara, K., (1983b) "Field and wind tunnel study of the flow and diffusion around a model cube--II. Nearfield and cube surface flow and concentration patterns, *Atmospheric Environment*, 17, 1161-1171.
- Oikawa, S. and Meng, Y. (1997), "A field study of diffusion around a model cube in a suburban area," *Boundary-Layer Meteorology*, Vol. 84, pp. 399-410.

- Parera, M.D., Tull, R.G., White, M.K. and Walker, R.R. (1991) "Assessing Intake contamination from atmospheric dispersion of building exhaust," 12th AIVC Conference, Ottawa, pp. 347-357.
- Petersen, R.L. (1986) "Wind tunnel investigation on the effect of platform-type structures on dispersion of effluents from short stacks," *J. of the Air Pollution Control Assoc.*, 36, 1347-1352.
- Petersen, R.L. and Wilson, D.J. (1989) "Analytical versus wind tunnel determined concentrations due to laboratory exhaust," ASHRAE Trans., 95(2): pp. 729-736.
- Petersen, R.L. and Ratcliff, M.A. "An objective approach to laboratory stack design," *ASHRAE Trans.*, Vol.97, No. 2., 553-561 (1991).
- S-2.1, r.15 (1994) "Regulation respecting the quality of the work environment," Quebec.
- Saathoff, P. and Stathopoulos, T., (1997) "Dispersion of exhaust gases from roof level stacks and vents on a laboratory building--Discussion," *Atmospheric Environment*, 31, 1087-1089.
- Saathoff, P., Wu, H. and Stathopoulos, T., (1996) "Dilution of exhaust from rooftop stacks -- Comparison of wind tunnel data with full-scale measurements," *Proc. of 9th Joint Conf. On Applications of Air Pollution Meteorology*, AMS/AWMA, Atlanta 341-345.
- Schuyler, G.D. and Turner, G.G., (1989) "Comparison of wind tunnel test results with empirical exhaust dilution factors," ASHRAE Trans., 95(2): pp. 737-744.
- Start, G., Cate, J., Dickson, C., Ricks, N. Ackerman, G. and Sagendorf, J., (1977) "Rancho Seco building wake effects on atmospheric diffusion," NOAA Tech. Memo. ERL ARL-69.
- Turner, D.B. (1994) Workbook of Atmospheric Dispersion Estimates, 2nd Ed., CRC Press .
- Wilson, D.J. and Chui, E. (1985) Influence of exhaust velocity and wind incidence angle on dilution from roof vents, *ASHRAE Transactions*, 91(2B) 1693-1706.
- Wilson, D.J. and Chui, E., (1987) "Effect of Turbulence from Upwind Buildings on Dilution of Exhaust Gases," *ASHRAE Transactions*, 93(2), 2186-2197.
- Wilson, D.J. and Lamb, B., (1994) "Dispersion of exhaust gases from roof level stacks and vents on a laboratory building," *Atmospheric Environment*, 28, 3099-3111.
- Wilson, D.J. and Chui, E.H. (1994) "Influence of building size on rooftop dispersion of exhaust gas", *Atmospheric Environment*, Vol. 28, No. 14. pp. 2325-2334.
- Wilson, D.J. (1995) Concentration Fluctuations and Averaging Time in Vapor Clouds, Center for Chemical Process Safety, American Institute of Chemical Engineers.

APPENDIX A

Analysis of Anemometer Data

The Gill ultrasonic anemometer measures three components of wind velocity using the time of flight principle. The anemometer consists of six transducers; one pair of transducers measures the vertical component, w_s , and the other two pairs measure the horizontal components, u_s and v_s , where the subscript indicates a measurement on the transducer axis. Each transducer acts alternately both as a receiver and a transmitter of ultrasonic pulses; by measuring the time of flight of the pulses, the velocity components are determined.

The transducer orientation in relation to the positive u_s and v_s directions is shown in Figure A1.

The relationship between u_s and v_s and the along-wind and cross-wind components of the wind, u and v , is shown in Figure A2.

The mean wind direction, $\bar{\theta}$, is determined by calculating the rotated mean wind direction, $\bar{\theta}_r$:

$$\bar{\theta}_r = \tan^{-1}(\bar{u}_r/\bar{v}_r) \quad \text{A1}$$

such that: $\bar{\theta} = \bar{\theta}_r - 90 + \phi$ A2

where an overbar indicates the mean value; and ϕ is defined in Figure A2. The mean along-wind and cross-wind components are:

$$\bar{u} = \bar{u}_s \sin \bar{\theta}_r + \bar{v}_s \cos \bar{\theta}_r \quad \text{A3}$$

$$\bar{v} = \bar{u}_s \cos \bar{\theta}_r + \bar{v}_s \sin \bar{\theta}_r = 0 \quad \text{A4}$$

The along-wind component can also be obtained from the following:

$$\bar{u} = (\bar{u}_x^2 + \bar{v}_x^2)^{0.5} \quad \text{A5}$$

The along-wind velocity variance is defined as:

$$\begin{aligned} \sigma_u^2 = & (\bar{u}_x \bar{u}_x) \sin^2 \bar{\theta}_r + 2(\bar{u}_x \bar{v}_x) \sin \bar{\theta}_r \cos \bar{\theta}_r + (\bar{v}_x \bar{v}_x) \cos^2 \bar{\theta}_r \\ & - (\bar{u}_x)(\bar{u}_x) \sin^2 \bar{\theta}_r - 2(\bar{u}_x)(\bar{v}_x) \sin \bar{\theta}_r \cos \bar{\theta}_r - (\bar{v}_x)(\bar{v}_x) \cos^2 \bar{\theta}_r \end{aligned} \quad \text{A6}$$

The anemometer records the mean and standard deviation of u_x and v_x , and thus, the mean square quantities can be calculated. (e.g. $\bar{u}_x \bar{u}_x = \sigma_u^2 + \bar{u}_x^2$). The covariance ($\bar{u}_x \bar{v}_x$) was not measured; however, it can be estimated by assuming that the cross-wind turbulence intensity is a fixed ratio of the along-wind intensity. By definition, the cross-wind variance is:

$$\sigma_v^2 = (\bar{v}_x \bar{v}_x) \sin^2 \bar{\theta}_r - 2(\bar{u}_x \bar{v}_x) \sin \bar{\theta}_r \cos \bar{\theta}_r + (\bar{u}_x \bar{u}_x) \cos^2 \bar{\theta}_r \quad \text{A7}$$

Previous studies [e.g. Ogawa et al. (1983), Oikawa and Meng (1997)] indicate that, on average, $\sigma_v \sim 0.8\sigma_u$, although in some cases σ_v may approach σ_u in magnitude.

Letting $\sigma_v = 0.8\sigma_u$, Equ. A7 can be re-arranged such that:

$$2(\bar{u}_x \bar{v}_x) \sin \bar{\theta}_r \cos \bar{\theta}_r = (\bar{v}_x \bar{v}_x) \sin^2 \bar{\theta}_r + (\bar{u}_x \bar{u}_x) \cos^2 \bar{\theta}_r - 0.64\sigma_u^2 \quad \text{A8}$$

Substituting the left-hand side of A8 into A6 yields:

$$\sigma_u^2 = 1/1.64[(\overline{u_s u_s}) + (\overline{v_s v_s}) - (\overline{u_s})(\overline{u_s})\sin^2\theta_r - 2(\overline{u_s})(\overline{v_s})\sin\theta_r\cos\theta_r - (\overline{v_s})(\overline{v_s})\cos^2\theta_r] \quad A9$$

or

$$\sigma_u^2 = 1/1.64(\sigma_{u_s}^2 + \sigma_{v_s}^2) \quad A10$$

Example:

The validity of the above method for calculating σ_u can be checked for those intervals when the mean wind direction was aligned with an axis of the anemometer. In such cases, the measured σ_u can be compared to that obtained using the Eq. A10.

Wind data obtained on June 26th at the Hall Bldg. are shown in Table A1. The 10:35 record indicates that the wind was aligned with the V_s axis since $U_s \sim 0$. Therefore, the turbulence intensity is: $\sigma_u / U = \sigma_{v_s} / U = 1.27/2.82 = 0.45$. Substituting values of σ_{u_s} and σ_{v_s} into Eq. A10, gives $\sigma_u = 1.253$ m/s. Thus, the estimated value of σ_u / U is 0.444, which is approximately equal to the true value .

References

ASTM D5527 "Standard practices for measuring surface wind and temperature by acoustic means" The American Society for Testing and Materials (1994).

Ogawa, Y., Oikawa, S. and Uehara, K., (1983) "Field and wind tunnel study of the flow and diffusion around a model cube--I. Flow measurements, *Atmospheric Environment*, 17, 1145-1159.

Oikawa, S. and Meng, Y. (1997), "A field study of diffusion around a model cube in a suburban area," *Boundary-Layer Meteorology*, Vol. 84, pp. 399-410.

Table A1 Wind data obtained on the Hall Building during Test 1

TIME	Hall Day 1					26-Jun-98	
	Mean Vel. (m/s)	Us (m/s)	Vs (m/s)	σ_{us} (m/s)	σ_{vs} (m/s)	σ_u	Turb.Int.
10:25	4.036	0.36	-4.02	1.17	1.56	1.522694	0.377278
10:30	3.369	-0.24	-3.36	1.3	1.56	1.585683	0.470669
10:35	2.82	0.01	-2.82	0.98	1.27	1.252631	0.444196
10:40	5.021	-3.5	-3.6	1.78	1.33	1.735093	0.345567
10:45	5.168	-1.45	-4.96	1.15	1.6	1.538629	0.297722
10:50	5.02	-1.09	-4.9	0.88	1.9	1.635058	0.325709
10:55	5.499	-0.93	-5.42	0.98	1.34	1.296336	0.23574
11:00	5.62	-0.75	-5.57	1.15	1.37	1.39673	0.248528
11:05	6.428	-1.12	-6.33	0.82	1.28	1.187023	0.184664
11:10	4.377	-1.56	-4.09	1.39	1.86	1.81318	0.414252
11:15	4.812	-1.24	-4.65	1.13	1.28	1.333275	0.277073
11:20	3.209	-1.14	-3	1.03	1.42	1.369818	0.426868
11:25	3.46	-1.67	-3.03	1.51	1.42	1.618585	0.467799
11:30	4.966	-1.82	-4.62	1.38	1.77	1.752577	0.352915
11:35	6.537	-1.18	-6.43	0.95	2.07	1.778496	0.272066
11:40	5.424	-1.79	-5.12	1.57	2.41	2.245999	0.414085
11:45	4.737	-1.09	-4.61	1.19	1.94	1.777176	0.375169
11:50	4.9	-1.82	-4.55	1.39	1.89	1.831999	0.373877
11:55	3.974	-2.82	-2.8	1.85	1.63	1.925344	0.484485

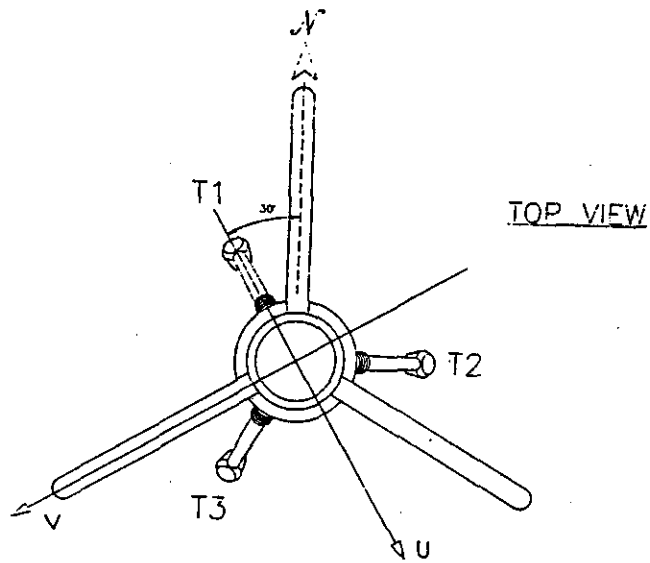


Figure A1 Plan view of Gill sonic anemometer showing orientation of transducers

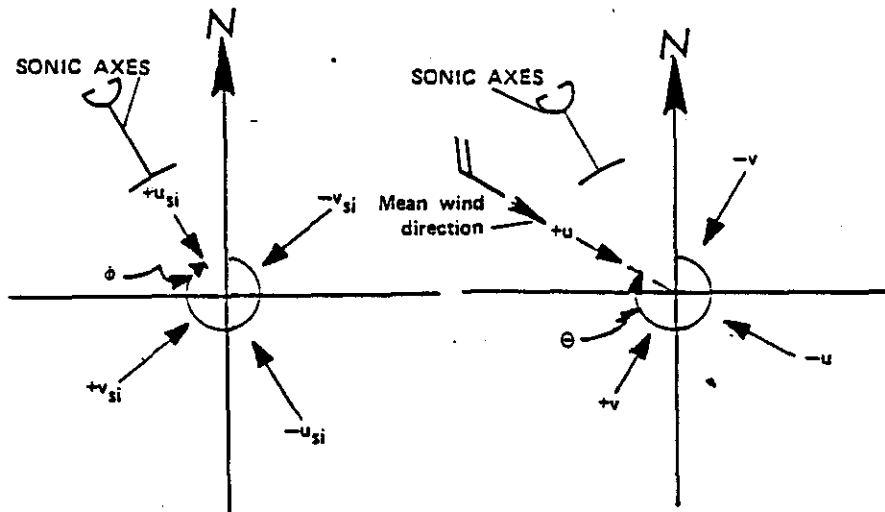


Figure A2 Sonic anemometer coordinate system (from ASTM D5527)

APPENDIX B

Design of Automatic Air Samplers

The automated sampling module shown in Figure B1 was designed and built at the IRSST for the sequential sampling of several air samples at predetermined time intervals. Each module is equipped with a low-flow sampling pump (MSA C-210) connected to a distributor to which 10 1-litre bags (Cali-5-Bond) are attached by flexible (polyethylene) tubing (see Figure B1). Each of the bags has a LUER type valve. This type of valve is normally closed, thus avoiding the loss of the contents should the connection tube accidentally disconnect.

Preliminary tests have confirmed that sulfur hexafluoride (SF_6) does not adhere to the bag material, thus preventing sample contamination. As a safety measure, each bag was purged with zero air between samplings.

The manual programming unit, shown in Figure B2, assigns the sampling time and the waiting period between samplings (if need be), and also, starts all the modules simultaneously. The operating parameters are transmitted to all the sampling modules by radio waves, with the antenna's transmission frequency being 49.830 MHz. Programming can also be done using a computer connected to the module's RS-232 communication port. This means of programming is useful when the sampling parameters differ from one module to the next, particularly when the modules are not started at the same time.

In normal mode, the liquid crystal displays the instantaneous sampling data, namely the number of the valve (or bag) being used, the sampling time, the elapsed sampling time, and the current drawn by the sampling pump. In view mode, the same information can be seen, but only for the valves that are not in use.

The module requires a power supply of 110/120 V or the use of a 12 V gel-acid type rechargeable battery with a capacity of 7.5 ampere-hours. The autonomy of the battery is approximately 8 hours.

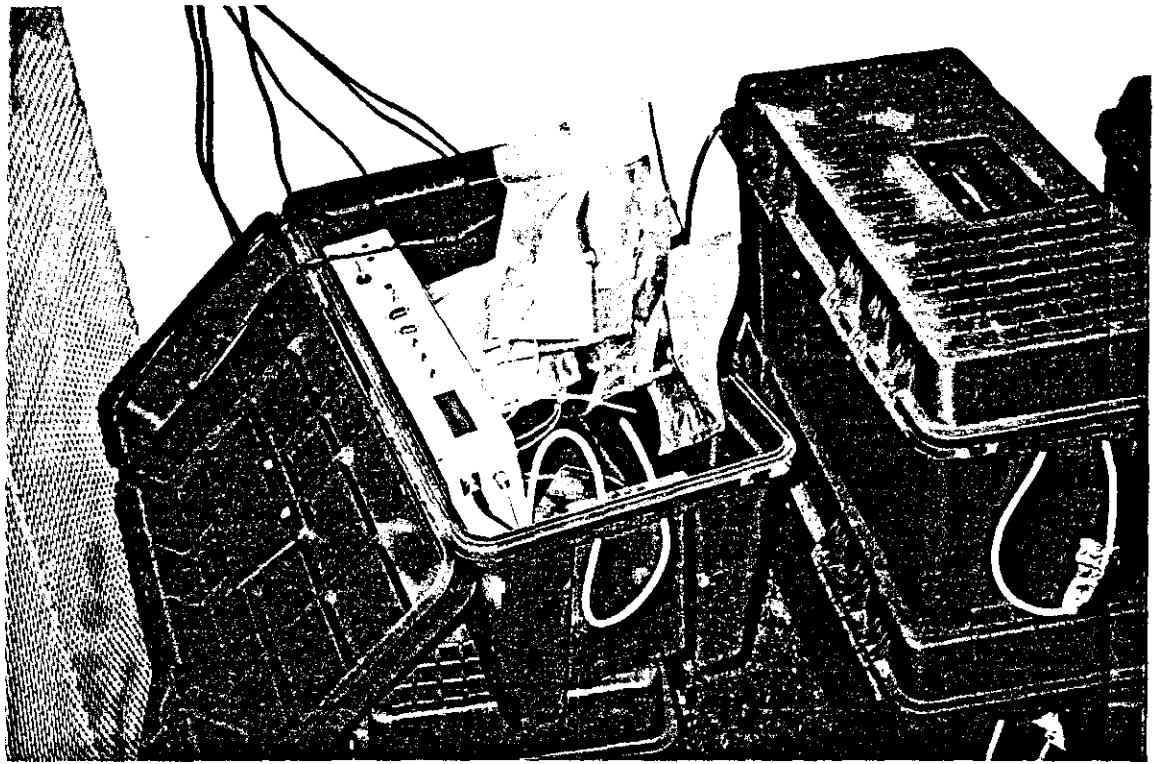


Figure B1 The automated sampler with sample bags attached

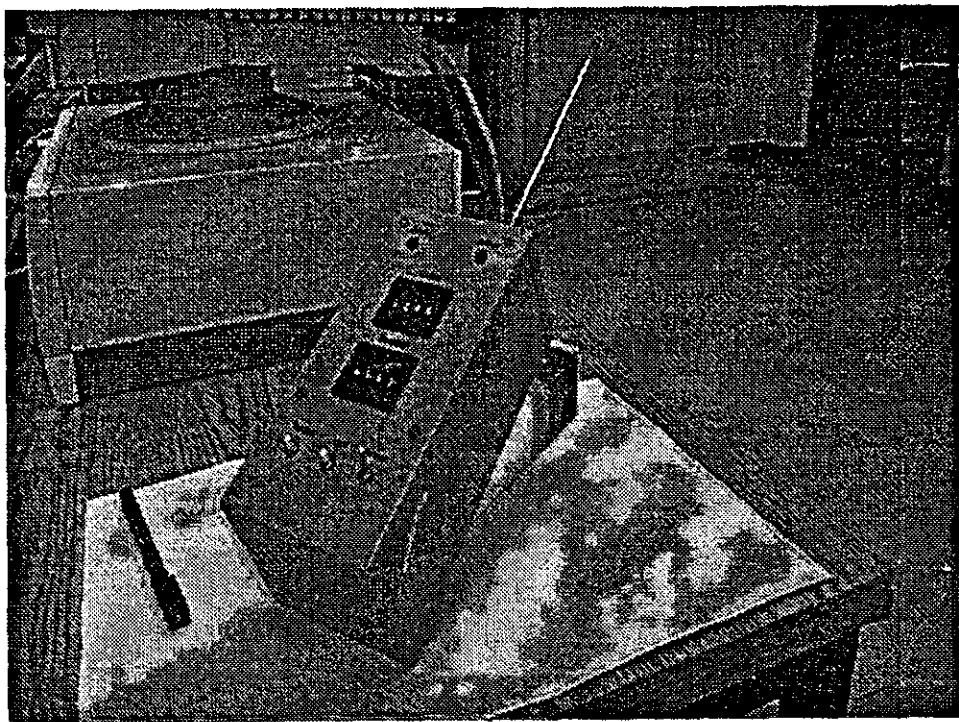


Figure B2 The manual programming unit of the sampling modules